Three Dimensional Simulation of Ultrasonic Cleaning Vessels and Verification of Results.

Jamie Peter Lewis

A submission presented in partial fulfilment of the requirements of the University of Glamorgan/Prifysgol Morgannwg for the degree of Doctor of Philosophy

This research programme was carried out in collaboration with Ultrawave Limited of Cardiff, manufacturers of ultrasonic cleaning devices under EPSRC funding.

June 2007

Acknowledgements.

"There is a theory which states that if ever anyone discovers exactly what the universe is for and why it is here, it will instantly disappear and be replaced by something even more bizarre and inexplicable"

"There is another theory which states that this has already happened..."

(Douglas Adams: 1980)

Any learning experience is a journey, and like any adventure, it is made all the more pleasurable by the companions who tread the path alongside you. In nearing the completion of this work I feel I must extend my deepest gratitude to those who have accompanied me on this journey.

First and foremost, to Valmai, who has made the transition from girlfriend, to wife and finally thesis widow during the past few years, and offered her unwavering love and support throughout.

Secondly, my supervisor, Steve, without who's patience, encouragement and professionalism in the face of adversary I could not have made it this far.

Finally, to all those who have commented, assisted, criticised, guided and aided. To friends, family, colleagues and acquaintances. My eternal thanks.

J.P.Lewis (2007).

Abstract.

Ultrasonics, that is mechanical waves with a frequency greater that 18 kHz, are employed in a number of diverse and distinctive industries. One important niche occupied by ultrasound, and the focus of this thesis, is its application in ultrasonic cleaning systems whereby the rapid pulsing of mechanical waves at ultrasonic frequencies forms thousands of microscopic voids (or cavities) in the liquid. It is the implosions of these voids during the positive pressure phase of the wave that assists the removal of contaminants from the surface of an immersed load and is known as cavitation.

A thorough literature review conducted as the foundation of this work uncovered a significant deficit in knowledge regarding the positions of cavitating fields within ultrasonic vessels. Further to this, the effects on the cavitating field of a number of industrially relevant parameters, such as transducer placement, the introduction of baskets and cleaning loads to the liquid and variations in the level of the cavitating medium, were found to be deficient within both academic and industrial knowledge base.

The outcomes of the literature review clearly indicated that it was evident that the development of a "toolset" capable of modelling the bulk cavitating fields within ultrasonic vessels would not only sustain the strong industrial relevance of the programme of work, but would also add significantly to extant knowledge concerning the design and production of commercial ultrasonic vessels. This work describes the development of such a toolset, detailing the mathematical modelling behind the simulation system and the logical progression of the work, from basic 2D models used for rapid prototyping to full 3D models used to simulate a wide variety of complex systems with parameters hitherto un-described within the literature. A variety of methods of quantifying the simulation outputs are reviewed and discussed during the

thesis, leading to the logical selection of one qualitative and one quantitative indicator of cavitating fields.

A comparison of the simulation outputs to the respective empirical data showed an excellent degree of correlation, leading to a high level of confidence in the simulation toolset. Use of the verified model together with the developed design methodology was used to address the industrially relevant issues detailed in the literature review and this further promoted the contribution to knowledge presented in this work.

As in any industrial design, pragmatic approximations were used in the production environment and this occasionally appeared to show discrepancies between the simulation outputs and the practical data obtained. Specific causes behind these differences are critically analysed, and along with further questions arising from such analysis. The outcomes formed the backbone of a future work proposal presented along with a comprehensive review and summary of the results and improved synthesis techniques.

Table of Contents

Chapter 7 – conclusions

List Of Appendices

List of Figures

List of Tables

List of equations

The Programme of Work

This programme of work is the outcome of a study designed by Ultrawave of Cardiff (UK) and the Faculty of Advanced Technology at the University of Glamorgan, to develop, test and implement a novel design process for ultrasonic cleaning systems. This work is supported under the EPRSC Industrial CASE Award scheme and the PRIME Faraday Centre in Loughborough (now the Electronics Enabled Product Knowledge Transfer Network).

The Partners

Ultrawave is a company dedicated to the design and development of high quality ultrasonic cleaning vessels for a wide range of applications, including medical applications and industrial cleaning tanks. The medium term objectives of Ultrawave include becoming a recognized leader in the creation of new solutions for its market through improved understanding of the overall process and the implementation of the knowledge gained into novel system designs.

To achieve this goal, the company vision is one whereby customer problems can be evaluated in terms of a process which uses product performance modeling and simulation as a major tool in the delivery of a solution. To that end it has formalized its links with the Centre for Electronic Product Engineering (CEPE) and with the Faulty of Advanced Technology at The University of Glamorgan via the EPSRC Scheme. CEPE is a recognized Centre of Excellence and has knowledge transfer role focused on partnering with SMEs in Wales. It primarily works in the Electronics area but practical implementation of hardware and software solution often mean that it has to relate to mechanical systems. CEPE has a long history of working on Mechatronic Systems both through this R&D work and via practical implementations for industry and thus this relationship was recognized as being well suited for support from PRIME Faraday.

Chapter 1: Introduction to Ultrasound and Ultrasonic cleaning

1.0 Introduction

The existence of ultrasound was first deduced by Lazarro Spallanzani in 1794 who deduced the navigation of bats was accomplished by echo location using sounds at frequencies outside of human hearing ranges [1]. In the three centuries succeeding Spallanzani's discovery, ultrasonics has flourished from a passively observed phenomenon to a tightly controlled science utilised in a wide number of disparate industries.

Ultrasound is defined as the propagation of mechanical waves in a medium that is above the human hearing range [2]. Figures for the range of frequencies at which ultrasonics commence are generally quoted as above 20kHz [3] (although some sources will quote as low as 16kHz [4]), with frequencies above 500kHz often referred to within some sectors of industry as 'megasonic' due to process differences between the higher frequency range of megasonics and effects due to ultrasound [5].

Industrial applications of ultrasound are many and diverse and can be roughly divided into two distinct categories, low powered and high-powered applications. Table 1.1 shows a list of applications relative to the high/low-powered spectrum.

Low Power	High Power
Flaw detection and inspection (NDT)	Atomizing
Flow detection	Biological Processing, cell disruptors
Distance sensing and control	Chemical processing (sonochemistry)
Bond and weld testing	Degassing of liquids and molten metals
Liquid level sensing	Surface cleaning applications

Leak detection	Emulsification and homogenization
Marine navigation	Drilling and cutting
Fish Detectors	Medical surgery (HIFU)
Medical diagnosis (Echo cardiogram)	SONAR ranging and tracking
Pest repellant	Welding and soldering of metals/ plastics

Table 1.1 division of ultrasound by high powered/low powered application

A further classification of ultrasonic industries can be made according to the frequencies commonly used. Figure 1.1 shows commonly used frequency ranges used by some of the aforementioned applications.

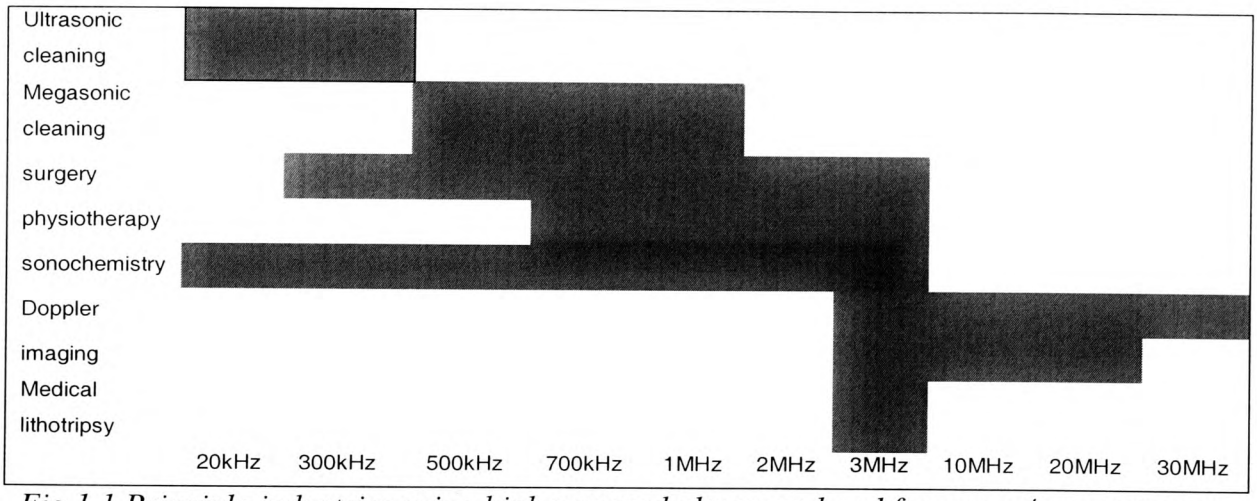

Fig.1.1 Principle industries using high powered ultrasound and frequency/power ranges

At the lower end of the frequency spectrum but utilizing high-powered ultrasonic energy lay the ultrasonic cleaning applications.

1.1 Ultrasonic cleaning.

The principle of operation of ultrasonic cleaning was first discovered in the early 1930's by a team from the Radio Corporation of America as a by product of experiments into vibrating crystals in Freon used to cool radio components[6]. The first patent on cleaning by ultrasound was filled in 1943[7] and the ultrasonic cleaning industry has since

expanded to cover a broad spectrum of particle removal ranging from heavy grease in car part manufacture to delicate removal of bio-burden from fine fissures in medical instruments. In ultrasonic cleaners cavitation is the primary mechanism for particle removal, although other secondary forces for cleaning have been advanced such as acoustic streaming, but within the ultrasonic range these forces are secondary to cavitation.

Ultrasonic cleaning has been shown in numerous studies to have significant advantages over other cleaning methodologies. A study by Cafruny *et al*[8] showed ultrasonic cleaners to be greater than a 100 fold more efficient at blood removal than traditional hand scrubbing of instruments and the basket based loading system of ultrasonic cleaners helped prevent sharps and needle injuries in medical and dental settings[9]. Numerous other studies have re-enforced the value of this view point[10, 11]

In cleaning systems that require sterilisation, ultrasonic cleaners are still routinely used as an essential part of the decontamination cycle. Sabir *et al* [12] defined decontamination as "A process that removes or destroys contamination. It always involves cleaning..." and they further identified the cleaning stage as "The most important part of the decontamination process. Its primary purpose is to lower the bioburden before disinfection or sterilisation". Pockets of bio-burden are known to form over fine fissures, hinges and blind holes in instruments and act as a shield against heat and chemical sterilisation agents. Ultrasonic cleaning technologies have been shown to penetrate such narrow crevices, removing the bio-burden and exposing any pathogens beneath to fresh cleaning chemistries, thus increasing the process sterilisation rate and pathogen kill percentage.

Claims have also been made[13] that ultrasonic activity alone can cause sterilisation effects without sterilizing chemicals by puncturing cell membranes, although evidence for this is not yet conclusive.

Although ultrasonic cleaners have been shown to present a clear advantage over many other cleaning methodologies, it has been shown that cleaning throughout the vessel is not homogenous. Rather a series of 'hot spots' and 'dead zones' in the cleaning activity exist within the vessel. This has been attributed to the development of standing waves in the ultrasound field arising from the superposition of the primary radiated wave[14].

A typical ultrasonic cleaning vessel arrangement is shown in figure 1.2.

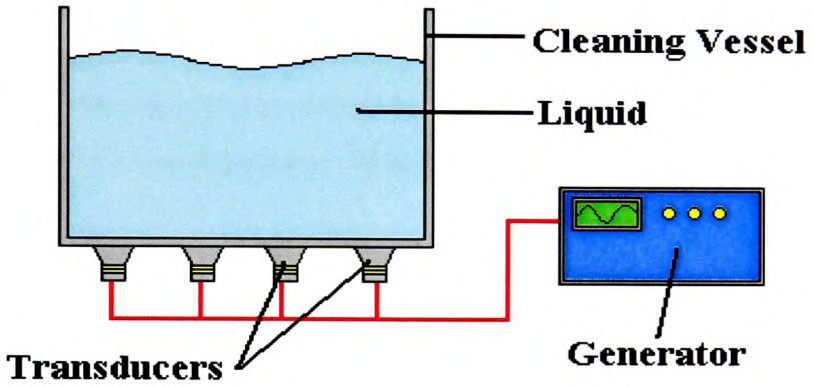

Fig. 1.2: Components of an ultrasonic cleaning vessel

The cleaning system can be divided into four components:

a) *Cleaning vessel* – An ultrasonic cleaning tank comprises of a vessel with a plurality of transducers bonded to the outer sides. The vessel is generally constructed of a stainless steel for durability and its acoustic properties. The dimensions and geometry of the vessel differ between applications ranging from 0.5L circular vessels used in optics cleansing to large bespoke industrial units ranging from 4.5L upwards. Cleaning loads are generally suspended in the vessel by means of a load carrier such as a basket or instrument tray, with the design, material and suspension height of the load carrier varying vastly between vessels.

b) *Transducers* – Ultrasonic transducers convert electrical energy supplied by the generator to the mechanical displacements necessary for ultrasonic cleaning. This

conversion can be accomplished by a number of methods which are reviewed in section 1.2. Transducers are generally bonded to the outer faces of the cleaning vessel, but in the case of extremely large vessels, a number of transducers may be submerged directly into the liquid load by means of a sealed stainless steel box known as a 'submersible transducer'.

c) *Generator* – The generator supplies the voltage and current required to drive the transducers and hence create the desired cleaning effect. The frequency and voltage of the generator output directly affects the displacement and frequency of the transducer output. The most simplistic generators operate with a high frequency sinusoidal output, although more complex output waveforms (such as square waves) have been tried as a response to the issue of inhomogeneous cleaning fields.

d) *The liquid* – Many of the properties of the liquid within the tank such as density, speed of sound, vapour pressure and temperature directly affect cleaning capabilities and therefore need to be monitored and controlled during experimental procedures. The height of the water column above the transducers also has an effect on cleaning capability by changing the standing wave structure of the vessel.

A summary of liquid properties and controls can be found in section 5.1: *Control of experiments protocol.*

1.2 Ultrasonic transducers

Ultrasonic transducers convert electrical waveforms to the mechanical oscillations required to produce cleaning effects in ultrasonic tanks with the frequency of oscillation dependant on both the frequency of the driving voltage and the characteristics of the transducer. A review of underwater sound transducers compiled by Charles Sherman on behalf of the IEEE [15] identified the following transducers as suitable for underwater application at the necessary frequency and power ranges and performed a maximum force comparison of each.

Transducer	Maximum force per unit area. (Pa)
Electrostatic	10
Moving Coil	8000
Variable reluctance	$4*10^5$
Magnetostrictive	10^6
Piezoelectric	$8*10^6$
Hydroacoustic	$7*10^6$

Table 1.2: Comparison of underwater transducers by maximum force per unit area

Of these transducer varieties only two are utilised for ultrasonic cleaning applications, the magnetostrictive and the piezoelectric transducers. Both the moving coil, electrostatic and variable reluctance transducers are limited by the maximum force they can exert.

By comparison, hydroacoustic transducer methodologies have comparable force exertion to both piezoelectric and magnetostrictive transducers. A further criterion of selection is the electromechanical coupling factor, the numerical comparison between electrical input and mechanical output. A higher electromechanical coupling factor leads to higher transducer efficiency, with piezoceramic and magnetostrictive transducers demonstrating a far higher electromechanical coupling factor than hydroacoustic transducers. [16]

1.2.1 Magnetostrictive transducers

Magnetostrictive transducers display a change in length when subjected to an alternating magnetic field. This effect is known as the Joule effect and is a property of some ferromagnetic materials. Although capable of generating greater strains than naturally occurring piezo crystals and providing a better match to relatively high acoustic impedance media such as water [15], modern piezo ceramic composites have largely

replaced magnetostrictive elements in designs due to greater strain capabilities, ease of generator design and drastically improved operational frequency bandwidth.

It is worth noting here that although out of favour at present, development of new 'rare earth' composite materials such as Terfenol-D developed by the USA's Naval Ordinance Labs exhibit 'giant magnetostriction' and lead to far greater strains and better electromechanical coupling coefficients [17], [18] than most magnetostrictive materials and even some piezoceramic composites. These developments may eventually qualify magnetostrictive materials as a candidate for industrial cleaning applications once the low frequencies of operation limitations are improved.

1.2.2 Piezoelectric transducers.

The direct piezoelectric effect (from the Greek *piezein* 'to squeeze') was first discovered by Pierre and Jacques Curie in 1880 using crude experiments on naturally occurring and prepared crystal structures (quartz, Rochelle salt, tourmaline), showing a relationship between applied stress and voltage. The mathematical deduction of the inverse piezoelectric effect (generating a strain from an applied voltage) was accomplished by Lippmann in 1881 and subsequently confirmed by quantitative data from the Curie's [19].

Initially, due to the superior deformation qualities of magnetostrictive materials over naturally occurring piezo electric crystals, development work was slow. The application of Paul Langevin's piezoelectric transducers in first world war sonar submarine detection bolstered interest in the field, accelerating development of new materials exhibiting highly enhanced piezoelectric properties such as Barium Titanate ($BaTiO_3$), Strontium Titanate ($SrTiO_3$) and Lead Zirconium Titanate $Pb(ZrTi)O_3$. Piezoelectric materials exhibit a higher coupling factor than its magnetostrictive counterparts [15].

At present, the most commonly utilized piezoceramic material used in industrial ultrasonic cleaning applications is Lead Zirconium Titanate consisting of mixed crystals of Lead Zirconate ($PbZrO_3$) and Lead Titanate ($PbTiO_3$), henceforth abbreviated to PZT,

and it is this composite material that will be used for further considerations of transducer application throughout the thesis.

PZT has a poly-crystalline structure comprising of cells exhibiting a Perovskite crystal structure, which initially show an arbitrary polling. Application of a strong electric DC field causes the electric cells to become aligned in the direction of the field, and this alignment remains (remnant polarization), thus enabling the piezoelectric phenomenon to occur.

Once poled, PZT disks and rings exhibit a number of oscillating modes that can be excited at particular resonant frequencies dependant on the geometrical ratios of the PZT design and certain properties associated with the piezoceramic material. A PZT disk for example displays two clear oscillation modes, Radial (or Planar) and Axial (or Thickness), as shown in figure 1.3. The resonant point of a PZT disk in the thickness mode of oscillation is given by the thickness mode frequency constant (N_t in kHz.mm) divided by the diameter of the disk and the planar mode vibration by the planar mode frequency constant (N_p) divided by the diameter of the disk. Ultrasonic cleaning devices utilize the thickness mode vibration for mechanical excitation of the tank. Although it is theoretically possible to have both resonant modes of vibration close together in the frequency spectrum, in practice this is discouraged and designs ensure a clear frequency gap between the two hence preventing unwanted oscillations in the planar mode.

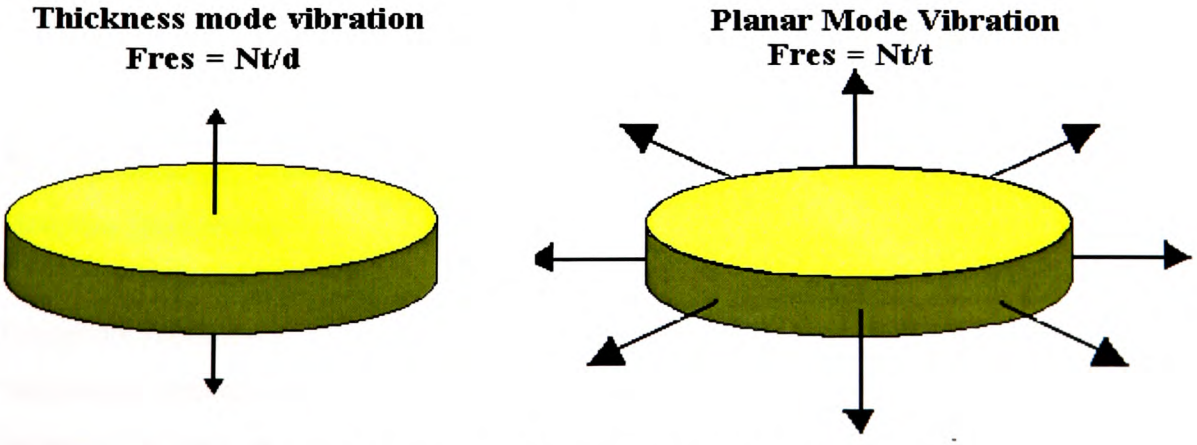

Figure 1.3: Resonant oscillation modes of a PZT disk

PZT transducers are subject to a capacitive ageing that effects the resonant characteristics of the transducer, this will also be covered further in section 2.3 and experimental steps taken to negate the effects of this ageing are described in the control of experiments protocol (section 5.1).

1.2.3 Topologies of piezoceramic transducers.

The most common types of topologies used for ultrasonic transducers are the Langevin type transducer and the bonded disk. Bonded disk transducers are attached directly to the base of an ultrasonic tank via an adhesive and are connected to the ultrasonic generator section via two electrodes. A single PZT disk with electrode connections is shown in figure 1.4.

Figure 1.4: Single PZT disk with electrode connectors

Single disk transducers have a voltage/strain relationship that is well documented and will be covered in depth in section 2.3 of the literature review along with investigations into the resonant characteristics of specific PZT materials used for industrial ultrasonic cleaning applications.

Langevin topologies, as shown in figure 1.5 are sometimes referred to as 'pillar' or 'sandwich' transducers and comprise of a plurality of piezoceramic rings held in tension between an end cap and a front section by a high tensile, electrically insulated bolt. Langevin transducers are capable of producing higher strain deflections that single

bonded disks and are used for high powered applications, but the characteristics of the voltage/strain relationship and the frequency response are less well defined due to the addition of the front mass and end piece as will be shown in section 2.3.

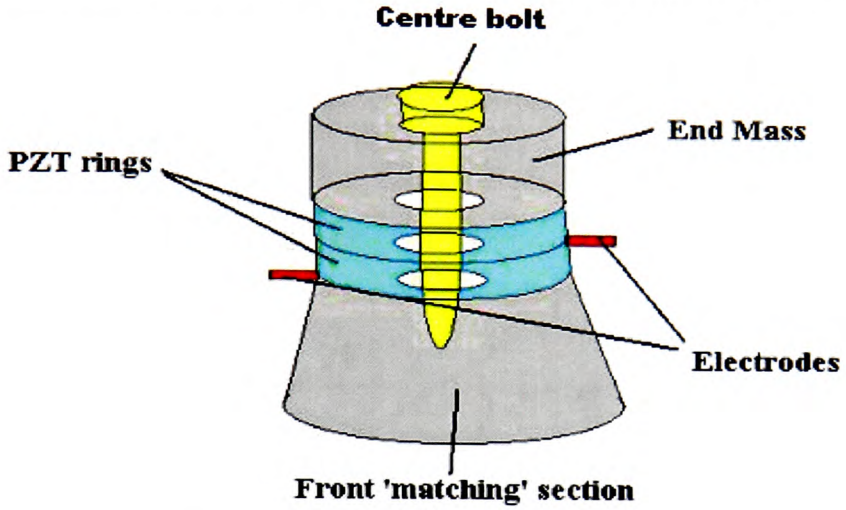

Figure 1.5: Langevin pillar type transducer

1.3 Introduction to Cavitation.

Ultrasonic vessels clean primarily through the mechanisms of cavitation. Cavitation has been studied since the 19th century due to damage caused by cavitation on ships propellers and has been described as 'The formation and instantaneous collapse of innumerable tiny voids or cavities within a liquid subjected to rapid and intense pressure changes'.[20] Cavitation can occur as a result of turbulent flow or pressure changes brought about by the action of propellers or mechanical pumps. However in ultrasonic cleaning baths, the required pressure change to induce cavitational activity is brought about by ultrasonic displacements of the PZT transducers bonded to the vessel base.

Cavitation is often referred to as 'cold boiling' due to the similarities between pressure induced cavitation and heat induced boiling. Figure 1.6 below demonstrates how cavitation can occur with the aid of a phase diagram. The liquid shown at point A is a substance under a constant pressure and temperature. Increasing the temperature of the

substance whilst keeping pressure constant results in a transition to the gaseous phase (point B). This is thermally induced boiling.

If however the liquid is kept at a constant temperature and the pressure is dropped, the transition to the gaseous phase also occurs (point C). This is the mechanism by which ultrasonically induced cavitation occurs.

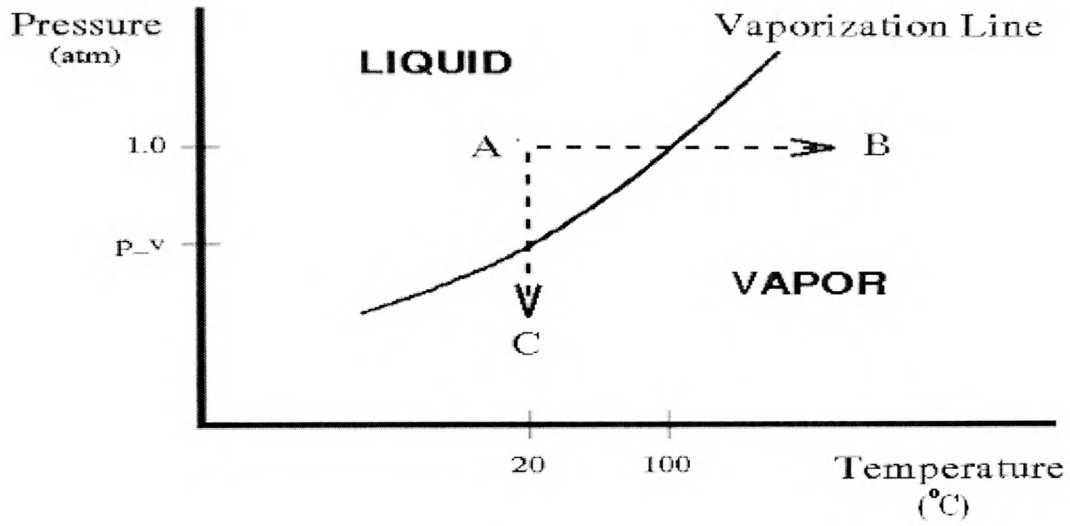

Figure 1.6: Cavitation with the aid of a phase diagram

A further explanation of the causes of cavitation states that when subject to an alternating pressure of sufficient amplitude, the molecular bonds between the molecules of liquid are stretched beyond their tensile strengths causing a void, or cavity to form. In theory, the tensile strength of water is far too high for ultrasonic cleaning systems to induce cavitation, but as noted by Moholkar *et al*[21]:

> "The theoretical pressure amplitude to cause cavitation in water is 1500 Bar. However, in practice, acoustic cavitation occurs at lower pressure amplitudes, less than 5 Bar"

This discrepancy between the theoretical value and that obtained practically can be attributed to the presence of contaminant 'weak spots' that act to lower the tensile strength of the surrounding liquid and act as seeds for cavitational inception. The value

of negative pressure amplitude that will result in ultrasonically induced cavitation is dependant on a number of variable liquid parameters and is therefore subject to variation unless experiments are tightly controlled. Thus, the nature of the liquid is a very important factor.

The collapse of these cavitations has been shown to produce extremes of heat and pressure in the locality of the void collapse with temperatures approaching 5000°C. It has also been shown that cavitational collapse is asymmetric in the vicinity of boundaries (either immersed loads or as a result of bubble-bubble interaction in cavitational clouds) and that this asymmetrical collapse creates a high pressure micro jet traveling at 100's of metres per second. These micro jets form the basis of the cleaning process by dislodging contaminants from the surfaces.

Further by-products of the effects of cavitation closely aligned to ultrasonic cleaning include:

- **Sonochemistry:** is described as driving and accelerating chemical reactions through ultrasonic energy[22] where the extremes of pressure and heat generated by cavitation are utilised to drive sonochemical reactions. Sonochemical reactions have been shown to improve some reaction times [23], create new chemical species and has been utilized in the production of nanomaterials[24].
- **Sonoluminescence:** picosecond flashes of light generated by the collapse of cavitational bubbles that fall into two categories. Initially observed in clouds of bubbles back in 1934 at the university of Cologne the phenomena of multi bubble Sonoluminescence (MBSL) was largely ignored due to difficulties in reproducibility and the complexity of expressing the bubble interactions. Renewed interest in the phenomena occurred as Gaitan *et al* succeeded in trapping a single, stable bubble in a standing wave field.[25]This form of Sonoluminescence is known as single bubble Sonoluminescence (SBSL)
- **Sonofusion:** A contentious application whereby evidence for nuclear fusion was observed by Dr Rusi Taleyarkhan using a similar device to an ultrasonic cleaner.

Sometimes referred to as 'bubble fusion', the debate about the validity of Taleyarkhan's results is ongoing[26].

Cavitation, as the primary cleaning mechanism differentiates ultrasonic cleaning from megasonic cleaning systems. Megasonic cleaning vessels, operating above the 700kHz range, are commonly utilised in highly delicate applications such as silicon wafer manufacture where the implosions of cavitational voids could damage the end product and fine particle removal is of critical importance.

1.4 Motivation for Study

It has been shown from the above that ultrasonic cleaners comprise a large sector of the high powered industrial ultrasound market. Ultrasonic cleaners are essential to a number of highly diverse industries, not least the critical cleaning of medical equipment where a clear advantage has been shown over other cleaning methodologies, especially in the processing of surgical instruments containing hinges, narrow lumens and blind holes.

Some of the reasons driving the growth of ultrasonic cleaners are the recent concerns regarding cross contamination and surgical transmission of both variant Creutzfeld Jakobs disease (VCJD) and AIDS through poor decontamination of hospital equipment and the fear of litigation this brings. A further factor in the popularity of ultrasonic cleaning is the phasing out and banning of rival solvent based cleaning methodologies due to their harmful environmental impact. This control on CFC, HCFC and 1,1,1-Trichloroethane is already in place in the UK and a number of other countries, with other jurisdictions following suit. Ultrasonic cleaning is widely regarded as the most viable alternative to these defunct solvent systems[27]. With this, the sales of ultrasonic cleaners are predicted to grow, both in the benchtop market and in the industrial cleaning market leading to competition between the existing companies for dominance of this highly lucrative business [28].

However it has also been shown that the bulk cavitating field, of ultrasonic vessels is inhomogeneous leading to 'hot spot' and 'dead zone' conditions in the cleaning field. This is wholly unacceptable, especially given the medical applications of the equipment and fears about the transmission of blood borne pathogens. Quality of cleaning is not consistent throughout an ultrasonic vessel and has been shown to relate to a complex standing wave effect that is a result of numerous factors, especially:

- The frequency of operation.
- The geometry of vessel design.
- The number and placement of transducers.
- Load carrying basket design and finally,
- The placement of cleaning items within the vessel.

Currently the design of ultrasonic vessels is conducted on a trial and error basis with no prior knowledge of the cavitational field. Assessment of the cleaning capabilities and the positions of cavitational hot spots and dead zones can only be conducted after the production of a prototype unit, which is a costly and time consuming process. Additionally the introduction of complex loads into the vessel and the cavitation effect presented to each surface of the load is unknown which leads to a high probability that areas of the immersed load may receive unequal cavitational/cleaning power.

Given the above, the ability to assess standing wave fields within ultrasonic cleaning vessels prior to prototype development would be of major advantage to industry.

Knowledge of how changes to geometry, liquid fill level and transducer placement can affect ultrasonic field coverage should lead to improved design methodologies providing, faster, safer and more energy efficient cleaning systems. Also desirable within the industry would be knowledge on how the introduction of differing loads to the liquid affect cavitational fields which includes an ability to evaluate novel designs of cleaning load holders in order to assess any possible negative effects that they may induce.

The aim of this study was to develop a system that answers many of the issues raised above through a theoretical framework mapped to practical results. The body of work will show the structured development of a design process whereby given a number of parameters, the bulk cavitating field within a given ultrasonic cleaning bath can be visualized, evaluated and compared when parameters are varied. This investigation should add a significant contribution to academic knowledge in the field by describing the design architecture developed and the strong industrial relevance by addressing shortcomings in the current body of knowledge identified.

1.5 Overview of Report

This report will aim to provide the reader with an in depth knowledge not just of the systems developed as part of this PhD proposal, but also into the necessity for the work conducted and the strong industrial relevance of the solution presented. The decisions taken in the development and evaluation of each step of the project will be presented and critically analysed allowing the reader to evaluate alternatives and follow the logical thought process utilised.

Chapter one has presented a strategic overview into some of the concepts involved in ultrasonic cleaning, and the position of ultrasonic cleaning as a large and lucrative segment of the high powered ultrasonics industry sector, together with its application to critical clean systems highlight the importance of this work under review. The basic components of ultrasonic cleaning vessels have been presented along with a brief introduction to the principle operating mechanisms of two of ultrasonic cleanings most important concepts – The Piezoelectric transducer and the cleaning mechanism of Cavitation.

Chapter two will consist of a literature review to inform the reader about the current state of the art regarding ultrasonics, with particular reference to the modeling and simulation of cavitating fields. Chapter two will also examine the methods currently employed to practically measure the effects of cavitation within ultrasonic cleaning

vessels, which will lead to a critical appraisal of the state of the art showing where deficiencies and gaps in the current knowledge exist.

Continuing on from the literature review, chapter three will state how this work aims to remedy some of the perceived deficiencies in the knowledge base and hopefully add a substantial contribution. A succinct list of aims for the project will be presented including those identified during the PhD registration process.

Details of the modeling and simulation methodology will be discussed in detail in chapter four expressing how parameters for the simulation were developed and the logical progression from initial models designed as proof of the concept, through to full 3D representations of commercially available ultrasonic cleaning baths. Chapter five will provide analysis of the practical methods used to verify the outputs from the simulations performed and a set of protocols developed to ensure consistent experimental conditions identified from the literature review.

A results section provides simulation outputs of models and model verification via comparison with the practical techniques selected. Results are presented as a progression from initial models to the more complex developments. Finally in chapter seven the results from the various test regimes are discussed. Accuracy of the simulation work under various conditions will be assessed and conclusions are drawn from the data. The relevance of the work is discussed both from an academic viewpoint and in terms of relevance to the ultrasonic industries. Discrepancies in the comparative results that have been identified will also be discussed along with possible solutions to these and future work that would be of interest.

Chapter 2: Literature review

2.0 Introduction

In order to build a solid foundation from which to progress studies, a substantive review of work already conducted in the field was undertaken. The purpose of this chapter is the review of available literature pertinent to the project and gauge the state of the art in ultrasonics, culminating in a critical appraisal of what research is lacking and therefore desirable in terms of the overall objectives of the programme.

This section will cover aspects of work conducted on general ultrasonics, such as environmental variables and wave propagation as well as specifics relating to ultrasonic cleaning such as cavitation cloud mathematics and previous attempts at modelling. It also considers the tools and techniques necessary for progress.

2.1 Environmental variables affecting cavitation

Much work has been conducted into the effects of environmental variables on the processes of ultrasonically induced cavitation. In the words of the prominent ultrasonic researcher Robert E Apfel "Know thy liquid!" [29] . The following is a non-exhaustive list of variables known to effect cavitation in ultrasonic vessels:

2.1.1 Temperature

The number and positions of cavitating zones has been shown to have a sensitive dependence on the liquid temperature[30]. A study by the NASA Langley research centre identified temperature of the liquid medium as a major factor in the effective sonication of items in an ultrasonic bath[31]. Further studies by Zeqiri *et al*[33] and Chivate and Pandit[34] confirm this finding implicating the liquid temperature as being essential in the formation of patterns of ultrasonic cavitating by affecting the speed of sound and liquid viscosity/density. Temperature in the medium is found to be controlled not solely by the temperature of the liquid introduced to the bath, or any heating system incorporated in

the vessel but also as a result of self-heating during operation. Two principle mechanisms are identified to cause this heating due to cavitation and heating caused from the diffusion of heat from the transducers' mechanical flexure.

2.1.2 Vessel Geometry and Transducer Placement.

Ultrasonic cleaning baths come in a number of shapes, depths and configurations of transducers. The geometry of an ultrasonic cleaning vessel has been shown by previous studies to alter the distribution of cavitational regions by causing standing waves set up from the primary radiated pressure wave and subsequent reflections from the boundaries.[14] [31]

Although limited, publicly available, empirical research exists on the effects of transducer placement other that truisms encountered on ultrasonic cleaning company websites, the work available shows the placement of transducers to cause variance of cavitational patterns[35]. This has been largely attributed to the directional nature of sound at higher frequencies and a treatment of this along with expected beam dispersal patterns from piston transducer sources (such as PZT transducers) is provided by Blitz[36] and Papadakis[37]. Both these sources show that the beam dispersal of ultrasound from a piston transducer in an unbounded medium is dependant upon the width of the transducer and the frequency of the source as shown in figure 2.1 and is related by the formula:

$$Sin\theta = 0.61\lambda/a \qquad \text{Eq. 2.1}$$

Where θ is the angle of the beam dispersal in degrees, "a" is the diameter of the transducer source (in metres) and lambda (in metres) is the wavelength of the ultrasonic source.

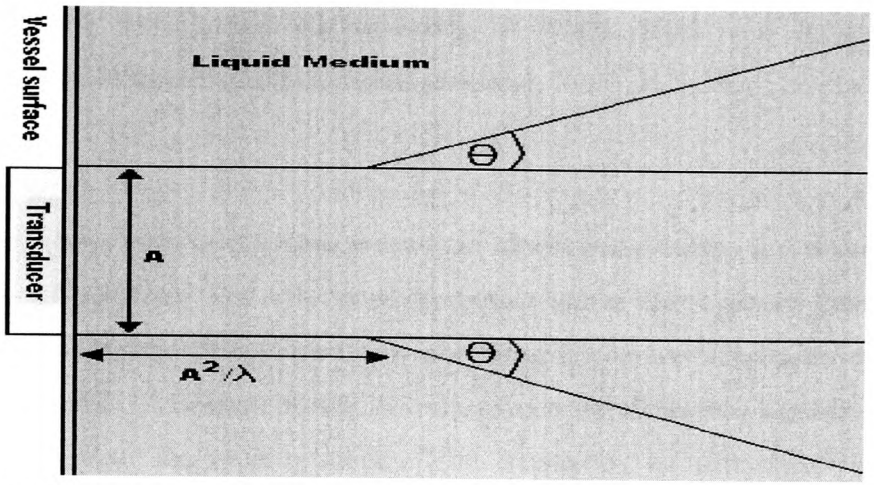

Figure 2.1: Beam divergence from an ultrasonic transducer

The variations in cavitational patterns make numerical simulation difficult. Bereziat *et al*[38] state this is a consequence of variations in incidence angles and plate geometries and that one of the main disadvantages of employing ultrasound is its geometrical limitations.

The liquid/air interface is also included here as part of the vessel geometry, forming one of the boundaries of the liquid medium[14]. Agitation of the liquid by ultrasound is found to cause a surface ripple effect that is a function of frequency, vessel geometry and liquid parameters (much like the standing waves in ultrasonic vessels). This ripple effect is shown to cause both a reflection and scattering of an ultrasonic wave rather that a neat reflection[37]. A treatment of how this will be represented in the modelling methodology with be discussed in section 2.4.

Having identified the water/air boundary as a geometrical feature in an ultrasonic vessel, note must be made of the effects of liquid depth. Generally in an ultrasonic vessel, all boundaries are fixed, all except the water/air interface which is subject to end user alteration. No significant literature was discovered during the review concerning the effects of water depth on either pressure/ cavitational profiles or locations of the bulk cavitating field. Given that the standing waves are noted, in part, to be a function of

vessel geometry, the setting and measurement of water depth will have to play a significant role in any control of experiments protocol.

2.1.3. Frequency

When examining the effects of frequency upon an ultrasonic cleaner. it is worth dividing the effects into two spheres: The effects of frequency upon the resonant characteristics of the vessel and piezo transducers and how changing frequency affects the inter-liquid properties of cavitation. As noted above, the frequency of ultrasonic agitation plays an important role in beam dispersal patterns. The frequency of ultrasound propagated within the vessel is directly proportional to the frequency of the electrical impulse supplied to the transducers. The transducers themselves display a sensitivity to frequency in their power transfer characteristics. Both disk and pillar transducers display resonant behaviour with optimum power transfer to the fluid occurring at the resonant point.

The resonant point and behaviour of a PZT disk is clearly identified in the manufacturers literature as a function of the disks geometry and chemical properties and can be easily identified or calculated[39]. The frequency response of a pillar transducer set-up is however more problematic with matching sections and front end spawning further mechanical resonant points and damping/distorting the calculated frequency response of the PZT rings. To further cloud the issue, the frequency response is also found to be partly reliant on the tension of the centre bolt of the pillar transducer[40] Thus frequency responses of disk transducer types are significantly easier to model than those of pillar assemblies.

The frequency of ultrasonic agitation also has a direct bearing on the threshold of acoustic power required to produce cavitation [36]. The amplitude of the sound/pressure waves in water is shown to diminish in intensity over distance with a proportionality relative to the frequency of the wave. Thus the acoustic power required to initiate cavitation over a distance will relate to the propagating frequency[41].

The number, radii and location of cavitation bubbles produced also shows a dependence upon the frequency of agitation[42]. A complex pressure standing wave set up within an ultrasonic vessel has been shown to be a function not only of vessel geometry, but also the frequency of the pressure source whereby it is acknowledged that only negative pressures below the threshold of cavitation will be significant to initiate cavitation, and the regions of peak negative pressure are standing wave dependant.

The relationship between bubble radius and frequency is uncovered in the literature review where Becker[43], McQueen[44] and Ziskin *et al*[45], all provide R_0=300/f as a simplified version of the derivation of equilibrium bubble radius proposed by Notting and Neppiras[46]. For practical purposes, this allows a value of 0.5uM to be substituted at the frequency range of interest and is used as such by Bretz *et al*[47] and Qi *et al*[48].

Given the dependence of bubble radius on frequency, we also find that the bubbles per unit volume (also referred to as bubble void fraction, or bubble equilibrium volume fraction) is dependant upon bubble radius and hence frequency. Qi *et al*[48] give the bubble volume fraction with equilibrium radii between an arbitrary distance R_0 and dR_0 as:

$$\beta_0 = \frac{4\pi}{3}\int_0^\infty R_0^3 f(R_0;x)\partial R_0 \qquad \text{Eq 2.2}$$

And from this they derive an attenuation coefficient per unit length for a cavitating bubbly liquid that is dependant on both speed of sound, frequency and bubble radius:

$$D = 8.69\left[\frac{2*4.2*10^{-4}}{3(2\pi)^{0.5}} - \frac{\omega_0^{\frac{3}{2}}}{c^3}\left(\overline{R_0}\omega_b\right)^2\right] dB/m \qquad \text{Eq 2.3}$$

From this equation they arrive at an attenuation coefficient of 0.02dB/cm for bubbly liquids over the frequency range of interest.

2.1.4 Liquid parameters

The parameters of the cavitating medium are also identified in the prior literature as having a direct effect on both strength and locations of cavitating fields for a given geometry. The tensile strength of the liquid has a bearing in that it is this tensile strength that the negative pressure phase of the ultrasonic wave has to overcome in order to initiate cavitation[33], [49], and [50].

The peak negative pressure required for cavitation to occur in a pure water sample has been calculated theoretically as high as 150,000kPa[21], although in practice this value is found to be significantly lower. This reduced threshold of cavitation has been attributed to the presence of contaminates in the liquid medium lowering the tensile strength and acting as nucleation sites[14], [51]. Moholokar *et al* state a practical negative pressure value for cavitational inception can be less than 500kPa due to the presence of such contaminate weak spots[21]. Indeed the energy required to form a void by mechanical application of negative pressure is provided by Or and Tuller [52] as a function of the surface tension with the equation:

$$\Delta E = 4\pi r^2 \sigma + {}^{4\pi}/_{3}\, r^3 \rho \qquad \text{Eq. 2.4}$$

A further discussion of achieved values for the cavitation threshold will be discussed in section 2.2.2.

Given the importance attributed to the liquid parameters in the literature, mention must also be made of surfactant dosing. Many ultrasonic cleaning companies recommend the addition of cleaning surfactant to the liquid medium to lower the tensile strength and viscosity and hence improve cavitational power. Due to difficulties in gauging the overall effects of adding surfactants and possible counter reactions with measurement methodologies (discussed in Chapter 4), no cleaning formulas or surfactants will be added during experimental procedures.

With the factors listed above established as having a significant effect upon cavitating systems, it is deemed necessary to provide control mechanisms during experiments in order to stabilise results and reduce a possible source of errors arising from 'environmental' variance. Full details of the control of experiments protocol (CoEP) can be found in Chapter 5 and was strictly adhered to throughout the course of investigations.

2.2 Mathematics

The literature review thus far has highlighted the effect of a number of variables in the formation of bulk cavitating fields. It has been shown that within an ultrasonic vessel, a complex standing wave will form in the pressure field as a result of environmental factors such as frequency, power, geometry and temperature. It has also been shown that in regions of the standing wave where the peak negative pressure exceeds a practical limit (the Threshold of cavitation) cavitation will occur. This section will now treat the cavitating and non-cavitating regions of the fluid as separate phases within the medium and examine some of the relationships proposed to deal with these fluid phases.

2.2.1 Linear pressure wave propagation

In those regions of the liquid medium where the peak negative pressure is not sufficient to initiate cavitation, it is proposed that standard equations for pressure wave propagation in fluids are sufficient to describe the time harmonic agitations of the fluid.

The general wave equation can be expressed as[53], [54]:

$$\nabla^2\phi - \frac{1}{c^2}\frac{\partial^2\phi}{\partial t^2} = 0 \qquad \text{Eq 2.5}$$

Where pressure (Pa)=p(x,y,z,t), c=c(x,y,z,t) and ∇^2 is the Laplacian operator

Derivations of this version of the wave equation can be found in Elmore *et al*[55] and numerous other textbooks and thus will not be repeated here. A particular case of

interest is noted in the literature where the agitating pressure wave is time harmonic (single frequency and continuous wave) such as that provided by the PZT transducers. Under such conditions it is shown that a Helmholtz solution to the pressure wave can be applied[54], [55], [56]

$$\nabla^2\phi + k^2\phi = 0 \qquad \text{Eq. 2.6}$$

Where ϕ is a time independent potential function given by $\phi = \phi_0 e^{-i\omega t}$

Etter[54] then proceeds to define the acoustic transmition loss in terms of this potential function giving the transmition loss (TL) as:

$$TL = 10Log_{10}\left[\phi^2\right]^{-1} = 20Log_{10}|\phi| \qquad \text{Eq. 2.7}$$

It has already been stated that reflections will occur from boundaries within the vessel. Ericson *et al*[57] state that the reflection coefficient of a linear pressure wave when encountering the boundary between two media with differing densities/acoustic velocities can be given by:

$$R = \frac{Z_1 - Z_2}{Z_1 + Z_2} \qquad \text{Eq. 2.8}$$

Where z is the acoustic impedance of the media.

The value of the acoustic impedance is a function of the density and speed of sound of each medium so that equation 2.8 above can be rewritten:

$$R = \frac{\rho_1 c_1 - \rho_2 c_2}{\rho_1 c_1 + \rho_2 c_2} \qquad \text{Eq. 2.9}$$

And the pressure amplitude transmition into the secondary medium if given by (1+R). A similar treatment of the reflection and transmition of sound waves at smooth boundaries is provided by Blitz[36].

A flat surface likely to produce a specular reflection is defined here as one that is flat over several acoustic wavelengths[37]. A specular reflection is assumed for simplicity, although it is acknowledged the actual reflections caused when the incident wave strikes either the stainless steel walls or the liquid/air interface are more likely to comprise a mixture of specular reflection and diffuse scattering. Potential consequences of this will be dealt with in the results discussion.

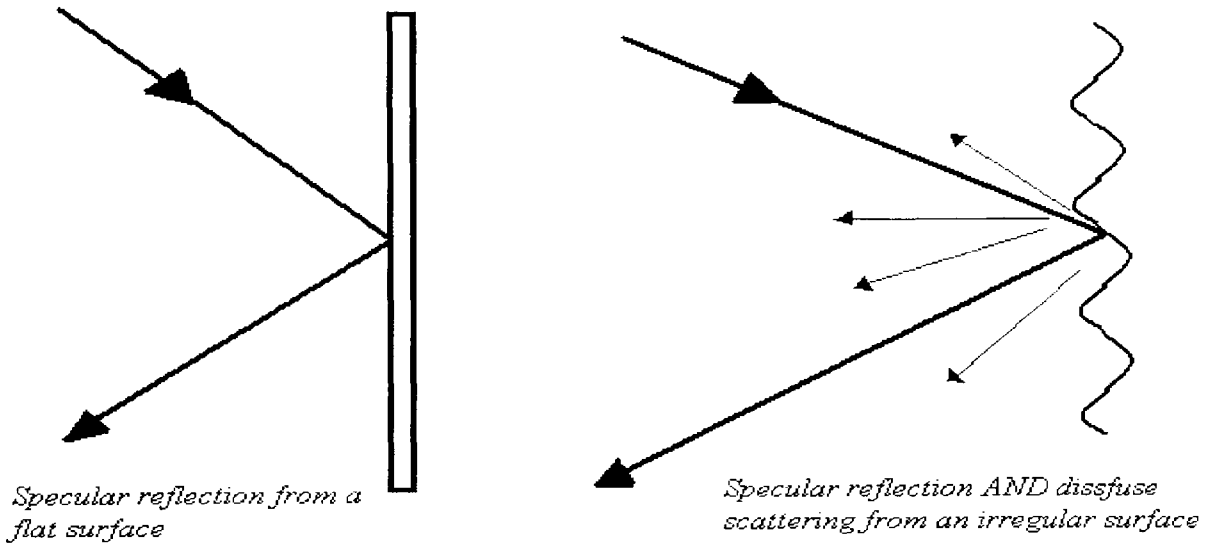

Fig 2.2. Specular reflection versus diffuse scattering

2.2.2 Bubble dynamics and effects

Although the options presented above can be used to adequately describe the propagation of pressure waves at ultrasonic frequencies, it has been noted that sufficient pressure amplitudes will induce cavitation. The values presented for the required pressure amplitude vary significantly within the literature; Kwak and Panton[58] give a theoretical value of $10x10^8$Pa for cavitation but also report practical values as low as $10x10^5$Pa as sufficient to induce cavitation whereas Moholokar *et al*[21] report $1.5x10^8$ Pa

and 500 KPa respectively for the theoretical and practical cavitation thresholds. Herbet *et al*[59] report experimentally obtained values ranging from 26MPa to 17MPa according to water temperature whereas Bretz *et al*[47] utilise a value of 50kPa as a cavitation threshold for simulation.

The wide range of values represented in the literature for the cavitation threshold is explained by a number of authors as a result of varying surface tensions, nucleation sites and liquid properties[60],[61],[62] and given the variability, some method of practical verification will be required to produce the value to be used in the simulations.

Knowing that cavitation is probable in regions of a standing wave of sufficient negative pressure, a case for introducing the non linear effects of cavitation upon the wave equation was introduced to the project at an early stage by Professor Joo Min Choi of the NPL[63]. In a review of the effects of a bubble/liquid mixture such as that produced during cavitation, Leighton *et al*[64] identify that both density and speed of sound of a bubble infused liquid mixture differ from that of a pure liquid stating a formula relating the speed of sound and density in a bubbly liquid as a function of the void fraction.

Qi *et al*[48] also derive the formula for transmition loss in terms of bubble volume fraction in a bubbly liquid. These equations are shown in equation 2.6 and 2.7 and are similar to those used by Bretz *et al*[47] as the basis of their wave equations for bubbly liquid when substituted into the wave equation (shown in equation 2.5).

2.3 Modelling Work

A review of the available academic literature shows that a number of research groups have already undertaken work in attempting to model ultrasonic wave propagation, both linear, and with cavitating systems. These range from the very basic, describing linear pressure waves in an unbounded medium, to quite sophisticated models of three dimensional cavitating representations. This section will review the work available to date highlighting both the achievements and what is deemed lacking or could be improved upon by this project.

Bechet *et al*[65] and Schechter *et al*[66] both describe the use of finite element techniques to simulate the propagation of a pressure wave through a non-cavitating field. Finite element (FE) is shown to have advantages over finite difference (FD) or finite-difference-time-domain (FDTD) in these papers due to the lower special discretisation and time steps required to produce steady state solutions and FE's ability to adjust for a generalised geometry and medium. Hughes and Harari[67] reinforce the suitability of FEM by stating its computational cost comparison to the boundary element method (BEM) is significantly lower for problems of acoustics. Nitkin *et al*[68] note that BEM is unsuitable for objects with a possible inhomogeneous interior density or a complex internal structure.

Indeed the FE method is generally presented as advantageous over other numerical simulation methods for solving complex fluid and pressure interactions as noted by a number of authors.[69]

Kirkup[56] and Elmore *et al*[55] also describe a general application of the linear wave equation in an homogenous fluid noting the suitability of the Helmholtz solutions for time harmonic applications (equation 2.6). The application of the Helmholtz solution has been shown to hold for time harmonic disturbances of the pressure field. A case is presented for the modelling of PZT disks as a time harmonic source by Huang *et al*[70] who note that a PZT disk driven by an AC voltage source whose voltage is represented by

$$V = V_0 e^{i\omega t} \quad \text{(Volts)} \qquad \text{Eq. 2.10}$$

will cause a similar time harmonic displacement in the thickness mode of oscillation. Further confirmation of this relationship can be seen in Xong *et al*[71]

Although the above describe the simulation of the wave equation with a Helmholtz solution as will be used in this project, they fail to represent ultrasonic cleaning systems

in that they do not exhibit the effects of cavitation, the boundary conditions, or dimensional scales encountered in ultrasonic cleaning vessels.

Two teams that apply the wave equation to vessels similar in operation to ultrasonic cleaning tanks are Wu *et al*[35] and a Sandia National Laboratories research team[72]. The Sandia team model pressure wave propagation at megasonic frequencies using spectral methods and Green's functions. They obtain the acoustic field by superposition of only the primary radiated and first reflected waves and investigate the effects of introducing a cleaning load in the form of a silicon wafer, noting a shadowing effect. Wu *et al*[35] also investigate at the megasonic range using a 2D model, they differ from the Sandia team however in that they define the need to represent boundary materials and note a correlation between the pressure field and the cleaning effects of megasonics. They also comment on the importance of transducer positioning in the model to provide an accurate solution, but do not go as far as to investigate the effects of altering transducer positioning.

Both Wu *et al* and the Sandia team provide valuable insights into ultrasonic modelling, but the techniques used are not wholly applicable to ultrasonic vessels due to differences in ultrasonic and megasonic agitation; namely the differences in beam spread and attenuation due to frequency and the almost negligible effects of cavitation at higher frequencies. The Sandia teams approach of only using the primary and first reflected wave, while permissible in a tank with dimensions very much greater than the acoustic wavelength, would not be suitable in most ultrasonic baths where geometries would necessitate the introduction of multiple reflections. This is especially the case in benchtop models, where the proximity of the liquid/air boundary and the vessel walls enhance the reflections of the primary radiated wave.

Harkin *et al*[73] address some of the issues in modelling bubbles by describing changes in bubble radius in relation to a time harmonic driving pressure field, but they do not develop this into a description of a bulk cavitating field. Crighton[74] expands this into a two-phase continuum model with the linear wave equation modified into a bubbly wave

equation, but despite noting how the speed of sound and fluid densities are altered, stops short of producing a model of a physical vessel.

A number of teams have approached the issue of actual ultrasonic vessel modelling using a two-phase continuum model. Olson[75], and Olson and Yang[76] do so in two dimensions, but with axis symmetric models that have limited applications as does Bretz *et al*[47] who utilise a technique very similar to the one developed by the author. Both teams introduce a continuum model, but do not further their models to higher dimensions or utilise them to investigate any ultrasound phenomena other than confirming the simulations validity.

Only one attempt at a full three dimensional model of a cavitating system was uncovered during this literature review. Dahnke and *et al*[77], [78] describe the modelling of a sonochemical reactor in two papers using time harmonic transducer agitation and assuming an ideal flat water surface. Although sonochemical reactors share many similarities with ultrasonic cleaning vessels, the power range and smaller volumes make a crucial difference to modelling outcomes. Dahnke *et al* do however use a full continuum model and describe the importance of transducer position and vessel geometry on the simulation outputs.

Although many different variations on ultrasonic vessel modelling are described above, many of these representing cavitation share the following common assumptions about the cavitation bubbles and cavitation clouds:

- A region of cavitating fluid can be treated as a continuum fluid phase.
- Bubbles are small with respect to the propagating wavelength and evenly distributed within the cavitating fluid region.
- Coalescence and fragmentation of bubbles can be ignored (i.e. there are no bubble-bubble interactions within the fluid).

These assumptions are postulated by Crighton[74], Shimada *et al*[79], Qi *et al*[48] and Bretz *et al*[47] as being sound for the mathematical description of cavitating bubble clouds. Despite the numerous models presented above, many are not capable of simulating numerically an ultrasonic bath of the kind commonly available and none are used to assess many of the factors affecting commercial ultrasonic cleaners during operation such as the effects of liquid depth, transducer placement or basket mesh.

These deficiencies in current knowledge of ultrasonic cleaner modelling will form the basis of this PhD and will be used to identify research that will add significantly to current knowledge.

2.4 Cavitation measurement techniques

Given that the models developed in this thesis will represent actual ultrasonic cleaning vessels, methods are required to assess the actual cavitating field for comparisons to the simulation outputs. This section will describe and review the methods uncovered in the literature review with regards to their suitability for this project. The types of measurement method can be broadly divided into two categories, qualitative and quantitative.

2.4.1 Qualitative

The category describes techniques that can provide a good indicator of the bulk field locations, but are generally limited in their ability to provide data on relative field strengths. One such technique is foil erosion or foil ablation testing as described by Lauterbourn *et al*[80] where cavitation erodes and pits aluminium foil samples immersed in the field. Foil erosion is an industry standard indicator even being described in the UK's Health Technical Memorandum (HTM2030)[81] as a method of assessing ultrasonic cavitation. Difficulties with the foil erosion method come from correct application of the method but has been successfully employed by Chivas and Pandit[34] and Bretz *et al*[47] to compare with simulation outputs.

A similar method to the above is the dye method described by Savazyan *et al*[82] and Watmough[83] whereby a chemical dye is introduced to the liquid, such as methylene blue, and a sheet of paper is immersed in the field. The measure of the cavitational intensity is then related to the uptake of dye to the paper. The potential drawback of this method is that the introduction of the chemical dye may affect the fluid properties outlined in section 2.1.4 hence invalidating the simulation parameters.

Further qualitative methods generally involve the removal of materials from surfaces[14] such as paint from a glass slide[80], or from actual instruments using and evaluating using a scanning electron microscope[84]. Although as qualitative as the foil technique, these methods are difficult to employ correctly due to the difficulty of precisely distributing contamination materials on the surface to be cleaned.

2.4.2 Quantitative

Most quantitative methods comprise of a form of probe measurement system. Most commercial probes use the inverse piezo-electric effect to produce a probe signal relative to cavitational implosions on the probe surface. These cavitational probes vary from manufacturer to manufacturer, but all can be broadly said to perturb the sound field by their presence in the liquid as noted by Dahnke *et al*[78].

One exception to this rule is provided by the National Physical Laboratory's (NPL) Cavimeter which was developed to be as unperturbing as possible to acoustic fields while being able to measure broadband emissions from cavitation bubble collapse. A description of the operation of the Cavimeter probes can be found in the paper titled *"Novel sensors for monitoring the occurrence of acoustic cavitation"*[85].

Through close contacts with the NPL throughout this PhD, the author was fortunate enough to have access to the Cavimeter through initial trails and secured permission to use the novel probe system for this work.

Other varieties of probe that do not utilise the inverse piezo-electric effect include those measuring sonochemical reactions caused by cavitation[86] or occasionally electrochemical effects as described by Yao *et al*[87]. Both these methods suffer the drawback of introducing chemistries to the fluid as described above.

A novel probe measurement method is described by Martin and Law[88] who note the use of a thermistor probe embedded in an ultrasound absorbing material. The rate of heating of the probe is used as an indicator of ultrasound field strength. This method however does not necessarily reflect cavitating fields as opposed to just the ultrasonic pressure field.

Some methods not easily categorised with the above include measurement of sonoluminescence, laser measurement of membrane displacement[89] and a light source synchronised photographic technique[87]. Whilst novel, all the above suffer limitations when employed to the measurement of cavitation fields in actual ultrasonic baths. Laser and photographic equipment would greatly perturb the sound field if introduced to the liquid and would not be capable of operating through the stainless steel walls of most vessels.

Having reviewed the possible measurement techniques it is acknowledged that a combination of qualitative and quantitative techniques would provide the optimum balance between bulk field overview and fine detail numerical detail. Selection criteria and the choices made for each method will be discussed in Chapter 5.

Chapter 3: Scope of Study

3.0 Scope of study

The preceding chapters clearly indicate that there exists a deficit in knowledge both in industry and academia regarding the modeling of ultrasonic vessels and in particular how certain parameters affect the bulk cavitating fields of ultrasonic cleaners [84],[90]. Although from the literature review it is clear that a large number of factors regarding ultrasonics and ultrasonic cleaners remain to be investigated, certain parameters have been identified as being of more importance than others to the ultrasonic cleaning industries by having a direct effect on the cleaning capabilities of vessels [91], [31]. These factors include the effect of vessel geometry and transducer placement on the standing wave locations (and hence cavitating field), how the depth of the liquid medium alters the cavitational field and what effects, if any, introducing a cleaning load to the liquid produces. The literature review also identified a deficit in knowledge regarding the effects of basket mesh upon the cavitating field.

This body of work will aim to address these shortcomings and add a contribution to the existing body of knowledge in a number of ways. Firstly it will aim to develop a simulation technique that can be easily applicable to commercial ultrasonic cleaners whilst avoiding many of the shortcomings in the current work identified from the literature review. Secondly it will aim to apply this simulation technique to solve some of the fundamental problems of ultrasonic vessel design and manufacture currently unanswered. Throughout the programme the rigorous testing of simulated outputs against practical verification techniques have been implemented to ensure the reliability, accuracy and industrial relevance of the work.

3.1 Modeling and simulation.

From the literature review it was shown that while attempts have been made to model the bulk cavitating field of ultrasonic vessels, many of these methodologies were impractical to industrial usage assuming idealised or unrealistic parameters such as ignoring the effect of cavitation [92] or developing axis-symmetric modeling systems [76] that would not be able to account for non-symmetric features that so often appear within ultrasonic vessels. A prime example of such a non-symmetric feature is the off centered location of drainage holes, common in larger bench-top ultrasonic cleaners and industrial units.

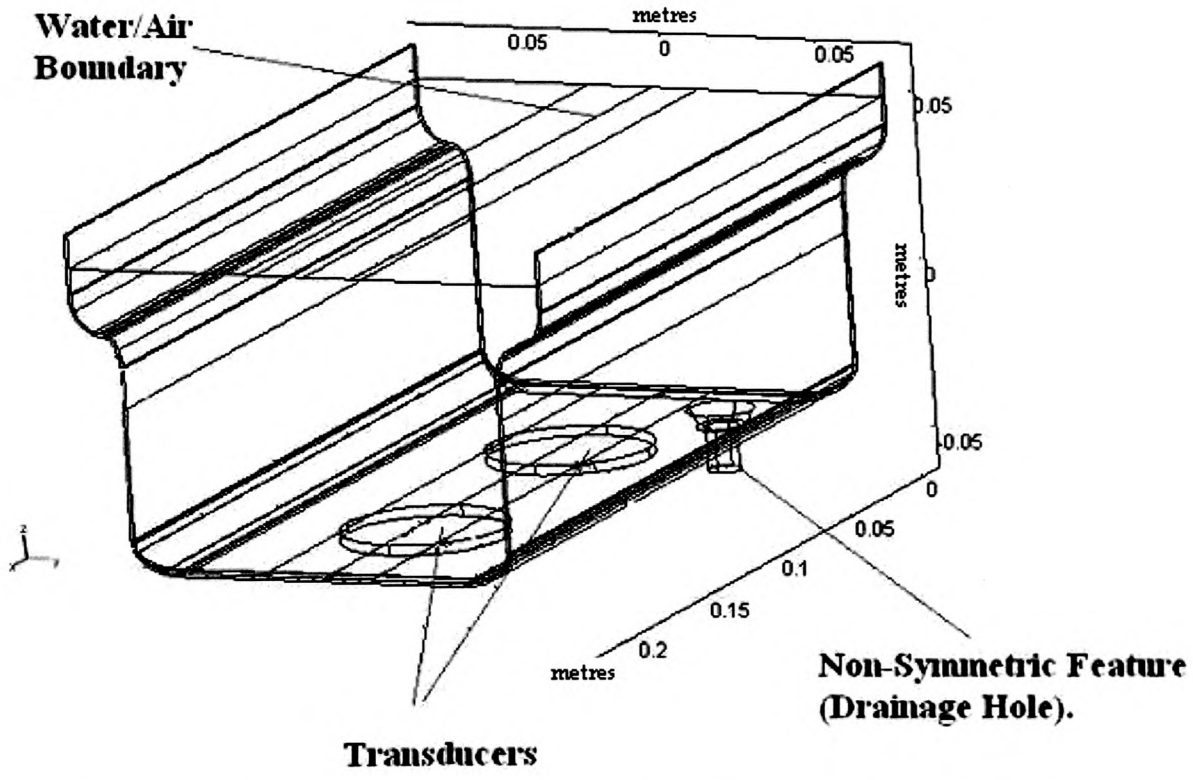

Figure 3.1: Cutaway of a sample Three-Dimensional Model Showing Non-Symmetric Feature (Drainage Hole) off vessel centre line

It was therefore proposed that a modeling and simulation methodology be developed that would be capable of simulating a whole range of vessels that were commercially

required. The model was necessarily capable of representing the time harmonic pressure field agitations of ultrasonic transducers at a range of commonly encountered frequencies whilst also taking into account reflections from the vessels geometry and the water/air interface. It has also been shown that in order to successfully model a cavitating system, the effect of wave propagation through bubbly liquids must be incorporated into the model [93] to take into account the effects of absorption and scattering of ultrasonic waves produced by the cavitating field.

Finite element modeling (FEM) techniques were identified from the literature review as most suitable for this purpose [94], [95] given the possibility of complex internal geometries within the model. Features such as work load placement and basket meshes can be more accurately represented with FEM, although it is acknowledged that FEM may experience some limitations in representing narrow geometry regions with respect to high frequency applications. This perceived limitation is due to the high computing cost theorised to be needed to accurately solve the dense meshes dictated by equation 4.1 in the chapter 4 (Finite element modeling).

The model was developed according to the spiral principle of development [96] allowing rapid prototyping and feasibility studies to be conducted on the effectiveness of the modeling techniques prior to development of a full 3D system. Incremental steps in the development of the system (as shown in figure 3.1) also allowed factors such as asymmetry and cavitation to be introduced and their effects on the accuracy of the output gauged. Initial testing of the system in two dimensions using much simplified cases will assess the effectiveness of the system and the gradual addition of features will allow for a modular testing approach.

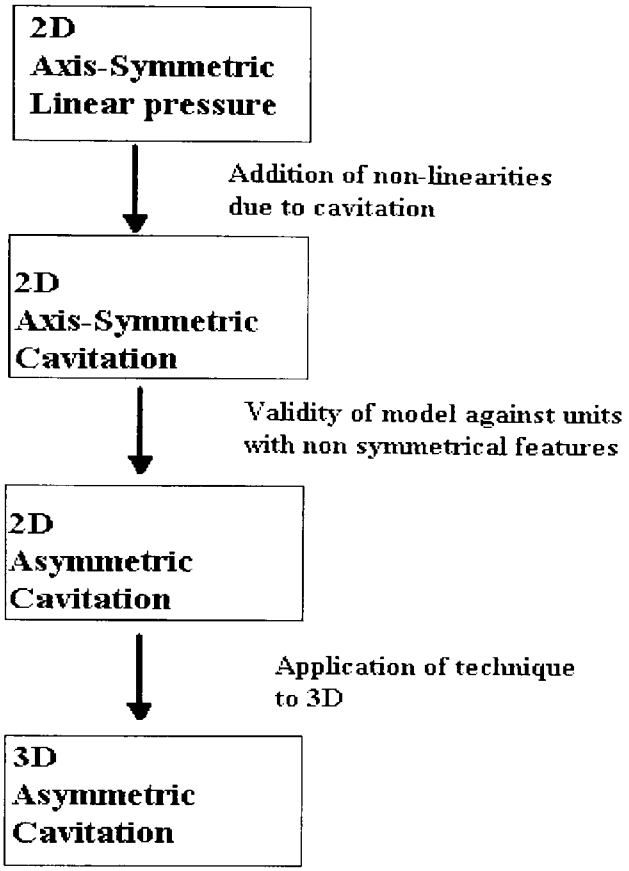

Figure 3.2: Incremental steps in the design of a full 3 dimensional model of an ultrasonic cleaner

Having developed a model that accurately predicts the bulk cavitating field of a given geometry of ultrasonic cleaner, the model will then be employed to test a number of parameters identified as of importance to the ultrasonic cleaning industry such as the effect of basket design, transducer placement and load introduction to the cavitating field. The wider a range of applications the simulation methodology can be accurately tested against, the greater the confidence in the methodology and the more useful the toolset to industry.

3.2 Testing and verification.

As noted by Mish and Mellow [96]:

"It is imperative for engineers to understand that computer problems are deterministic: They will construct a numerical solution to the problem and will generate results, regardless of whether the physical solution exists."

Given the above and the desire to tie the project to a problem of industrial relevance, methods of verifying the output of the simulation and relating those outputs to a relevant quantity are deemed highly important to this PhD. Many theses concerned with simulation make comparison against other forms of simulation [97], [98] as a benchmark of accuracy; in this body of work the outputs of the simulation will be assessed directly against the physical ultrasonic cleaning vessel model it represents. Not only will this bolster the industrial ties of the project but is also required since no firm ultrasound cavitation standard exists at present which can be utilized as a benchmarking tool (Although work currently underway by the National Physical Laboratory is attempting to address this issue)

The literature review has noted and assessed a number of possible means of indicating the cavitating field within ultrasonic baths [99], [100], [35]. The methods found tend towards one of two broad classifications, qualitative indicators and quantitative measurement systems. The qualitative, such as the foil ablation test [81] and Sarvazyan dye test [83] are shown to give a good visual indicator of the bulk cavitating field and are thus useful for developing full field maps to compare to any visual simulation output. The disadvantages perceived from the literature concern the disturbance of the pressure and hence cavitating field produced by suspending a reflective sheet within the liquid [101].

A number of diverse quantitative methods for measuring the ultrasonic field were also noted [35], [102], chiefly those that used the force generated from the collapse of the cavitating bubbles as an indicator of field strength. Methods such as laser inferometry and high speed photography were discounted as impractical due to the perturbing nature of the equipment to the sound field. Most the probe methods identified had the advantages of providing a numerical output to match against the

simulation data whilst also being less perturbing to the cavitating field than the immersion of large objects required for qualitative examination [103]. The perceived disadvantage of using such probes lay in the length of time required to obtain data points for a full field map given the unstable nature of ultrasonic cavitation with changes in temperature and dissolved gas content for example [104].

Given the relative strengths of both the qualitative and quantitative indicators of the cavitating field, the project employed methods from both. Qualitative representations of the full field were used for an initial comparison to the visual simulation outputs; this was particularly useful during the design verification stages of the project whereby rapid testing to assess changes in the simulation were desirable and also to assess the accuracy of the model in predicting the *locations* of the bulk cavitating field.

Qualitative outputs in the form of data from the chosen probe systems will be used to provide numerical data on the changing cavitational field. Although such testing would take longer than qualitative methods, it was envisaged that the data gathered would be more effective that visual indicators when assessing the effects of changing parameters on the strength of the cavitating field at given locations. Data from a probe system could also be deployed to construct field maps of the cavitating system for direct comparison with the simulated outputs.

3.3 Strategic aims of the programme

The literature review, proof of concept studies and commercial input form Ultrawave all combine to crystalise a set of programme objectives. These can be defined as follows:-

- Development of a modeling methodology using a Finite element toolset to assess the cavitational field distribution within ultrasonic cleaning vessels. This will entail evaluation and selection of appropriate modeling and simulation packages

and application of the mathematics identified in the literature review to produce an accurate representation of the cavitating field of a given geometry.

- Application of the methodology to full three dimensional representations of vessels manufactured for commercial use (i.e. without idealized parameters)
- Selection and assessment of appropriate test methodologies leading to testing and verification of the simulation outputs by means of both qualitative and quantitative means.
- Application of the modeling methodology to assess some common questions arising from industrial use of ultrasonic cleaners:
    1. What effect does changing water level have on the bulk cavitating field? Testing will consist of simulating finite decrements in the liquid level above the radiating face of the transducers and assessing the effects on both the bulk cavitating fields locations and the relative strength of the field.
    2. How does introducing a cleaning load change cavitational patterns? Does the introduction of a load alter the strength of the cavitating field or produce a shadowing effect alluded to in the literature review.
    3. Does transducer placement change the cavitating profile of the ultrasonic vessel?
    4. How does the design of cleaning load carriers (i.e. basket mesh type) affect cleaning capabilities? Baskets are the most commonly used type of load carrier in both industrial and bench-top settings yet no body of work addresses the effects of basket design or the effects of mesh type on a cavitating field.

By addressing the issues noted above, it is foreseen that the body of work undertaken will add significantly to the current knowledge concerning ultrasonically induced cavitation, both by extending the boundaries of current academic literature to encompass previously un-researched areas and assist the ultrasonic industry by providing answers to some fundamental design issues concerning ultrasonic cleaning vessels.

Chapter 4: Finite Element Modelling

4.0 Introduction

The outcome and direction of the project were well informed by the literature review which identified that a method of modelling and simulating the bulk cavitating fields of commercially available ultrasonic cleaning vessels would be desirable both to industry and add substantially to knowledge in an academic field with limited recent research. Furthermore, any modelling system developed needed to be compatible with 'realistic' ultrasonic systems, as opposed to some systems identified in the literature review which used idealised parameters. Given the aims and constraints identified for the modelling system, such as the need to solve two phase cavitating systems and possibly handle models with complex internal geometries, a finite element approach was considered most suitable.

A further aim of the project was that the modelling methodology developed be applicable within the limitations of computing power available to most industrial manufacturers of ultrasonic vessels. Ideally the system would be able to run on a widely available PC platform making it accessible to the majority of ultrasonic manufacturers.

The FEMLAB[105] finite element modelling package from COMSOL was identified above other simulation packages such as AQUABUS and ANSYS for the project. FEMLAB is a multiphysics package with model CAD, simulation and post-processing capabilities. FEMLAB was deemed a particularly suitable candidate not only due to its specialist acoustics and fluid physics packages, but also its multiphysics mode, enabling the coupling of the PDE's to reconstruct the two-phase medium and acoustic effects outlined in the literature review.

It is worth noting that comments from an external reviewer suggested that using the same package to model, solve and post process results may be seen as a weakness from a simulation perspective. However on reflection, it was decided that this approach would

be suitable for this part of the programme given that simulation results would be verified against practically obtained results from actual vessels, rather than simply comparing with previous benchmarked studies.

The following section will outline the process behind the modelling and simulation technique used, identifying not only the equations and constraints placed upon the system, but also the higher level process and consideration involved in its development.

4.1 Modelling methodology

Using FEMLAB to model ultrasonic cleaning systems allowed for the task to be divided into smaller sub-sections. Figure 4.1 shows the order of steps taken in the model development process. Geometries could either be created using FEMLAB's own CAD capabilities or International Graphics Exchange (IGES)[106] files imported from the 'Solid Works'[107] and other commercial packages. The dimensions of the models were taken directly from the ultrasonic unit to be tested (Figures 4.3 and 5.2 show the respective Y-Z and X-Z dimensions of the model); this was deemed necessary due to some process variances in the manufacture of ultrasonic cleaners that could introduce a source of error, such as off centre positioning of PZT transducers during the bonding process. Figure 4.2 shows a sample 2D geometry created within FEMLAB. Note the distinct geometrical sub domains created.

After development of a geometry, a finite element mesh was created. In order to undertake 2D modelling, the FE package supplies triangular mesh elements and for 3D modelling a tetrahedral mesh element is provided. Figure 4.2b shows the previous cross section geometry with a sub domain meshed. FEMLAB provided controls to adjust the mesh density over differing sub domains. This was important as the literature review identified the minimum mesh quality that could be used to provide accurate results was dependant upon the minimum wavelength in that material by the formula[108]:

$$Mesh_{\min} = \lambda_{\min} / 20 \qquad \text{Eq. 4.1}$$

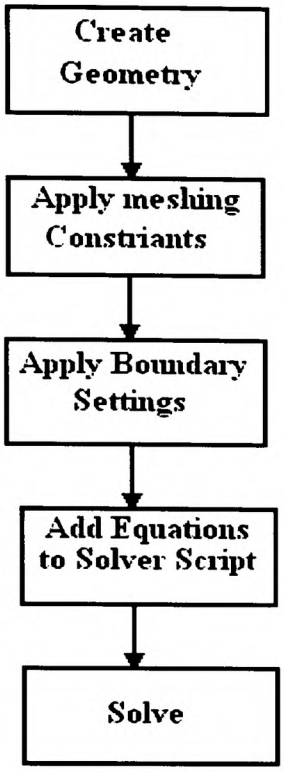

Figure 4.1: Basic modelling methodology

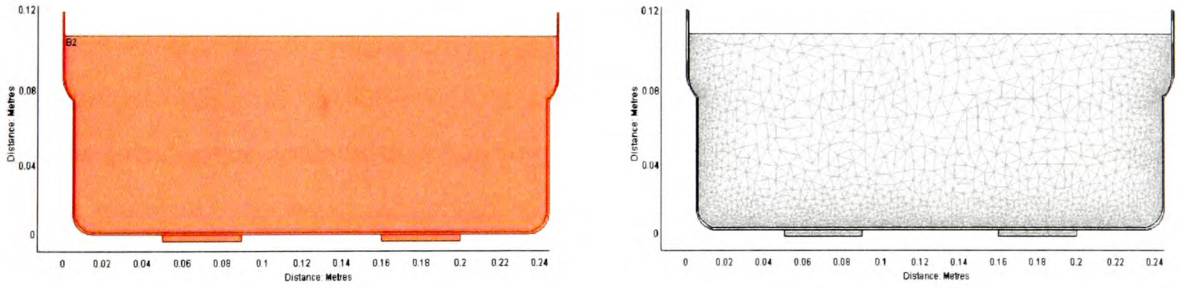

Figure 4.2a and 4.2b: A Sample 2D geometry created within FEMLAB and the same geometry showing mesh detail on a sub domain

One potential pit-fall identified with using finite element software for the task was the resolution of meshing in relatively narrow geometrical regions. The mesh density of a thin structure within a large sub domain, such as the wires of a load holding tray, would require an immensely dense mesh over the range of Ultrasonic frequencies under evaluation leading to excessive memory demands. FEMLAB provides a method of

dealing with such narrow geometries by allowing an anisotropic mesh to be specified. The net reduction in elements noted as a result of this feature varied between a 23% reduction in overall mesh elements to a 74% reduction during the meshing of thin wire sub domains encountered in section 5.3.6.

Adjusting mesh quality for different sub domains allowed the quality and accuracy of the mesh to be tailored for each material hence improving accuracy whilst keeping memory constraints manageable during the solving process. FEMLAB also allowed for manual adjustment of the mesh over precise regions within individual sub domains and this was performed in areas within the geometry where complex reflections could be expected, such as corner points, singularities and near reflective surfaces. Figure 4.2b shows the 2D slice with a section meshed according to the formula.

Once the meshing process was complete, boundary constraints were applied to the model and sub domain settings to reflect those of an actual ultrasonic vessel.

4.2 Sub domain settings

Each model was sub divided into a number of distinct sub domains. Allocating a separate sub domain to each material involved in the model allowed settings appropriate to each material's acoustic properties to be entered. Table 4.1 shows a list of materials used and the appropriate acoustic properties:

Material	Speed of sound ($m.s^{-1}$)	Density ($kg.m^{-3}$)
Water	1480	1000
Stainless steel	5970	6690
PZT	3200	7500
Air	345	1.29
Bubbly fluid	*	*

Table 4.1: Material properties of sub domains.

Note that the properties for cavitating fluid are not entered as these are frequency and pressure amplitude dependant and are therefore applied not as a sub domain, but as part of the equations set where negative pressure exceeds the cavitation threshold. All values above are taken for the materials properties at 25°C, a common temperature for benchtop ultrasonic cleaners.

These properties not only dictate the propagation of pressure waves through the medium, but also help calculate reflections and transmition of pressure at the boundaries between media.

4.3 Boundary Conditions

FEMLAB support includes a number of boundary conditions suitable for this project.

All boundaries between two media (as shown in figure 4.3) are given an 'Impedance' boundary condition, where the acoustic input impedance is calculated by the ratios of the speeds of sound (as identified within the literature review), and separately specified in table 4.1 above. This in turn is used to calculate the reflection and transmission coefficients between the media along each finite element

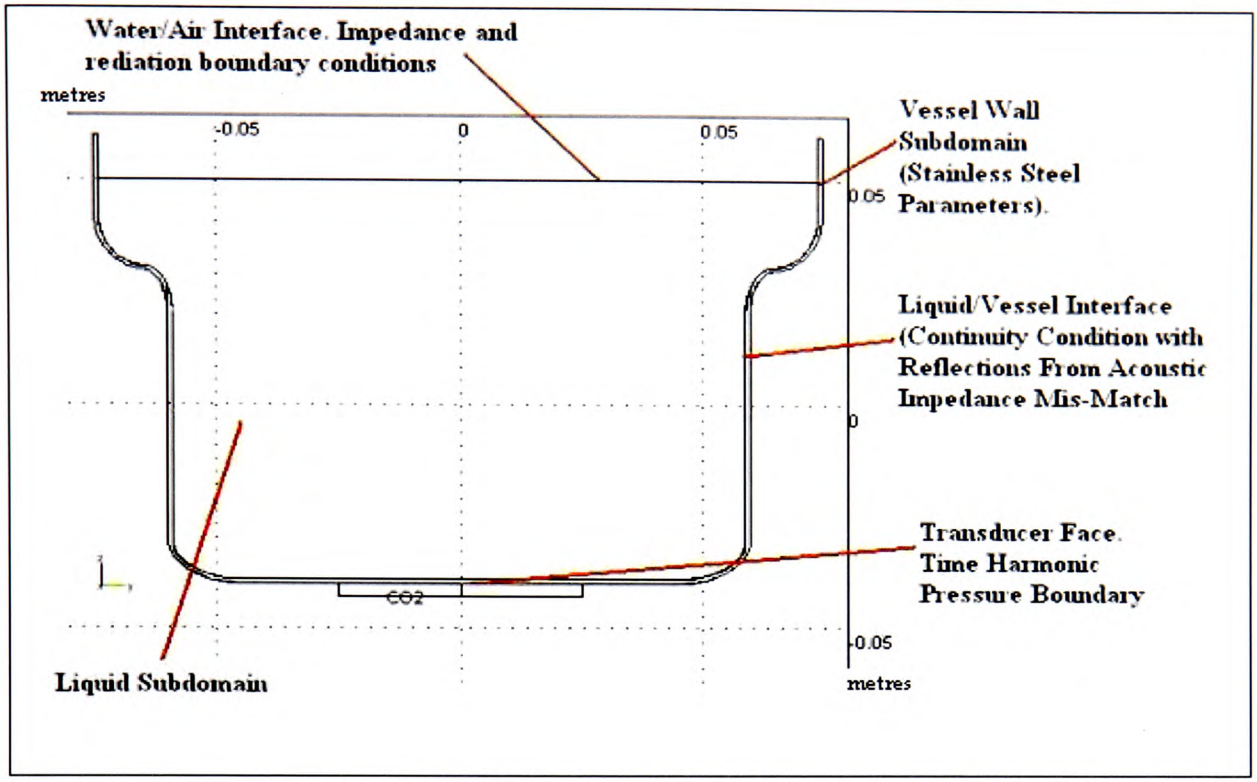

Figure 4.3 boundary conditions.

In addition to the impedance boundary condition, two further boundary conditions were used, the first of which described the vibrating source of the transducer face. As revealed in the literature review, the vibrating face of the transducer could be considered also as a number of distinct point sources that coalesce to form a united wave front at a given distance above the transducer face. However for the purposes of ultrasonic modelling, a valid assumption would be to represent the transducer face as a piston source oscillating at the driving frequency. FEMLAB simulates this by use of the pressure boundary condition, which facilitated the value of the pressure source to be entered directly along with the frequency of oscillation, which can both be determined from the PZT and generator parameters.

The final boundary condition was the radiation condition and was employed above the water/air interface and anywhere the pressure wave dispersed into an unbounded medium. The equation this used in the simulation was:

$$-n.\left(-\frac{1}{\rho_0}\nabla p+q\right)+\left(\frac{ik}{\rho_0}+\frac{R\left(\left|\bar{r}\right|\right)}{\rho_0}\right)p=\frac{\left(ik+R\left(\left|\bar{r}\right|\right)-i\left(\bar{k}.\bar{n}\right)\right)\rho_0 e^{-i\left(\bar{k}.\bar{r}\right)}}{\rho_0} \qquad \text{Eq. 4.2}$$

Where for the spherical wave case used by FEMLAB in 3D simulations:

$$R\left(\left|\bar{r}\right|\right)=1/r \qquad \text{Eq. 4.3}$$

A special case was also made for the water/air interface. In absolute terms it should be acknowledged that the water/air interface may not be a flat boundary, but rather it oscillates with ripples caused by the pressure wave disturbances. However, for the purposes of this thesis it will be treated as such, with a full discussion of the reasoning is presented in section 4.8 (Modelling trade off's and memory constraints) and is also discussed along with future improvements identified for the project in section 7.7 (Future work).

4.4 Wave propagation

The use of the linear wave equations for pressure wave propagation is well documented in the literature review and given the time harmonic source conditions of the transducer vibrations, the integrated Helmholtz solutions for both the 2D and 3D wave equations were used in the regions of the liquid where negative pressure was not sufficient to induce cavitation. The implemented pressure wave equation has the form:

$$\frac{1}{\rho_0 c^2}.\frac{\partial^2 p}{\partial t^2}+\nabla.\left(-\frac{1}{\rho_0}\nabla p+q\right)=0 \qquad \text{Eq. 4.4}$$

Given the time harmonic pressure variations of the transducer are identified as:

$$p=p_0 e^{i\omega t} \qquad \text{Eq. 4.5}$$

This reduced Equation 4.4 to the Helmholtz solution for pressure wave propagation

$$\nabla\left(-\frac{1}{\rho_0}\nabla p + q\right) - \frac{\omega^2 p}{\rho_0 c^2} = 0 \qquad \text{Eq. 4.6}$$

In those regions within the liquid medium where negative pressure was sufficient to induce cavitation, a different set of equations can be employed to define the propagation of the wave. Within these cavitating regions, both density, speed of sound and ultimately wave propagation are defined by the bubble volume fraction present. The equations governing this are derived in the literature review, but are presented here for clarity.

$$\frac{1}{c_l^2}\frac{\partial^2 p}{\partial t^2} - \nabla^2 p = \rho_l \frac{\partial^2 \beta}{\partial t^2} \qquad \text{Eq. 4.7}$$

This in turn gives rise to the attenuation coefficient for bubbly liquid in dB/cm for known frequency and bubble radii.

$$D = 8.69\left[\frac{2*4.42*10^{-4}}{3(2\pi)^{\frac{1}{2}}}.\frac{\omega_0^{3/2}}{c^3}\left(\overline{R_0}\omega_b\right)^2\right] \qquad \text{Eq. 4.8}$$

4.5 Fluid structure interactions

Throughout the programme several conflicting requirements have been set. Amongst these has been the tension between the use of idealised parameters to preserve modelling accuracy, and the introduction of certain concessions to expedite the simulation process and widen the practical use of the tool-set. The interaction between pressure waves in the fluid and the stainless steel structure of the ultrasonic vessel is one such area. The literature review revealed that an incident pressure wave upon the structure could possibly produce vibration of the structure and time harmonic deformities (depending on thickness and other properties of the vessel wall), leading to a deformation of the sound

pressure wave in that area. The simulation developed assumes a structurally rigid boundary with reflections of the incident sound wave dependant only on reflection coefficients produced by a mismatching of material densities and relative sound speeds in each media.

Although this decision is justifiable in that the small disturbance due to limited structural vibration is negligible in comparison to the radiated and reflected pressure waves, it is mentioned here both for completeness and as a source of potential variance and further improvement to be commented upon later in this thesis.

4.6 Two Dimensional versus Three Dimensional Modeling

Many of the previous attempts at modelling ultrasonic cavitational systems employ a two dimensional or two-dimensional axis symmetric approach to the simulations[76]. If the accuracy of a two dimensional model can be demonstrated, as some previous approaches have done, then what would be the motivation for a three dimensional modelling system with the increased computing requirements and additional design time?

This thesis posits that a three dimensional approach is required for the ultrasonics industry for the following reasons:

i) Two dimensional axis symmetric cases, although useful for initial proof of concept with the lowered solution time and memory constraints can only be applied to a very limited number of ultrasonic vessels such as that tested by Bretz *et al.*[47] The reality of industrial ultrasonic tank manufacture is that two-dimensional axis-symmetric vessels are a rarity and are impractical for industrial usage.

ii) Full two-dimensional cases are acceptable for demonstrating activity along the centre line of a vessel, where pressure reflections from the sides of the vessel which are not represented in the model are small or negligible. In a

vessel with a relatively large ratio between the driving sources wavelength and distance to the unrepresented vessel walls, where reflected pressure can be discounted, such as the Liga megasonic vessel, two-dimensional simulations can be used to show how the pressure wave propagates and how objects suspended in the liquid affect it.

However two-dimensional cases suffer drawbacks in that they make no predictions regarding the cavitating profile off the centre line and are unsuitable where vessels have a non-symmetric feature that is not included on the centre line of simulation, such as a drainage hole. This is highlighted in the author's own work which shows errors arising from a slightly off-centred feature when trying to predict bulk cavitating fields.[109]

The majority of benchtop and industrial ultrasonic cleaners also comprise of geometries where, due to power amplitude of the pressure wave or proximity of the non-represented geometries, reflections *will* be of significance and must therefore be represented.

A case for three dimensional simulations is thus made in that it presents significant opportunity to increase the prediction scope and accuracy of previous two dimensional attempts and is capable of representing a large range of commercially available ultrasonic vessels. Both two dimensional and axis symmetrical modelling will however play a role in this project as rapid development and proof of concept tools as discussed in chapter 3. The difference in accuracy and an appraisal of the values of two versus three dimensional modelling is presented both as a result set and in the conclusions (sections 6.2 and 7.6.2 respectively).

4.7 Data results and post processing

Having simulated the model under the aforementioned parameters, the resultant data needs to be presented in a clear, concise fashion that can be presented to a range of

audiences. The FEM modelling suite is capable of calculating a wide range of predefined quantities, such as pressure, local particle acceleration, or calculating user defined quantities from the raw data and any applied formulae. The literature review identified that the onset of cavitation is intimately linked to the maximum negative pressure attained in a region of liquid and it was also identified that several research teams have used the pressure profile of simulations as a means of representing and uncovering cavitational areas. A similar approach will be used for this project whereby the peak negative pressures achieved during the simulation will be displayed, highlighting those regions where the pressure drop is significantly sufficient to overcome the tensile strength of the liquid and produce cavitation.

The chosen FEM suite provides a number of post processing styles that can be used to graphically display results. The two modes of display identified as most suitable for this project are the line plot and slice plot facilities. The line plot can be specified between any two geometric locations (X,Y,Z) within the solved region and displays the solver data as a graphical line plot of the quantity of interest (e.g. peak negative pressures). The advantage of the line plot representation was that it provided a quantified indicator of the pressure field over a precise set of locales, e.g. the centreline above the radiating face of a transducer or for detailed examination of changing conditions in a small region when a load or basket mesh was introduced. The perceived disadvantage of the line plot was that it could only represent a very narrow region and thus could not give a full field map of the cavitating field.

For the representation of the bulk fields we utilise the slice plot facilities of the FEM tool suite were used. In two-dimensional mode the slice plot could be specified to produce a contour plot of a sub-domain, such as the pressure profile of the liquid medium or the vessel walls. In three-dimensional cases the slice was specified according to X,Y,Z coordinates and then produced a contour plot as in the 2D example. In both two and three-dimensional cases constraints could be placed on the simulation slice output to only display those regions where the literature review deemed cavitation was likely to occur (I.e. above 50kPa).

The FEM suite toolset also contained software to specify the solution at a given time and to display movie plots of the simulation over pre-defined time steps. The literature review identified that standing waves should predominate the bulk cavitating field and movie plots could thus be utilised to track the evolution of the pressure field and verify that the simulation did indeed converge to a standing wave solution.

Chapter 5: Verification and test methodologies

5.0 Verification and testing

From the outset of this project it has been posited that a strong industrial relevance should be maintained and that all simulation outputs should be tested, not against other simulated outputs or benchmark studies, but against the actual manufactured ultrasonic cleaning systems under consideration.

Studies cited in the literature review have noted that the cavitating field in ultrasonic cleaning systems exhibit a standing wave setup and that the positions of these standing waves are highly dependant on a number of design and environmental factors.

In this chapter, the procedure for the verification of the simulation outputs will be discussed along with the methods to be used, tests to be conducted and a protocol developed to stabilise the cavitating fields sufficiently to produce repeatable results during the testing cycle.

5.1 Test methodologies

A further outcome of the literature review identified two principle categories for evaluating cavitating fields, qualitative field representations and quantitative measurement techniques. During chapter three ('Scope of Study'), one of each method was selected from the literature review to incorporate into the verification routines; the foil ablation test and readings taken by an ultrasonic probe.

5.1.1 Foil ablation testing

Cavitational activity within ultrasonic baths has been shown to pit and erode foil. Use of tin foil sampling has been used throughout industry as a means of visualising patterns of cavitation within vessels and has even been adopted as a recommended test method by

the UK's Health Technical Memorandum (HTM2030)[81] on the validation of ultrasonic cleaners. Foil testing will be used in this project as a means of qualitatively assessing the cavitating field by comparing sheets of foil suspended in an ultrasonic bath to the simulation outputs showing the cavitational field along slices of the ultrasonic bath geometry.

Attempts have been noted to use foil testing quantitatively by weighing foil erosion or counting the number of pits under a microscope, but these have significant disadvantages in comparison to other quantitative methods.

Foil ablation, or foil erosion testing was performed by suspending a sheet of tinfoil cut to dimensions at the required location within the ultrasonic bath. Due to the pliant nature of tin foil, some form of securing needed to be accomplished in order to hold it secure within the pressure field. This was accomplished by preparing a cut sheet of tin foil with a thin layer of clamping plastic along the edges of the sample. This was deemed to be less perturbing to the sound field and more secure than the alternative method of clamping some weight to the base of the foil. A prepared sheet is shown in figure 5.1.

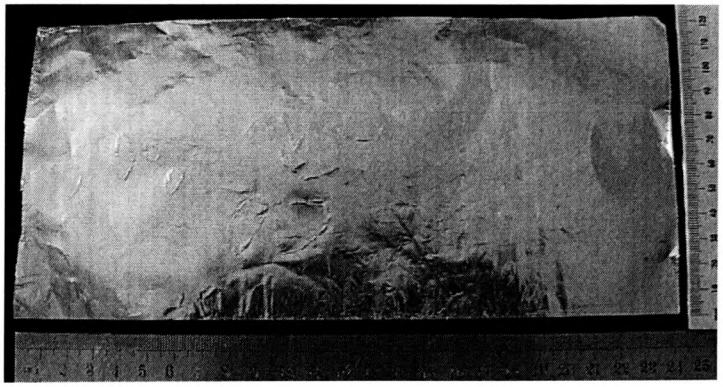

Figure 5.1: Prepared sample for foil ablation testing

The clamping mechanism also aided the positioning of the sample within the vessel and held it secure during testing. Each sheet of foil was immersed for a 3-minute period to allow sufficient erosion of the sample. The figure for the length of time to erode foil was

arrived at experimentally during initial testing. A point of note is that the addition of certain surfactants was liable to increase the erosion rate of foils and cause an effect known as 'run off' whereby foil samples would continue to erode *after* removal from the ultrasonic field unless thoroughly rinsed afterwards.

5.1.2 Ultrasonic probe testing

A number of methods for quantitatively assessing the cavitational field were reviewed, ranging from chemical species reaction rates produced as a by product of sonochemical reactions at cavitation sites to the use of fibre-optic hydrophones to measure the noise generated by cavitational collapse. From these methods a commercially available cavitation meter was chosen as a trade off between accuracy, design for purpose and ease of use.

From the available measurement system a PPB Inc[110] ultrasonic energy meter was selected. Designed for operation within the ultrasonic range, the PPB ultrasonic meter directly measures the implosion of cavitational bubbles on the surface area of the receiver providing an output display in Watts/inch^2. A metric conversion of 1W/in^2 equates to 1550J/(s*m^2).

The PPB meter also contains a number of additional features to facilitate large scale mapping of ultrasonic vessels. Table 5.1 lists some of the features of the PPB Ultrasonic probe.

Feature	Application
Operating range 0-500KHz	Operates well within the range anticipated for ultrasonic cleaning systems
Numerical energy display: Accuracy +/-0.2 Watts/Inch^2	Provides a definitive numerical output for quantitative comparisons.
Measured Frequency display: Accuracy +/-0.1kHz	Auxiliary check on operational frequency of vessel during testing

100 locations of memory storage. Data dump to PC and spreadsheet.	Expedites mapping process. Direct transfer to an application for data analysis.
Statistical data gathering. Stores Minimum, maximum, average and standard deviation values	Monitoring of stability of results by reference to deviation and peak values during testing.

Table 5.1: Features and applications of the PPB ultrasonic meter

The meter was calibrated at fortnightly intervals using a reference ultrasonic vessel. Under a set of tightly controlled conditions (Appendix 1), the probe tip was placed at fixed X,Y,Z locales within the reference vessel and a reading taken for comparison to the previous periods. The accuracy of the location of the reference ultrasonic bath was in turn tested by monitoring the voltage output from an inverse piezoelectric probe placed at that output. Appendix one shows the weekly calibration data, and it can be seen that it was consistent to an accuracy of ~ +/-6%.

Field mapping using the PPB meter was conducted by dividing the cross section of the tank under scrutiny into a series of equally sized squares in the Z,X or Z,Y planes (as shown in figure 5.2. The probe's receiver was then placed within the centre of the grid reference location and readings for the cavitational energy noted

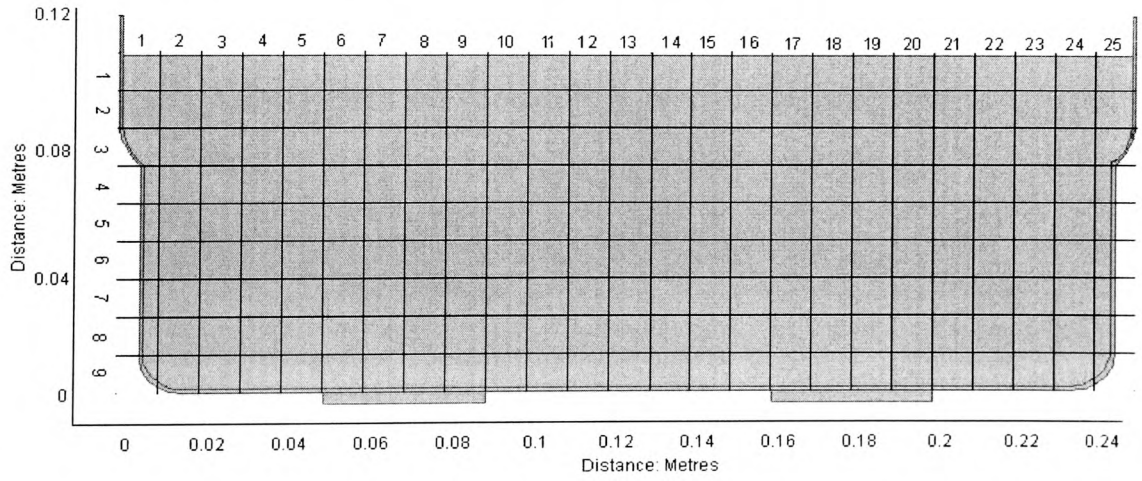

Figure 5.2: Sample division of the X,Z plane (at a fixed Y location) of an ultrasonic bath into a finite grid for field mapping.

The data received from the probe was then used to reconstruct a contour plot of a slice or test variance of regions under altered conditions. Contour plots of the data were constructed using the Minitab software tool (version 12.23).[111] Minitab was selected due to its ability to manipulate data into value banded contour plots, allowing a quantitative representation to be presented in a clear, graphical nature.

5.1.3 NPL Cavimeter

An extension of the work relating to the conducting of measurements with an ultrasonic meter was contact with the UK's National Physical Laboratory (NPL) providing an opportunity to take part in the initial trailing of the NPL Cavimeter. Permission was sought and obtained to use the new equipment as part of this PhD investigation, and to interact with the highly respected NPL team of scientists whose work appears in the literature review.[102], [103] and [112]

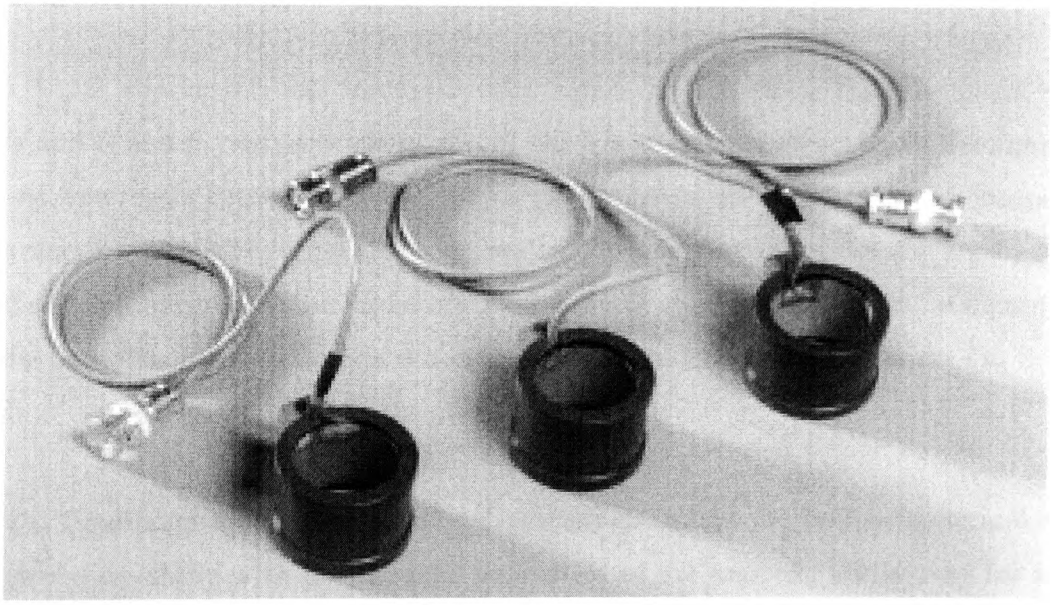

Figure 5.3: NPL Cavimeter probe receiver

The Cavimeter was designed and developed under the NPL's acoustic metrology program to provide a more reliable means of characterising the activity of ultrasonic baths by directly quantifying the cavitating field. Like the PPB ultrasonic meter, the

Cavimeter uses the inverse piezoelectric effect to convert pressure amplitude to a voltage representation, but in contrast to most commercially available cavitation probes (including the PPB meter), the NPL cavimeter measures cavitation as a function of its broadband noise spectrum rather than measuring implosion events at the driving frequency. This prevents distortion of the readings from the pressure of the radiated sound on the receiver.

The NPL meter is defined fully in two papers published in the IEEE transactions on ultrasonics, ferroelectrics and frequency control[103], [112], in which the NPL authors detail how the Cavimeter operates by integrating the broadband emissions radiated during cavitation in the MHz frequency range. The integrated broadband energy (in joules) between a given frequency range is defined in the paper as:

$$E = \int_{f1}^{f2} Vc(f)^2 \, df \qquad \text{Eq. 5.1}$$

Where Vc(f) represents the frequency dependant output from the cavitation sensor outputs and f_1 and f_2 represent respectively the lower and upper scales of the frequency range of interest (Taken from the paper as 1 MHz to 5 MHz). The rational in measurement in the MHz ranges as opposed to the fundamental of the driving frequency and subsequent harmonics lies in taking a measurement of the effects of cavitation away from the possible interference of the driving frequency of the transducers (In the kHz range).

The NPL Cavimeter also has a perceived advantage in that the hollow spherical design of the probe tip along with the acoustic properties of the material allow only for signals arising from the area under scrutiny (i.e. the centre of the probe) to register. Other probes considered for use, including the PPB meter, presented an open receiver face to the cavitating field and therefore could possibly be susceptible to noise distortion from surrounding regions.

The NPL cavimeter was used for testing as per the PPB cavitation meter, providing readout in mili-volts. Although only available in the latter stages of the project, the Cavimeter was applied to the same test scenarios as the PPB meter and used as a further indicator of the accuracy of the results both from the PPB meter and the simulation outputs.

5.2 Equipment Arrangement

A block diagram of a typical ultrasonic cleaner is shown in figure 5.4 below:

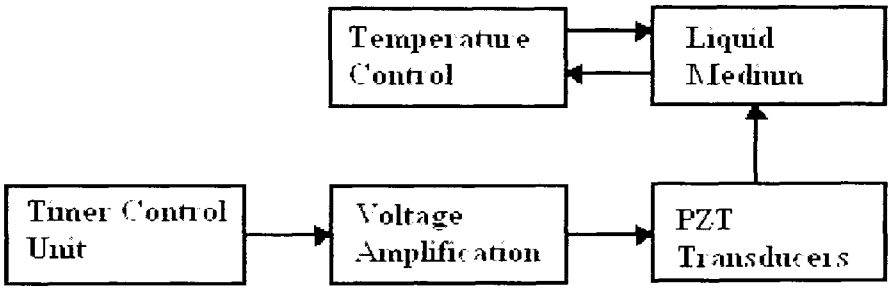

Figure 5.4: Typical ultrasonic cleaner equipment set-up.

As part of the manufactured benchtop units of the sponsoring company used for the experiments, the frequency control was accomplished by an oscillator circuit with a resistor-capacitor (RC) network used to set timing. Adjustment of the frequency was performed by means of a potentiometer in parallel to the resistor in the timer network.

The square wave output of the timer circuit was then fed to a voltage amplification circuit via two field effect transistors (FET's) to produce voltage amplification to the required level to drive the piezo-ceramic transducers into the liquid load, thereby producing cavitation. Although adequate for cleaning purposes where small variations in power/frequency would not be noticed in the bulk cavitating field of a cleaning cycle, the inbuilt circuitry was deemed unsuitable for test purposes due to the following points:

1. The RC based timer of the frequency control circuit was not deemed stable enough to drive the amplification unit. The poor selectivity of the potentiometer coupled with an observed tendency to drift over small time and temperature

ranges meant that the frequency of the output signal to the transducers could shift significantly over the time and temperature ranges used in testing. This is important as it was previously noted that changes in the driving frequency would result in an alteration in the complex standing wave set-up, as highlighted in the literature review.

2. The piezo ceramic transducers, especially the disk varieties, show a highly selective resonant behaviour in their power transfer characteristics. Small drifts in the frequency from the timer control unit could result in a large difference in power transfer to the vessel. The power/frequency curve shown below is for a single unbonded piezo-ceramic disk and shows how a frequency drift of just 0.3 kHz from the central resonant point can result on a power drop of +/-3dB.

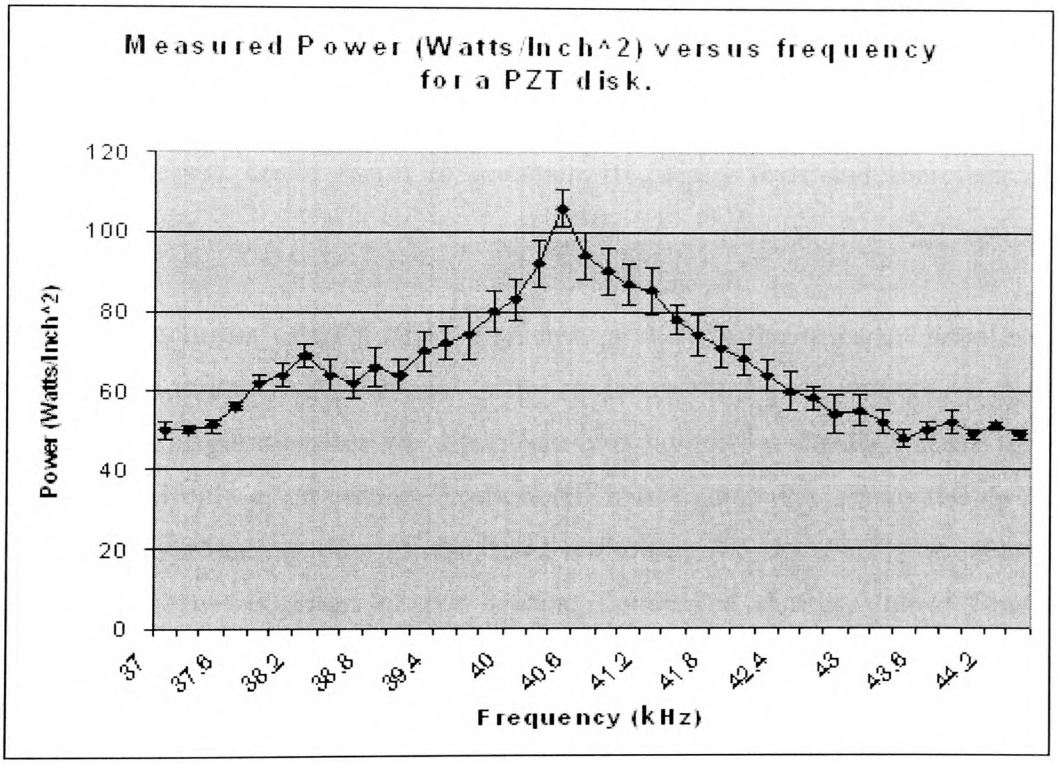

Figure 5.5: frequency/power curve of a single piezo-ceramic disk (data from tests for sponsoring company.)

3. The manufacturers of the piezoceramic disks used by the sponsoring company note a shifting of the materials resonant peak characteristics over time. This was due to the aging and partial de-polarisation of the material resulting in decay in

the capacitance of the disk. The relationship between the intrinsic capacitance of the PZT disk and its frequency of operation is given by:

$$f_r = \frac{N_t}{t} \qquad \text{EQ 5.2}$$

Where 'f_r' is the resonant frequency (kHz), 'N_t' is a constant provided by the manufacturers for a given PZT composite and 't' is the thickness cut of the piezoceramic disk (Metres).

This ageing is an exponential decay after the manufacturing process decreasing by -3.4% per decade[39]. Bonding of the transducers to the vessel at temperatures close to the materials half curie point (90°C) could cause a repolarisation of the crystals resulting in a resetting of the capacitive characteristics of the PZT. Although remote, there is still a possibility that using a tank shortly after the bonding process could result in resonant frequency drift and therefore affect power transfer.

4. The manufacturers of PZT disks also note a shift in the resonant behaviour of disks due to temperature variance in the environmental surroundings. A standard company configuration for the ultrasonic unit layout has the PZT disks directly above the circuit in an enclosed, uncooled metal surround, where the circuit is prone to overheating due to the hard switching of the FET's at ultrasonic frequencies. Investigation of the heating conducted during studies found an exponential heating rise per minute in the cavitating medium (Appendix 3). Heating of the disks could also occur as a result of continuous operation and convection from the self heating of the liquid medium.

Taking the above points into consideration, the revised experimental set up is shown below:

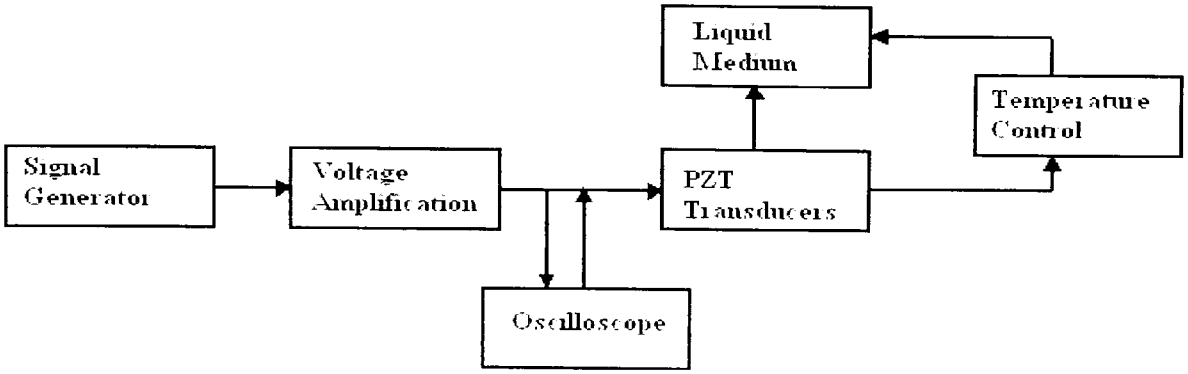

Figure 5.6: Revised experimental test equipment set-up

It is worth noting that many benchtop and industrial ultrasonic baths come equipped with heater pads bonded to the walls of the vessel. These were not used during experimentation as the heater pad bonding process added an asymmetric stiffness to the vessel walls and the inbuilt temperature monitoring systems were not sufficiently accurate for the purpose (The displayed temperature on the units with such monitoring facilities was found to be accurate only to within +/-3°C of the liquid temperature when compared with independent monitoring of the liquid temperature).

As an alternative to the supplied heater pads, models without heater pads attached were preferred and liquid for experimentation was heated by external means to the desired temperature before experimentation. Liquid temperature during the experiments was monitored both before and after with a digital thermometer (accuracy +/-0.5°C) to ensure the liquid temperature remained within the parameters outlined in the CoEP (Chapter 5.4). The temperature of the PZT disks was maintained during each experiment by means of a forced air cooling beneath the support structure.

5.3 Testing regime

The nature of this programme of work emphasised a desire to stress an industrial relevance and had a philosophy of testing the model against as many experimental

parameters as possible, thereby validating the model and contributing to an improved understanding of Ultrasonics. This necessitated that a large number of experiments be performed with the arrangement described above and in strict accordance with the CoEP outlined in Chapter 5.4. This sub section will detail the experiments performed and the applicable methodology in the same sequence as presented in the results section. The desired aim of each test has been outlined noting where each test will add to the existing body of knowledge and hopefully show how experiments were constructed in complexity from simple proof of concept to fully-fledged simulations.

5.3.1 Two-Dimensional Axis Symmetric Model

This simulation entailed the modelling of a single disk, geometrically symmetric model with a depth of 0.09m and a width of 0.08m as shown in fig.5.7. The sub domain and boundary settings are as described in sections 4.2 and 4.3 respectively but with a symmetry boundary along the line shown in figure 5.7.

The rationale for this was that a simplified geometry and simulation technique could be chosen for initial proof of concept, as the relatively small geometry and single transducer tank allow fewer chances of experimental variance to occur. The axis-symmetric modelling mode was employed due to the suitability of the vessel geometry for rapid prototyping and testing the viability of the simulation.

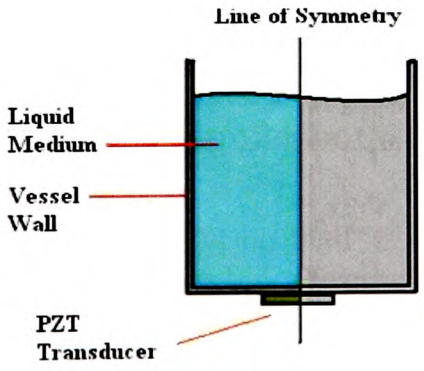

Figure 5.7: 2D axis-symmetric vessel

In order to undertake, the simulation and validate a 2D surface plot of the centreline in the liquid medium was produced and comparisons drawn to both the foil erosion and probe readings.

The desired outcome of the experiment would then be used to assess the simulation concept accuracy against a simple model. Detailed analyses of the results would inform if the simulation technique required structural alteration, fine tuning of parameters, or can progress to more complex vessel geometries. The results of this experiment are shown in section 6.1.

5.3.2 2D versus 3D modelling for non-axis symmetric cases

In this arrangement a 2D centreline plot of a less symmetric geometry than the prior arrangement could be compared to the centre line plot of the same model constructed in full 3D.

The aim of this simulation would be to assess the need for full 3D modelling or whether 2D modelling is sufficient in this context.

Comparisons of the centreline plot of both the 2D and 3D cases with each other and with, foil ablation and probe data from the actual vessel would be facilitated. Causes of variation or discrepancies, if any, would allow model feedback to occur. Results of this experiment are shown in section 6.2 with conclusions drawn in section 7.6.2.

5.3.3 Effects of liquid level upon the bulk cavitating field

Effects of reducing the height of the liquid medium in preset quantities on both the locations of cavitational activity and its relative strength would be investigated.

Consideration of the review of academic publications on this field and on industrial websites indicated the role of liquid level in the formation of cavitation is at best poorly

understood and at worst completely neglected. This was a significant area and opportunity for adding knowledge

Using both the simulation and practical measurements, the effect of lowering the baths liquid fill level would be noted. Liquid level, as measured from the radiating face of the base of the bath to the fill level would be reduced from 3λ max to 1.5λ min in decrements of 0.5λ. The maximum and minimum fill levels would be dictated by the vessel geometry whereas the decision to lower the fill level at 1/2λ intervals was deemed most likely to produce information of value given the theoretical standing wave set-up occurs at λ/2 intervals.

The intended outcome would be to produce significant results addressing the gap is ultrasonics/cavitation literature regarding the role of liquid level. It would address the importance of whether the function of depth/strength would be negligible or whether there would be a need for the ultrasonics industry to factor in maximum, minimum and optimum fill levels when considering the physical design of vessel geometries. Results are presented in section 6.3.

5.3.4 Introduction of a free suspended load to the cavitating medium

Ultimately, ultrasonic baths should be designed to clean items suspended in the liquid medium, within the practical engineering constraints of the best available science and quantitative models available. This set of experiments would compare the cavitating field of an unloaded system to one with a pre-selected load introduced.

Given the stated primary function of an ultrasonic cleaner, it was of concern that very little literature exists regarding the effect of introducing a solid load to the cavitational field. Much extant literature was often found to be contradictory or unsupported by empirical evidence. Knowledge of how and whether this does indeed affect cavitation would be of utmost importance to industry, especially given observed the end user

tendency to overfill baskets, and manufacturer's design of basket holders to facilitate stacking.

Foil erosion testing would be of limited use in this set of tests due to the difficulty of securing a foil sample above the load, therefore probes would be utilised both to conduct comparative field maps and line plots of regions of interest (i.e. the regions above the newly introduced load). It was considered that the load should consist of a rectangular aluminium block of dimensions 0.16m*0.10m*0.01m (Length, Width and Depth). Aluminium was chosen as it is representative of a common material cleaned in ultrasonic baths. The shape of the block would be random as the items placed in ultrasonic cleaners would have disparate geometries, but the flat, rectangular block was deemed likely to produce a worst-case scenario in terms of shadowing of ultrasonic activity.

The outcome would be to critically evaluate the impact, if any; the introduction of a cleaning load may have on the ultrasonic field in terms of possible shadowing or scattering of the field above the object. The relevance of the results (shown in section 6.4) would be applicable to the loading protocol for ultrasonic cleaners, particularly in cases where overloading and multiple stacked trays were commonplace.

5.3.5 Positioning of bonded transducers on an ultrasonic bath

The introduction to this thesis noted that the most common configuration for an ultrasonic benchtop bath is with its transducers bonded to the base of the vessel. Following on from the prior investigations further tests would examine the effect of alternative configurations of transducer placement on the cavitating field.

This evaluation emanated from the research conducted, the literature review and investigations within the sponsoring company. It is evident that the positions of transducers on the base of the vessel is wholly random and is adhered to not because of any empirical research in the field, but through maintenance of manufacturing status

quo. An investigation into possible alternate transducer bonding patterns could provide industry with improved cleaning results and would add to academic knowledge by defining transducer placement in ultrasonic baths as a possible critical factor to be further investigated.

The approach would allow for three topographies of transducer placement to be investigated. More would be desirable but the cost and experimental nature of producing and bonding many vessels is prohibitive. The three topographies considered of highest interest are listed below.

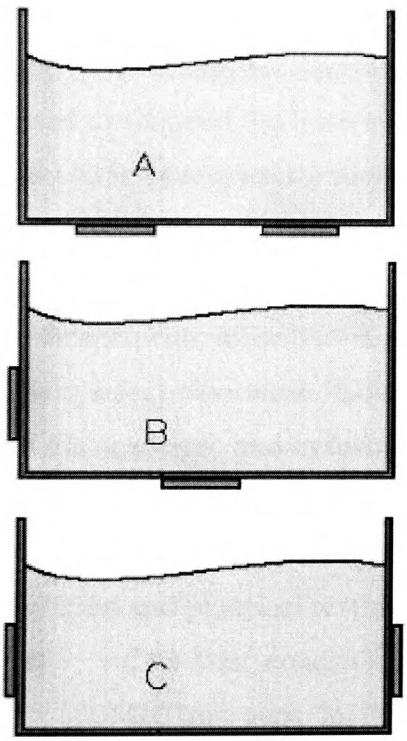

Type A is the standard configuration on an ultrasonic bath. Both transducers are placed at the base of the vessel radiating towards the base of any cleaning load. This raises the possibility of obstruction of the propagating pressure wave by any object suspended directly above the transducers.

In configuration B, a single transducer will radiate towards the base of the load and a second is bonded to the side of the vessel. This configuration may theoretically allow simultaneous radiation of the base, sides and top of the vessel.

Figure 5.8: Alternative configurations of ultrasonic transducer bonding

The final configuration has both PZT disks bonded to the sides of the vessel and no coverage of the base. This method may prove advantageous with long narrow workloads suspended in the bath such as the aluminium test block.

The goal would be to assess the configuration of transducer bonding in relation to cavitational field locations and strengths. Although limited in scope by the small number of tests, the results of these experiments (Section 6.5) will provide an insight into whether the issue of transducer location would be of significant industrial relevance and will provide a base for future academic research.

5.3.6 Effects of basket mesh design on bulk cavitating fields

Unlike in the previous examples of a load freely suspended in an ultrasonic vessel, in the majority of examples encountered during the literature review a basket or tray was utilised to suspend the load in the cavitating field. This batch of experimental procedures would attempt to identify the role of basket design on the cavitating field.

The rationale is based on the ubiquity of baskets in ultrasonic cleaning and, no significant prior information was uncovered during the literature review on how load carriers affect cavitation. Knowledge of the effects produced would add significantly to both the academic and industrial understanding of the issues.

The procedure would incorporate two types of basket mesh to be assessed both by simulation and practical testing.

i) The first consisting of a wire mesh grid with 0.001m diameter wiring and $0.01m^2$ gaps in the mesh as shown in figure 5.9a. This was the standard arrangement used by the sponsoring company.

ii) The third basket would be less common for industrial usage, but has applications in the medical fields. The basket consisted of a flat sheet of stainless steel with circular holes of 0.005m diameter, punched at intervals of 0.02m as shown in figure 5.9b.

Both mesh types will be simulated and compared to experimental results gained from probe testing as shown in section 6.6.

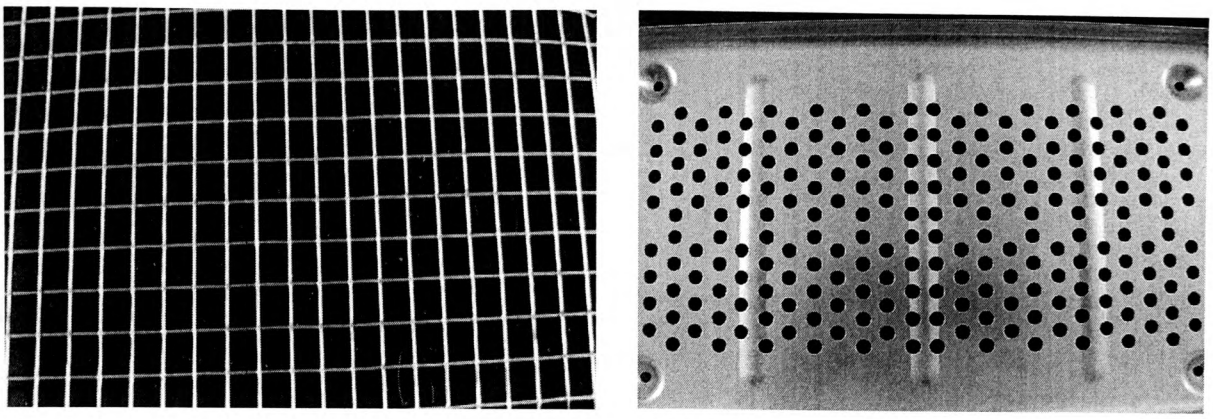

Figure 5.9: 'open mesh' and 'punched hole' basket varieties used as load carriers for immersion in ultrasonic cleaning vessels.

The aim of this part of the work would be to uncover the effects of basket design and ramifications for industry. The examining of these two distinct meshes would indicate the suitability of each and provide information that could be used in the future design consideration of basket meshes. As no prior information was uncovered in this field, the results gained will add significantly to the academic body of knowledge and feed directly into a design methodology process.

5.4 Control of experiments protocol

The literature review identified that the cavitating field in an ultrasonic cleaner was subject to fluctuations both in field strength and location based on a number of variables. The results of varying many of these parameters, such as liquid level and transducer placement form an integral part this thesis. Variation in other parameters that affect the bulk cavitating field could cause an adverse change leading to a skewing of practical result data. These considerations lead to a protocol being devised to stabilise as many undesirable variables as possible during testing and was adhered to during all experiments.

The list of potential sources of error during experimentation may be broadly categorised as instability in the liquid medium, variances introduced by the surrounding

environment, issues induced by measurement methods and instability in the equipment and drive electronics.

5.4.1 Liquid medium controls

I. The depth of the liquid medium is to be set according to the parameters of the simulation for the type of vessel modelled. Liquid depth is set measured by a suspended ruler along the centreline of the tank with an accuracy of +/-0.5mm

II. Tap water was most commonly used as the liquid medium within ultrasonic cleaning baths[33]. In keeping with the industrial relevance of this project, simulations have been performed using the properties of tap water and testing is conducted as such. Since dissolved gas content was revealed in the literature review as having a significant effect on cavitating liquids, each solution used for test purposes was degassed for a period of three minutes prior to experimentation to allow dissolved gas to coalesce and disperse from the liquid.

III. No Chemical surfactant/additive was introduced to the liquid medium during experimental procedures.

IV. The temperature of the fluid would affect the pressure wave propagation in the medium and also the negative pressures required for cavitation to initiate. In the simulation, parameters were specified for water at 25°C. Temperature in the bath was measured by means of a digital thermometer with an accuracy of +/-0.5°C. Temperatures were taken at the start at end of each experimental run with a variation of +/-2°C permitted. Appendix Three and Appendix Four provide justification for this value of +/-2°C given the variation of the strength of cavitation with heating of the liquid medium. Any readings out of this scale result in a void experimental run.

5.4.2 Environmental controls

I. Both the ultrasonic bath and test measurement placement systems should be mounted on a smooth surface without any slope.. Similarly the mounting of the probe/foil samples should be undertaken such that the probe receiver and foil sample would be suspended in the vessel at 90° to the normal of the water surface.

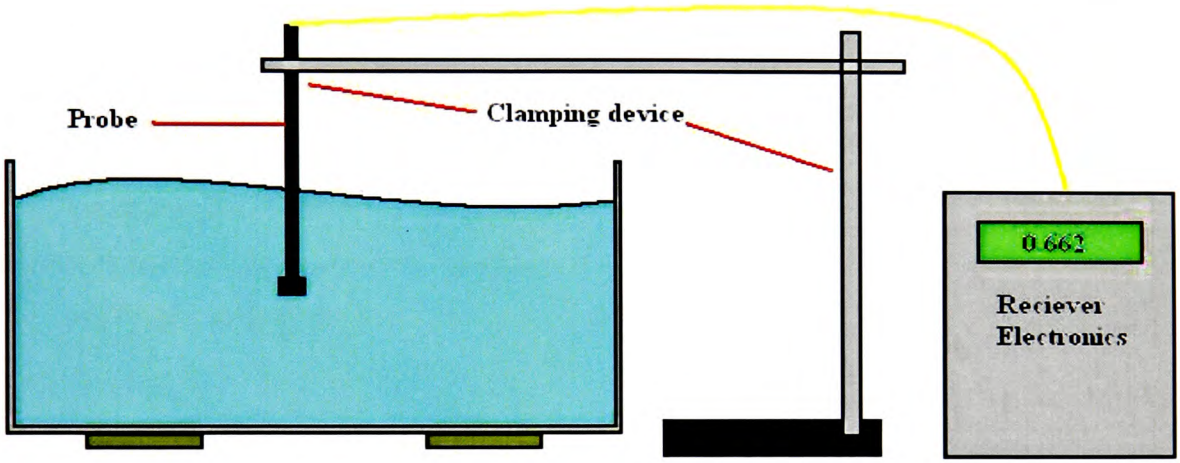

Figure 5.10: Probe clamped and suspended at 90° to the normal of the liquid surface.

II. The test equipment should be mounted away from any strong sources of external vibration that could cause displacement of the tank sides or water.

III. The literature review noted that free floating contaminants in the liquid medium lower the tensile strength of water facilitating cavitation by acting as nucleation sites. To this end the vessel under test was rinsed and cloth cleaned prior to each test.

5.4.3 Test measurement controls

I. Given the unstable nature of the cavitating fields and fluctuations in the field strengths, a method of time averaging the cavitational values to reduce the effects of sudden spikes in energy was employed. The PPB meter contained an internal method of time averaging the results, displaying an averaged value, standard deviation from that value and local maxima and minima for the location. The NPL probe, although providing a 3 second rolling point average of data values, was still susceptible to the influence of cavitational spikes. therefore the output of the probe was also averaged over three readings to normalise the data values.

II. Probes were clamped into position as shown in figure 5.10 within a jig to ensure accuracy of position within the bath and to prevent movement of the probe during measurement of the cavitating field.

III. Foil sheets were similarly clamped within the vessel to secure location and position within the ultrasonic vessel.

Chapter 6: Results

6.0 Introduction

The results presented in this chapter depict the simulation, probe and foil test data obtained from the experiments detailed in the chapter 5. The simulations were performed as indicated in chapter 4 and built sequentially into models of increasing computing and geometrical complexity, ranging from a two dimensional axis-symmetric case to the highly complex models containing thin mesh structures used to represent baskets as commonly used in ultrasonic cleaners.

The first images presented for each set of results show the simulation outputs from the various models, highlighting the peak negative pressures present in the liquid during time harmonic agitation by the piezo electric transducers. Having identified and selected a suitable cavitation threshold pressure form a variable range of values in the literature review, 40kPa is used in the simulation outputs as a cut off point for demonstration of pressures, allowing only those regions above the threshold of cavitation to be shown in the graphical output. The results are presented along the centre lines of the vessel and they represent the most dramatic and conclusive results from each case, allowing the regions directly above the transducers case to be examined.

Each simulation was tested over a number of time steps using the FEM simulation packages time solver capabilities. A time step of $6.25*10^{-6}$ seconds was used allowing four outputs per cycle at 40kHz to be tested over a period of several seconds. This time stepping of the result verified the output of the simulations and lead to a standing wave steady state as identified from the literature review. A negligible distortion of the pressure field was noted during the time stepping and therefore the results in this chapter reasonably represent a static standing wave in the pressure field and this should be reflected in the practical test outputs.

The first practical results presented are the foil ablation tests, which were identified from the literature review as commonplace for Ultrasonic bath testing. The foil samples were compared against the simulation outputs for the number, position and sizes of erosion caused by the cavitating field. To assist the comparison the output of the simulations and the foil samples, they are presented with both images overlaid for each test scenario. This overlaid image will be the second result image in each test grouping.

Although foil sampling can present a visual representation of the cavitating field, it provides no quantitative representation. To assess the numeric strength of the field at locations within the ultrasonic bath, it was determined that a probe capable of reading the cavitating field should be utilised. To this end the third set of results presented are the data outputs from the PPB cavitation meter.

The PPB meter was used to develop a contour plot of the cavitational field as described in chapter 5.1.2. The PPB meter was partly chosen due to its capability of storing a time averaged value of the results from a given location, thereby negating small fluctuations in the cavitating field (See Appendix 1). The raw data output of the probe, although useful for some point comparisons to the simulation outputs, was unsuitable for presenting an overall image of the cavitating field. To assemble the probe output into a more manageable form the data values were processed using the Minitab spreadsheet program (REF). Coloured contour plots of the values were then created by dividing the absolute range of values encountered into ten data ranges and assigning each a separate colour within the Minitab program.

Additionally, co-operative research links had been developed with the UK National Physical Laboratory (NPL), which resulted in an opportunity to test the new prototype NPL 'Cavimeter' towards the end of the research period with the industrial sponsoring company and permission was granted to use the Cavimeter to provide additional experimental results for this PhD.

The PPB and NPL probe results are presented respectively as the fifth and sixth results in each test scenario and can be compared directly to both the simulation and foil results by number, position, size, strength and location of the regions of cavitation.

6.1 Two Dimensional Axial-Symmetry

The axial-symmetry test case was performed on a single transducer, axially symmetric vessel operating at 40kHz. Due to the nature of the axial symmetric mode of simulation, only one half the simulation was produced under the assumption that the right hand side of the simulation will be identical to the left hand side (shown in figure 6.1 below). The corresponding reduction in computing power required and practical implications of this mode of modelling will be discussed in the conclusions.

6.1.1 Two Dimensional Axial-Symmetric Simulation Output

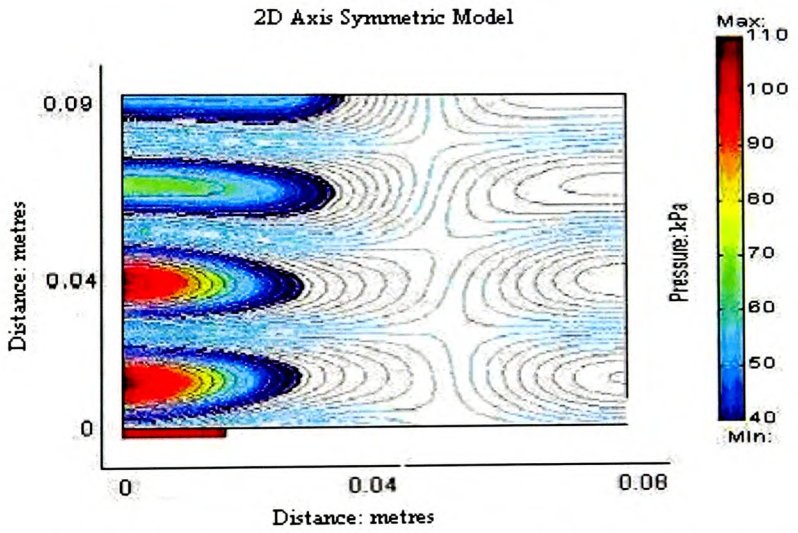

Figure 6.1: Two Dimensional Axial Symmetric Simulation Output of a Single Disk Radiating at 40kHz.

The output of the simulation shows a pressure field radiating from a single disk transducer located on the left hand side of the model. The number of nodes on the pressure standing wave can be shown to be accurate for the frequency, speed of sound and distance between source and the reflective boundary of the water/air interface. The

walls of the vessel were idealised as perfectly rigid in this mode of simulation and the right hand side of the model shows that although contour lines of pressure are present, no regions exist that exceed the 40kPa limit set for the onset of cavitation.

6.1.2 Two Dimensional Axial-Symmetric Foil Sampling

The foil sample shown represents both sides of the ultrasonic vessel. The line of symmetry is superimposed in red for clarity.

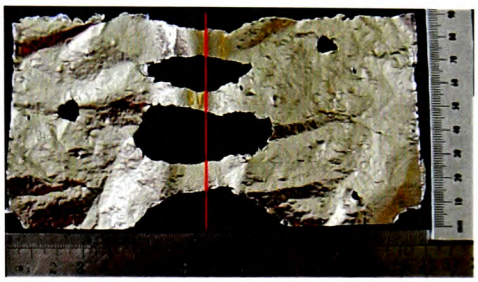

Figure 6.2: Foil Sample Taken along the Centre line of the Vessel

The number of areas of foil erosion match those predicted by the simulation outputs and the major areas of erosion are also along the central line above the transducer, as indicated by the model. The foil sample however shows several small regions of foil ablation not noted on the simulation. The left-right symmetry of the errant regions of erosion point to a region of variance within the simulation parameters and will be expanded upon within the conclusions.

Of particular note are the unpredicted regions of cavitation at the bottom corners of the vessel and the along the upper edge of the foil representing the water/air interface. These regions deserve special note at this stage as they are recurrent issues throughout the results. Possible causes and solutions to these differences in theoretical and practical outputs will be discussed within the conclusions and future work sections.

To obtain a clearer view of the relationship between simulation and foil sample, the results of figures 6.1 and 6.1 are shown below superimposed where the correlation between erosion areas and pressure maxima should be noted.

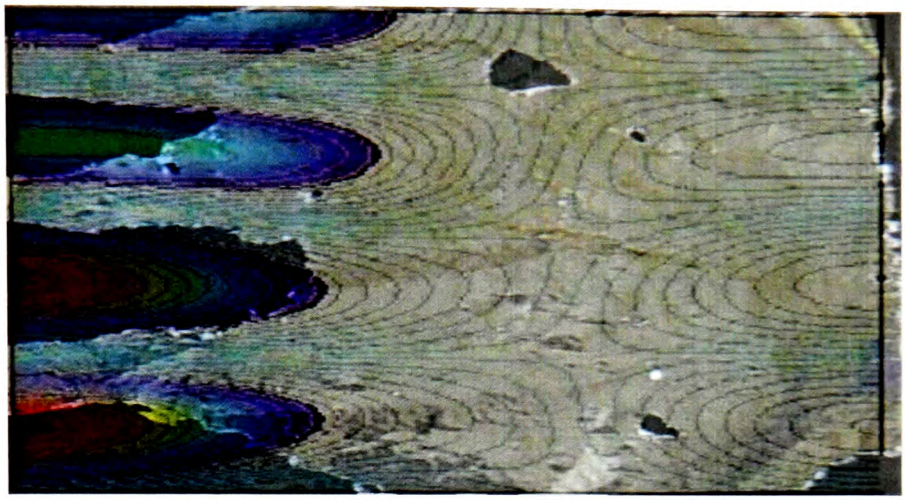

Figure 6.3: Overlay results of foil and simulation for Two Dimensional Axial Symmetric vessels

6.1.3 Probe plot of the cavitating field from the two dimensional axial-symmetric vessel

The probe output (placed in contour plot form) can be utilised to demonstrate graphically the cavitating field whilst still maintaining the quantitative approach the probes were selected to solve. The output shows the cavitating field primarily along the centre line predicted by the simulation output. The results of the PPB meter also show the strongest cavitating field present directly above the transducer face and beginning to dissipate as it rises, also in line with the simulations predictions concerning the strength of the pressure field.

However the probe also detects areas of cavitational power not predicted within the simulation, and some of these coincide with the areas of erosion in the foil not predicted within the simulation. These are discussed in sections 7.4 and 7.5.

The results of the NPL probe are presented in figure 6.5 and show similar cavitation patterns to the PPB output, also showing the bulk of the cavitating field in a direct line

above the transducer. Some subtle differences in field strength can be noted between the NPL and PPB meters but overall a good correlation exists between the two probes with the NPL Cavimeter appearing to match the foil and simulation output more closely.

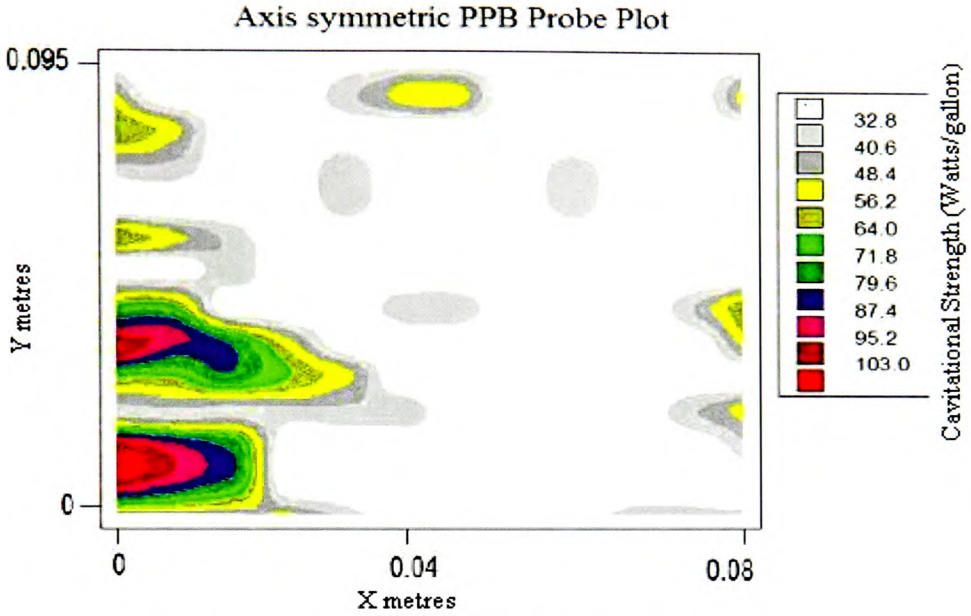

Figure 6.4: PPB probe outputs along the simulation lines of the 2D axial symmetric model

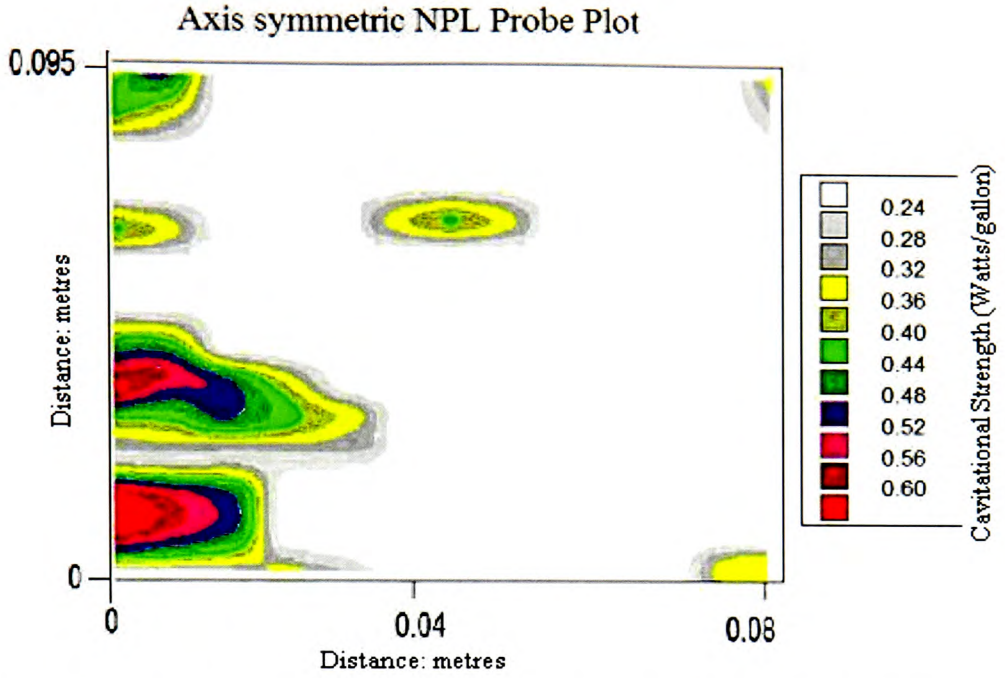

Figure 6.5: NPL Cavimeter probe output for two-dimensional axis symmetric vessel

Although it is noted that the major regions of cavitation are indicated on the foil by large areas of erosion leading to a complete hole in the suspended foil sheet, it must be noted that these are not the only places within the vessel that cavitation occurs. Closer examination of the foil samples shows that the foil is covered with a large number of minor indents caused by bubble implosions, which points to the fact that despite heavy erosion in regions of the standing waves, a cavitational field is in fact present throughout the entire vessel.

Figure 6.6 below shows a close up image of a region of foil taken from a sample, showing some of the aforementioned 'small pitting' in a region where the simulation indicates insufficient peak negative pressures to induce a cavitating field.

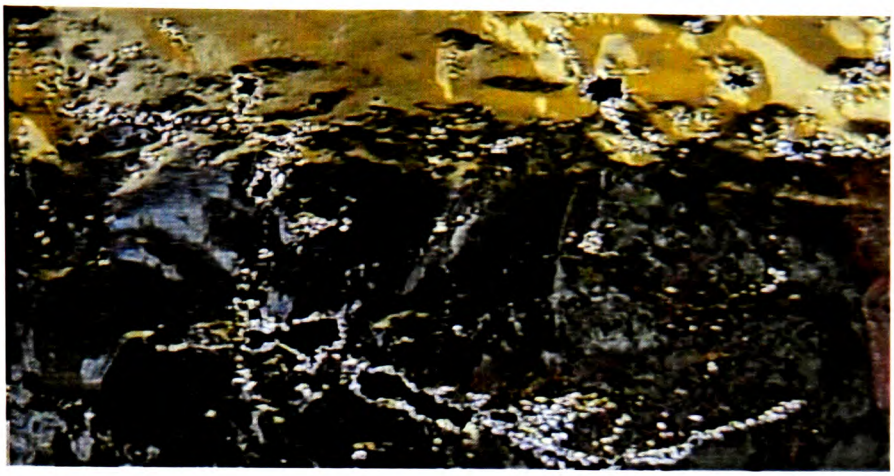

Figure 6.6: Close up image showing regions of 'small pitting' and minor erosion

Possible causes for these unpredicted regions of pitting and its implications for ultrasonic cleaning are discussed in the conclusions of this thesis (section 7.6.1).

6.2 Two dimensional versus three dimensional simulation

The implementation of a two dimensional axis-symmetric model, with its prediction of the major cavitating field gave rise to a greater confidence in the modelling methodology. However, the incidence of vessels exhibiting axial symmetry in commercially available vessels is very rare.

Given the stated aim of this project to produce a method of predicting bulk cavitating fields applicable to commercially available ultrasonic cleaners, this project proceeded to assess whether a typical ultrasonic cleaning vessel could be represented with a simplified two dimensional model, or whether a full three dimensional modelling approach would be required for accuracy and completeness.

In this sub set of experiments, the same region of an ultrasonic cleaner was assessed by both a two-dimensional and three-dimensional model and the results compared to the foil and probe values obtained for that region. The ultrasonic vessel utilised was a two

disk transducer model, operating at 40kHz and was geometrically presented as an exemplar of the standard 'benchtop' ultrasonic cleaner.

6.2.1 Simulation outputs for two and three dimensional models

Figures 6.7a and 6.7b represent respectively the comparative axial simulation outputs of the two and three-dimensional models aforementioned. Note that both predict the strongest field strength in the regions directly above the transducers, spreading and diminishing as the field moves towards the water/air interface. Both models contained the appropriate number of antinodes for the stated wavelength and both exhibited symmetry along the centre of the simulation as would be expected from the geometrical layout of the vessel under investigation.

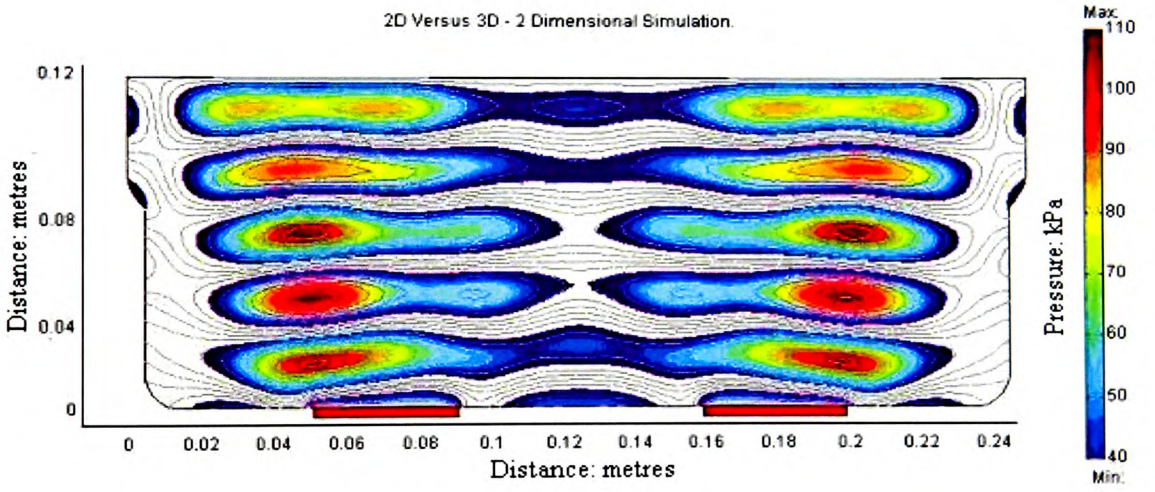

Figure 6.7a: Simulated output of the two dimensional model

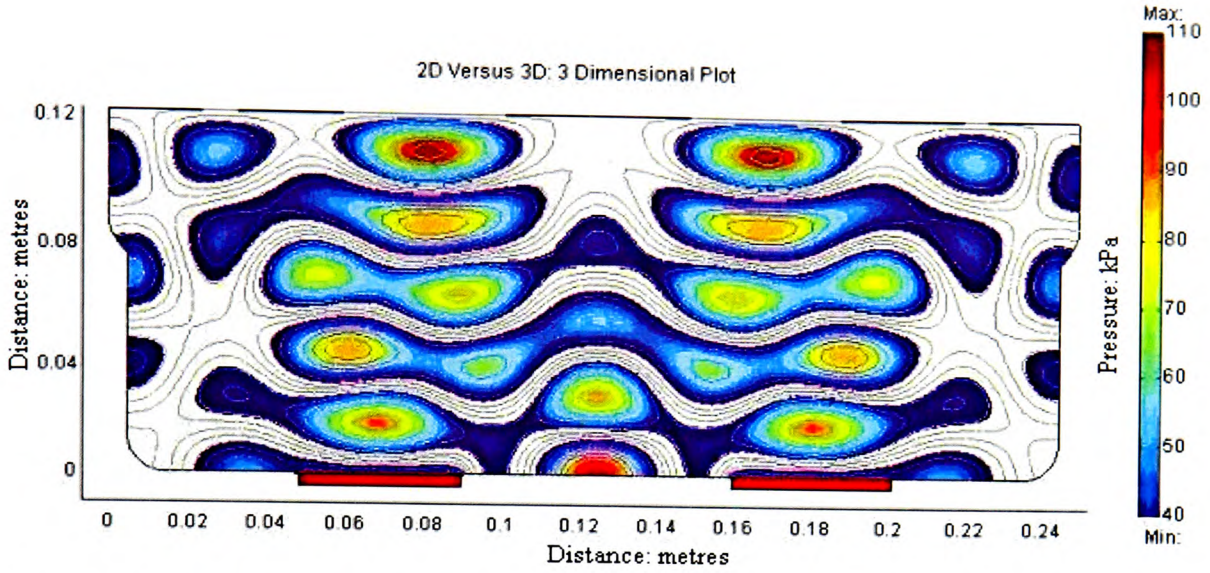

Figure 6.7b: Comparative cross-section of the simulated output of the three dimensional model.

There are however subtle differences in the pressure fields of both models. Although the number of antinodes between the transducer face and the water/air interface were the same for both models, slight variations in both the position and strength of the fields were noted; whereas the two dimensional case presented clear bands of activity within the vessel, the three dimensional case presented more of a blurring of fields where the left and right transducer fields superimpose.

Both also display a variation along the edges of the vessel and these differences were accounted for by the extra reflections in the three dimensional case superimposing upon the wave field noted in the two-dimensional case and altering the pressure profiles.

6.2.2 Foil sampling of the two/three dimensional test

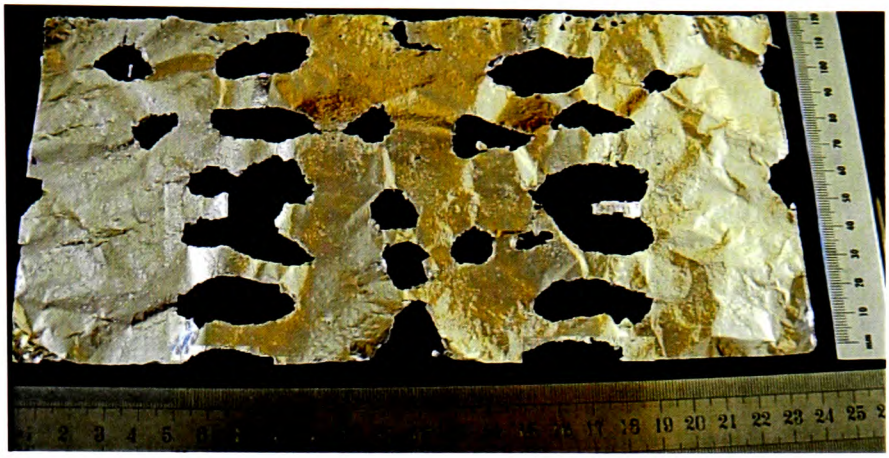

Figure 6.8: Foil sample taken along the centreline of the vessel in the two/three dimensional test scenario

The foil sample taken along the axis of simulation indicated the number of antinodes predicted by both simulation outputs extending directly above the transducer face towards the water/air interface. The foil sample however shows distinct erosion patterns between the main radiation paths as predicted more accurately by the three dimensional case. Indeed an overlay of the foil and simulation outputs (shown in fig 6.9) for the three dimensional cases highlighted the similarity between the two cases.

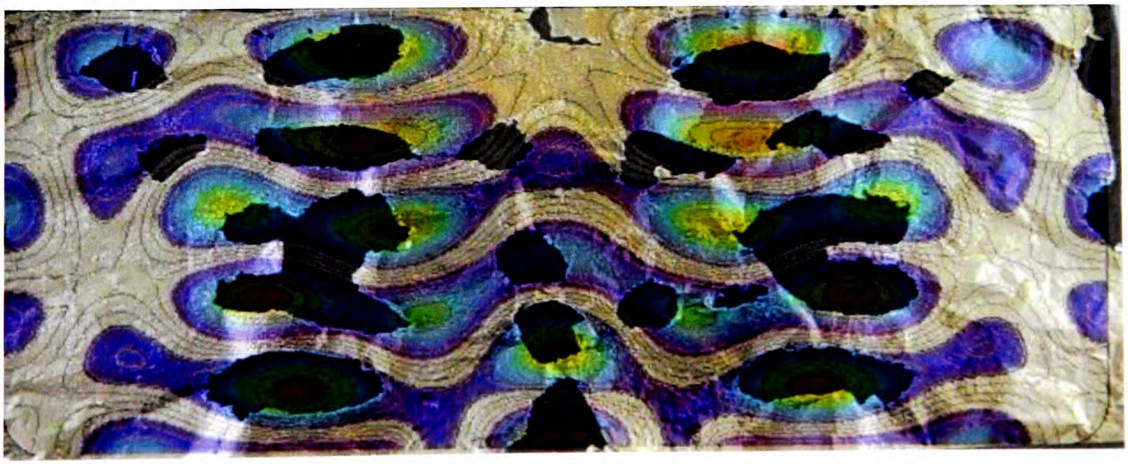

Figure 6.9: Overlay of foil and simulation results for the three dimensional test case

An inspection of the overlaid images indicated the number and locations of antinodes in the pressure field corresponded well to those found in the foil tests both directly above the transducer faces and between the two radiating faces.

Erosion patterns towards the side of the vessel were also partly accounted for in this simulation (note the two erosions towards the right hand side of the vessel), but some others were not. Accuracy of location appeared to diminish slightly in the results as we move further away from the radiating field and towards the air boundary. There was also the ubiquitous region of heavier that expected pitting along the water/air interface. Both these issues will be discussed in section 7.6.2.

It could also be seen that due to proximity of fields and their strength, the third and fourth set of antinodes appeared to have merged within the foil sample. This was found to be not uncommon and was found in later sets of results.

6.2.3 Probe data for the two dimensional/three dimensional comparative test

Both the results from the PPB and NPL probes are shown below in figures 6.10a and 6.10b. The field locations and relative strengths of both appeared more closely related to the three dimensional case than that of the two dimensional example.

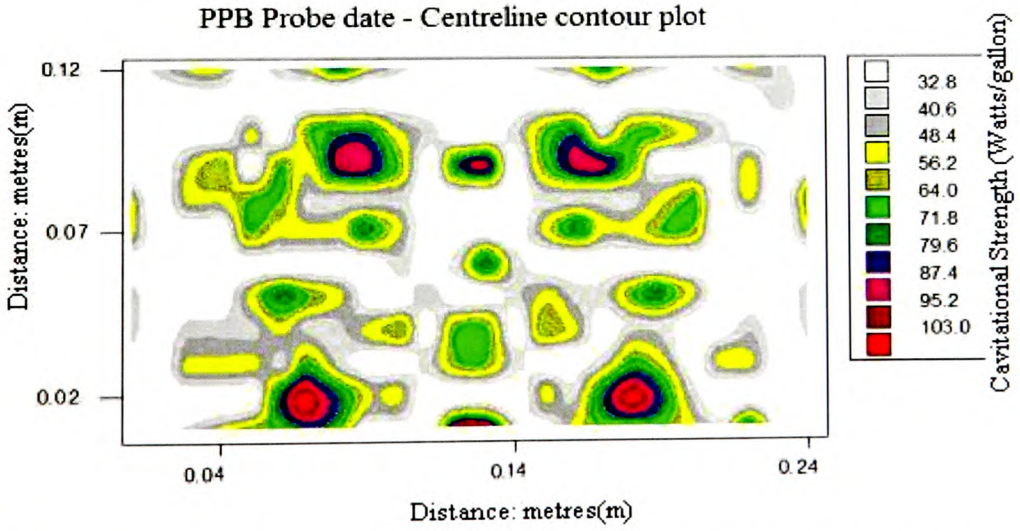

Figure 6.10a: PPB probe showing cavitational field for the two/three dimensional tests

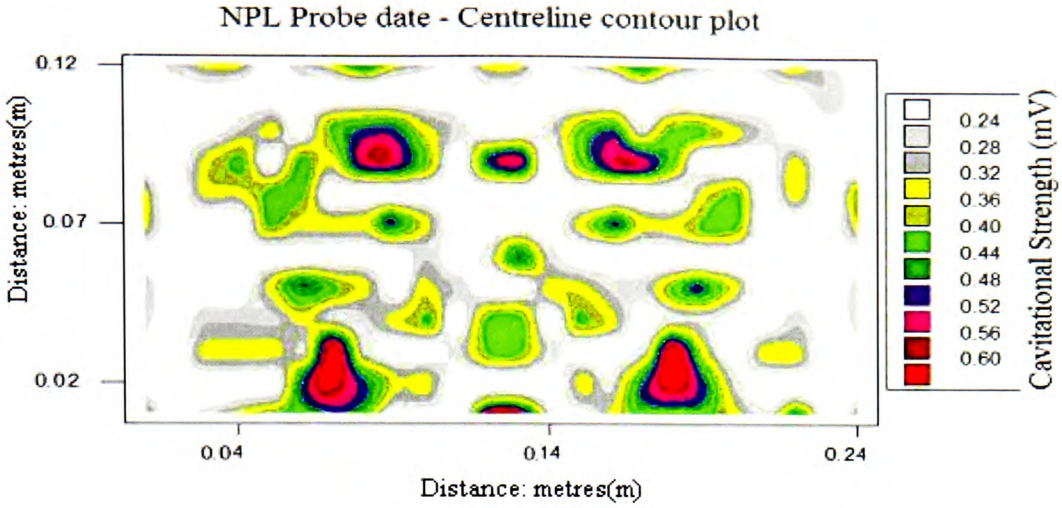

Figure 6.10b: NPL probe data for the two/three dimensional test cases

Both sets of probe results appear to concur with the foil, three dimensional simulation and each noting the chief activity occurring in a line extending above the transducer faces to the water air interface but also with significant regions of cavitation appearing in between the transducers, as predicted by the three dimensional simulation.

Both probes showed the greatest concentration of cavitational energy concentrated directly above the radiating face of the transducer and both sets of probe results showed a blurring of the first and second antinodes. This was possibly a result of insufficient resolution of data points when performing the experiment or that the strength of field was sufficient to cause this blurring.

6.3 Effects of reducing liquid level

A close examination of the literature concerning ultrasonic cleaning and cavitation uncovered very little with regards to the effects of liquid level in bulk cavitating fields, indeed the industrial sponsor, although seeing fit to include a fill level line upon their benchtop ultrasonic vessels was unaware of whether the depth prescribed was beneficial, neutral, or indeed had an adverse effect on the strength and positions of the cavitating fields within the vessel.

This section of the results will show the simulation and practical results obtained from varying the liquid level in steps of 0.5λ to a maximum of -1.5λ. The maximum level by which that the liquid could be reduced was dictated by the maximum fill level at one extreme and the technical limitations of operating the ultrasonic bath at low liquid levels at the other, as will be discussed in the conclusions.

The results from this section of work will present the simulation results for all three cases followed by foil and finally probe data for all allowing comparison not just between individual sets of simulation with its respective results, but also between all three liquid depths examined.

6.3.1 Simulation results for depth variations of -0.5λ, -1λ, and -1.5λ

The results of lowering the liquid levels as described in section 5.3.3 are presented below in figure 6.11a, 6.11b and 6.11c detailing a varying of the liquid level by -0.5λ for each successive image. A comparison of the first simulation image (-0.5λ) with the full liquid depth shown in figure 6.7b provided an indication as to how the fields are remarkably similar despite the slight reduction in the liquid level. Both demonstrate a similar pattern of pressure radiation and similar ranges for the locations of the pressure maxima.

Subsequent reductions in the depth of the liquid show a change in the locations and strengths of the field. The white regions in the centre of the maximum pressure areas of figures 6.11b and 6.11c represent pressures that exceeded the maximum pressure scale set in the simulation (i.e. above 110kPa) and the size and locations of these pressure extremes become more apparent with diminishing liquid level.

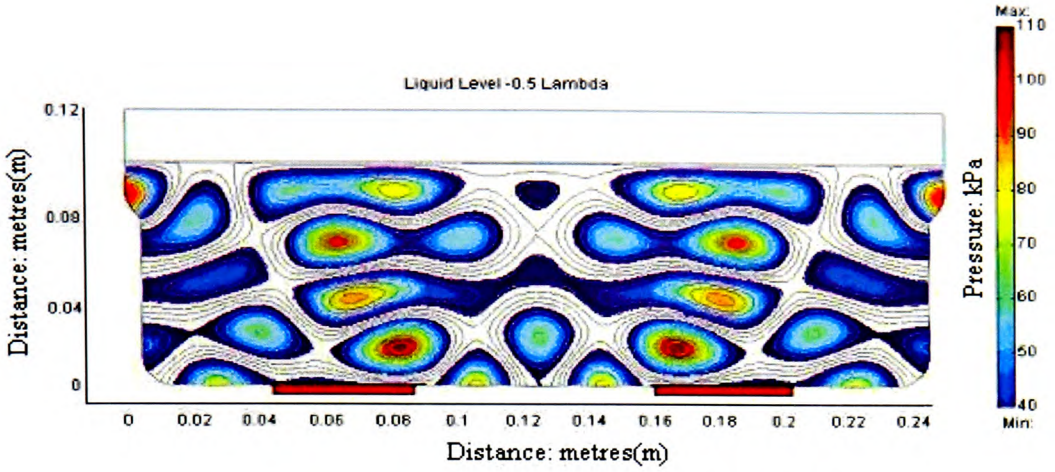

Figure 6.11a: Simulation at depth=-0.5λ

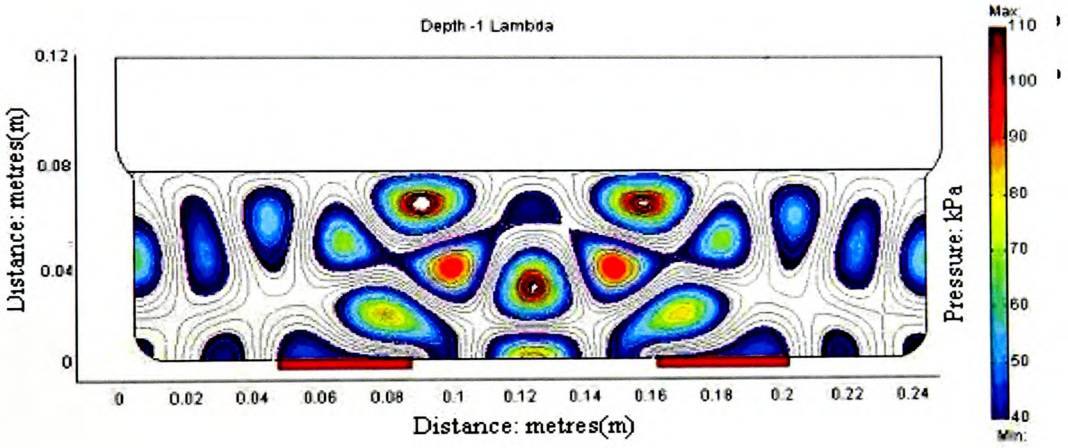

Figure 6.11b: Simulation at depth=-1λ

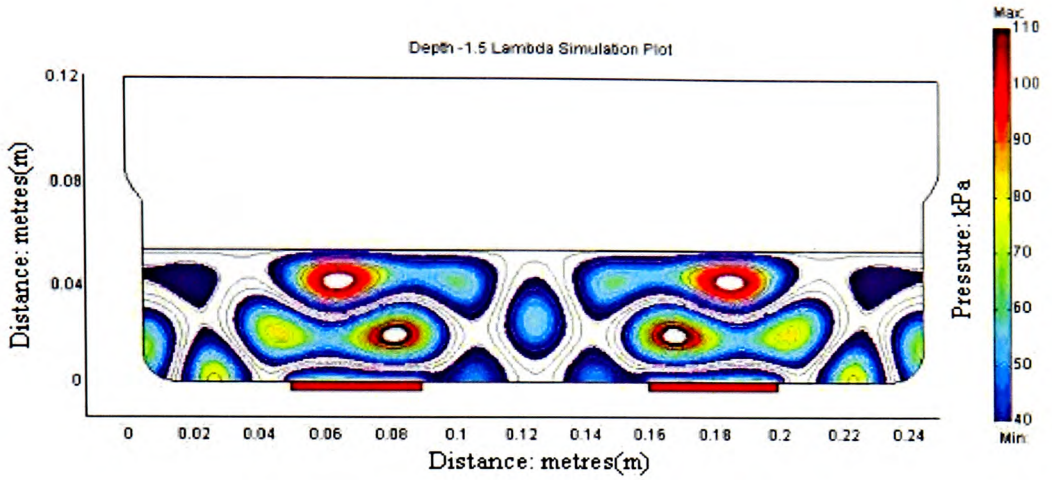

Figure 6.11c: Simulation at depth=-1.5λ

6.3.2 Foil sampling of the reduced liquid level values

Figures 6.12a to 6.12c show the foil samples suspended along the centre lines of the simulation for the reduced liquid levels and the corresponding overlay of the foil and 3D simulation results.

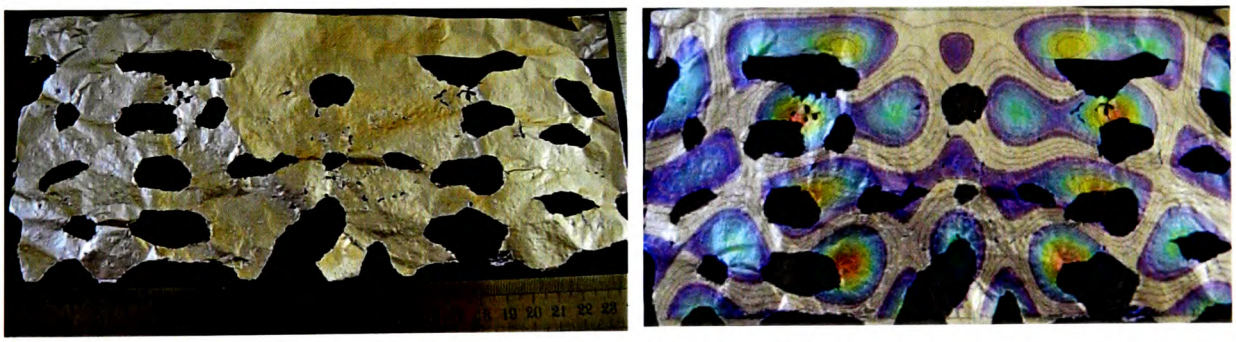

Figure 6.12a: Foil sample and Three Dimensional simulation/foil overlay at depth=-0.5λ

Figure 6.12a shows a good correlation between the foil and simulation outputs, with both the numbers and positions of the pressure maxima corresponding to areas of erosion on the foil sample. Again the further distances from the radiating face of the

transducers, the less accurate the simulation becomes in terms of the expected position of areas of erosion.

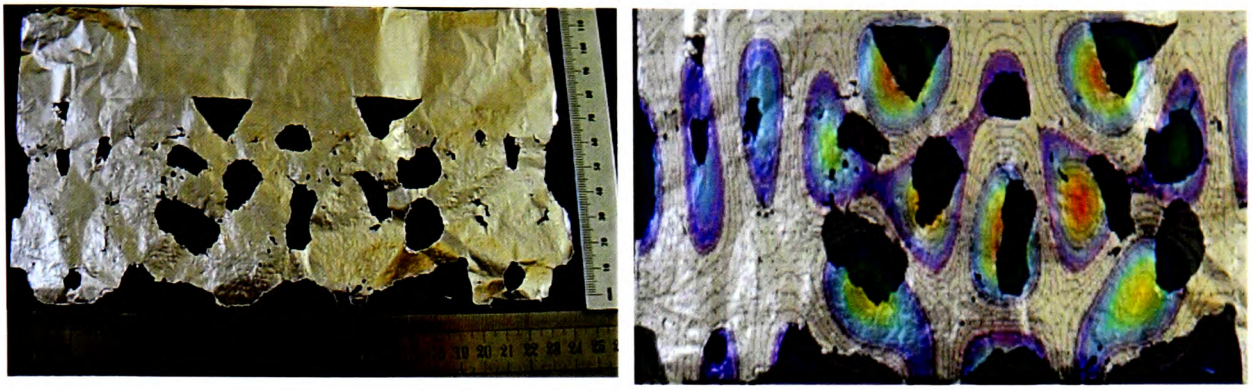

Figure 6.12b: Foil sample and 3D simulation/foil overlay at depth=-1λ

The foil results and the overlay at a depth of -1λ (presented in figure 6.12b) again show a very good correlation between regions of predicted cavitation within the simulation and those areas of heavy erosion on the foil sample. The deviation of the locations of cavitation from the simulation to the foil test appears far less pronounced than that in figure 6.12a at a depth of -0.5λ, perhaps indicating that the error in location of the cavitation 'hot spots' may be a function of the depth of the liquid. This possible facet will be discussed in depth during the conclusions.

If the accuracy of the simulation were to deteriorate with distance from the transducer face, it would be expected that a final lowering of the liquid levels would present a greater accuracy between foil and simulation outputs. Figure 6.12c shows the foil and overlay samples at the final liquid level of depth=-1.5λ and appeared to have an improved accuracy over the two previous examples with the positions of the erosion matching almost perfectly with the simulation output results.

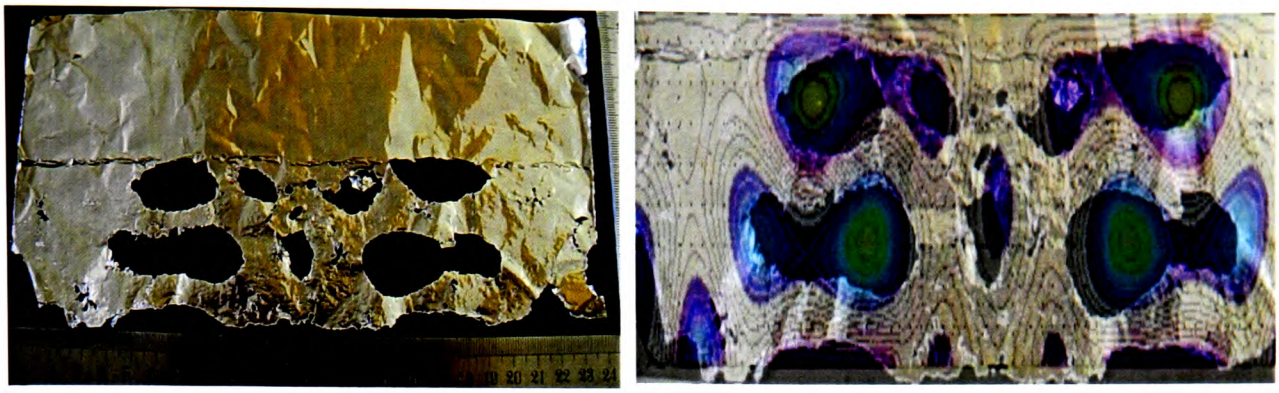

Figure 6.12c: Foil and simulation/foil overlay for depth=-1.5λ

Again a line of heavy foil pitting extending along the line of the water/air interface that was not predicted by the simulation output is most clearly visible in the foil sample of figure 6.12c. As a recurrent feature in the simulations which was not predicted but so prominent within the foil samples, this will require explanation during the conclusion phase of this thesis.

6.3.3 Probe results for varying liquid levels to depth -0.5λ, -1λ and -1.5λ

For each of the three liquid depths simulated, probe readings were taken with the PPB and NPL probes along the axis of simulation. Figures 6.13a, 6.13b and 6.13c depict the results for depth = -0.5λ, -1λ and -1.5λ respectively.

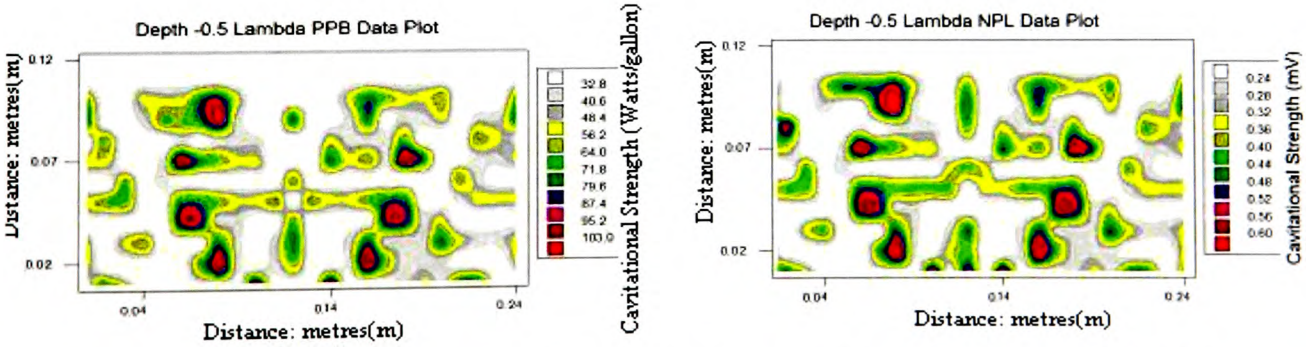

Figure 6.13a: PPB probe readings (Left hand side) and NPL probe contour plot (Right hand side) for -0.5 λ

Both the PPB and NPL plots here show a very close correlation in the results obtained relative to each other, the foil sample and the simulation outputs in terms of field locations and the relative strengths of cavitation. Although both show a good correlation, the NPL probe had a slightly better resolution in terms of the positioning of the cavitation locales throughout the vessel.

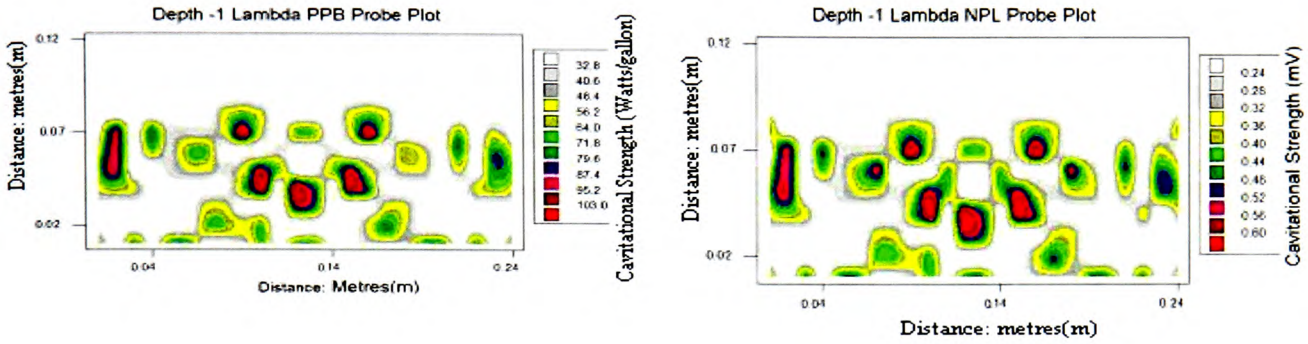

Figure 6.13b: PPB probe readings (Left hand image) and NPL probe contour plot (Right hand image) for depth = -1 λ

Once again, both sets of probe readings indicate consistency between each other and the simulation/foil results. Both probe readings also demonstrate higher strengths in the cavitational fields in those locations where the simulations show a relatively high pressure field, indicating a potential correlation between higher peak negative pressure values and higher bulk cavitating strengths.

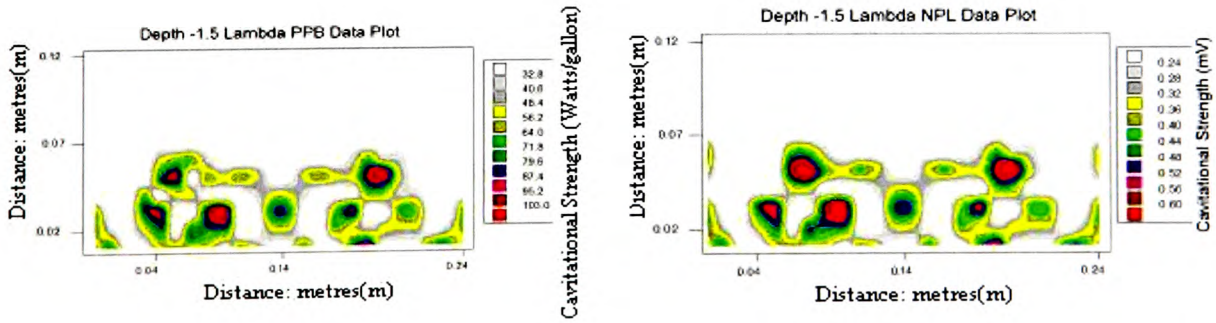

Figure 6.13c: PPB probe readings (Left hand image) and NPL probe readings (Right hand image) for a liquid depth -1.5 λ

The plots for PPB and NPL probe at the lowest of the tested liquid levels again continue the trend of matching both the simulation results and the suspended foil tests. As with previous tests, both sets of probe readings showed symmetry in cavitational locations and strengths along the centre line as predicted from the simulation outputs.

Although an increase in cavitational strength is noted, as compared to the previous examples, they are not totally inline with the expected increase due to the large peak negative pressures predicted from the simulation results. A possible cause for this discrepancy will be discussed in the conclusions along with a general discussion of the implications of the liquid level tests for industrial usage.

6.4 Results and Implications of introducing a free suspended load to the liquid medium

It was noted during the literature review that despite the fact that ultrasonic cleaners are designed to operate with objects suspended in the liquid, the majority of attempts at conducting simulation work neglected the placement of and form of object into the vessel and any subsequent effects this may have had on the cavitating field. This section of the results aims to address this by placing a typical load within the ultrasonic vessel and comparing the results to those from the free radiating field described and tested in section 6.1.

6.4.1 Suspended load simulation output

The image in fig 6.14 shows the pressure contours in the liquid sub domain with a load introduced to the liquid. It may be noted that below the level of the load, pressures were so high that they exceed the maximum level of 110kPa placed on the simulation, as a result of reflections from the lower surface of the load in the liquid.

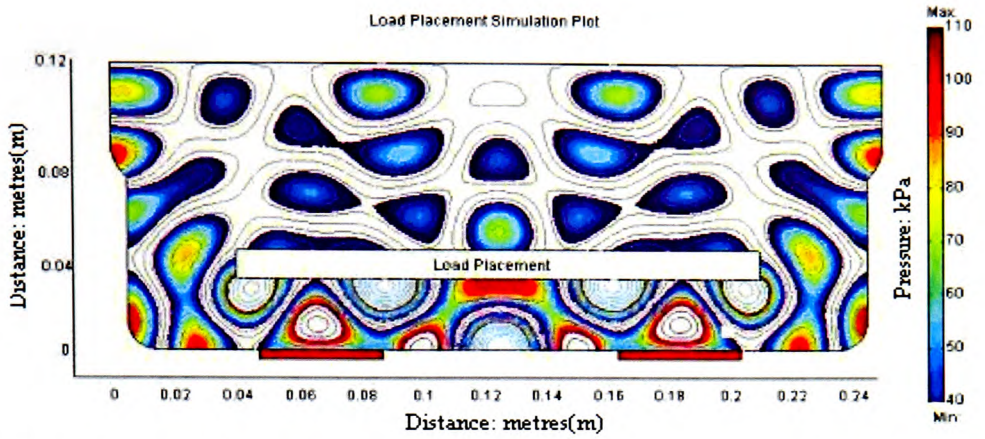

Figure 6.14: 3D Simulation of an ultrasonic vessel with a suspended load

Pressure above the surface of the load however showed that most regions were only just above the peak negative pressure identified as necessary for cavitational inception. The result of this should reflect in the foil and probe readings where low activity should be noted above the suspended load.

One area of interest on the simulation output was the regions directly to the sides of the load, where pressure wave radiation seeped through to the region above the load, giving a higher pressure profile to the sides of the vessel that were directly above the transducer faces as was usually the case in these tests.

6.4.2 Suspended load foil comparisons

A direct comparison between the foil and 3D simulation outputs again showed a reasonable level of correlation between both images. The foil sample shown in figure 6.15 and the corresponding simulation/foil overlay image were only of the region above the load placement and showed a reasonable agreement between simulation and foil. In comparison to the images from the free radiating transducers it was noted that there was far less major erosion above the load than in the comparable area without a load.

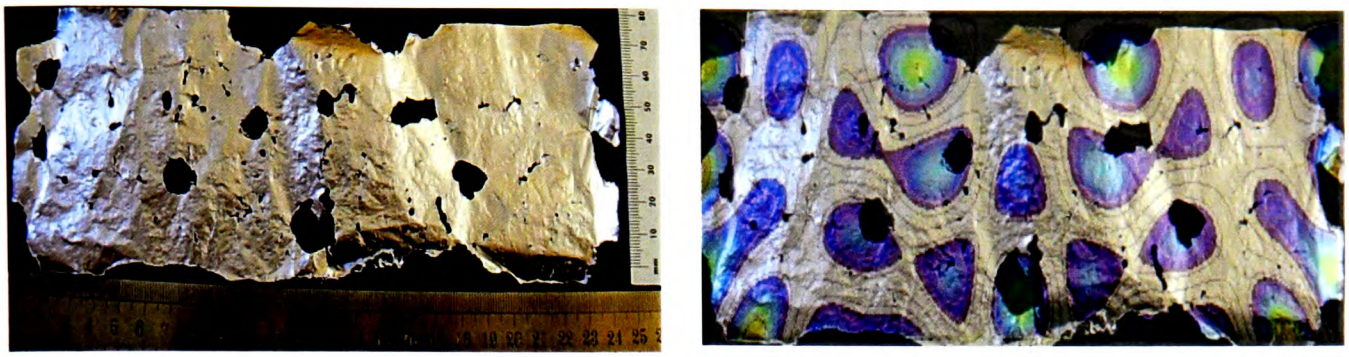

Figure 6.15: Foil sample of region above the suspended load and simulation/foil overlaid images

Careful examination along the edges of the image also showed how the higher pressure profiles predicted during the simulation had translated to a higher incidence of cavitational erosion on the foil samples.

6.4.3 Suspended load PPB and NPL probe results

The probe results from the PPB meter showed a spare scattering of cavitational zones above the line of the suspended load. In line with the predictions of the simulation a region of higher density cavitation could be noted to either side of the load.

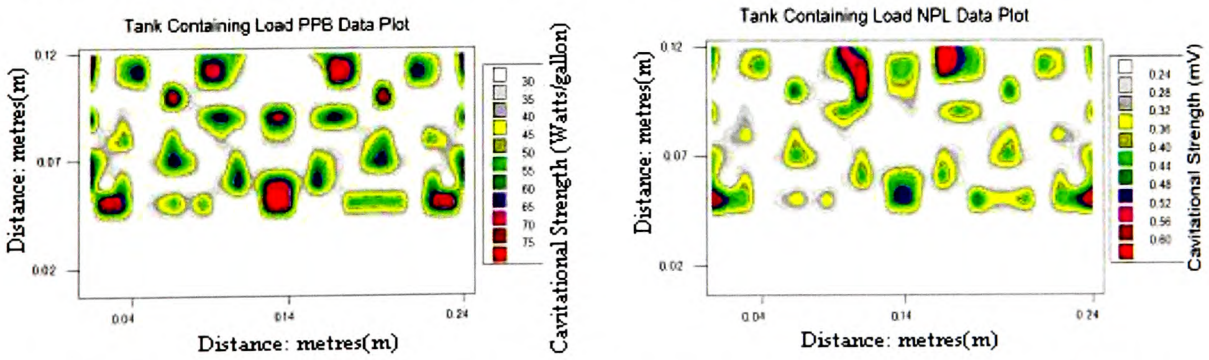

Figure 6.16: PPB and NPL plots of the cavitational densities in the region above the suspended load

The Results for the NPL probe were again similar to those of the PPB meter showing the same scarcity of cavitational density throughout the liquid above the load line. The implications of this 'cavitational shadowing' above a suspended load would have serious implications for the design and use of ultrasonic vessels and will be expanded upon during the conclusions and future work sections.

Data values could not be obtained for the regions below the load due to the dimensions of both probes being unable to fit below the suspended load.

6.5 Results of alternative transducer placements on an ultrasonic bath

Both the literature review and discussions with the industrial partner noted that although the bonding of transducers to the base of the vessel was commonplace, no sufficient explanation for this choice of location seemed to exist. As such one of the aims of this project was to examine the feasibility of alternative patterns of bonding transducers to the vessel walls and what effect this would have on the resultant cavitation field, if any.

The response of the ultrasonic field to a suspended load and the shadowing effect this produced directly above the face of the load that would require cleaning, and alternative transducer placement pattern should be investigated with reference to the standard radiating patterns noted in figure 6.7b.

The two alternatives to this standard placement of transducers are described in section 5.3.5 and are evaluated here using simulation, foil and probe tests.

6.5.1 Simulation results for alternative transducer placements

The simulation results shown below in figure 6.17 show the patterns for the two alternative transducer placements. Fig 6.17a has one base bonded transducer and another placed on the side of the vessel (The transducers positions are noted in red) and Fig 6.16b shows both transducers bonded to the sides of the vessel.

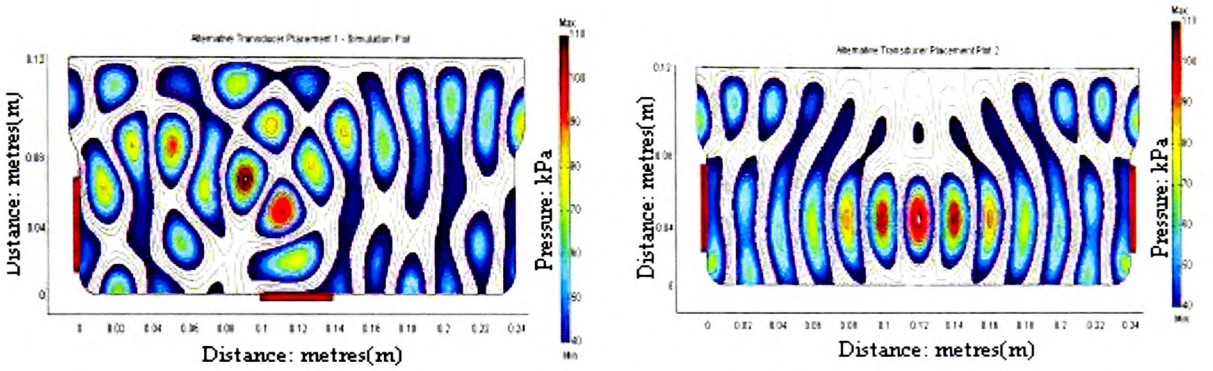

Figure 6.17a and 6.17b: Alternative positioning of transducers on the ultrasonic bath walls.

In the first configuration the resultant wave pattern from the superposition of the two radiating transducers was vastly different from the standard configuration of figure 6.7b. Note how the highest concentration of peak negative pressure amplitude appeared in the region where the primary beams of both transducers cross. The dispersion of pressure amplitudes above the cavitation threshold appeared greater than that of figure 6.7b, but the symmetry of the previous simulations results was lost due to the lack of symmetry in the transducer placements.

The second configuration shown in fig. 16.6b shows both transducers bonded to the opposing sides of the ultrasonic vessel. In this configuration, the pressure amplitude field appeared at its maximum towards the centre of the vessel directly in between both transducers. There appeared in both cases a reasonable coverage of the interior of the ultrasonic vessel with cavitational activity.

6.5.2 Foil test results for alternative transducer bonding configurations

Figures 6.18 shows the resultant foil sample from the first transducer configuration of one transducer on the base and one towards the side of the vessel. There was a reasonable correlation between the simulation and the major pitting of the foil as shown in figure 6.18.

It was also noted that, as predicted by the simulation output, the largest region of major erosion, reflecting the highest cavitational energy was located towards the left side of the images. Indeed the right hand side of the foil was largely devoid of any major cavitational erosion patches. A closer inspection of the foil sample showed that even the small pitting that occurred across the face of most the foils samples was less frequent along the right hand side of the foil.

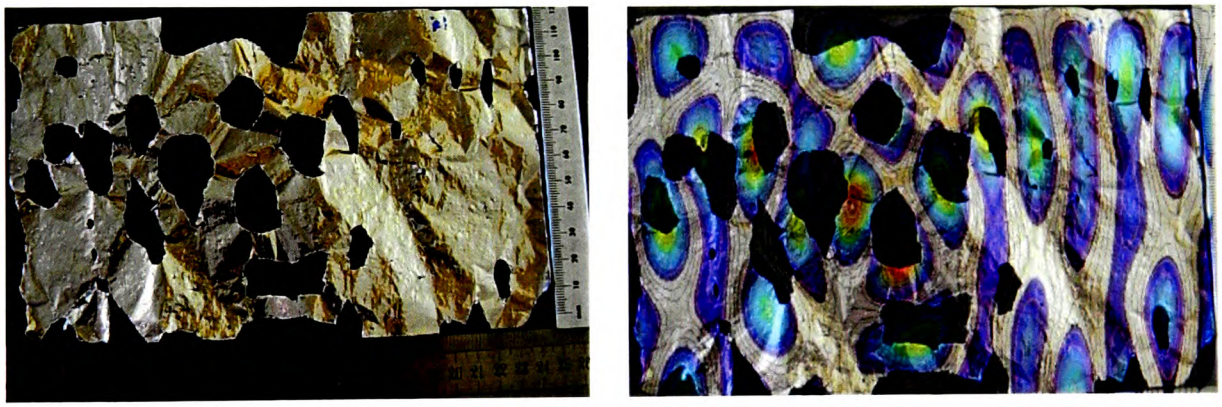

Figure 6.18: foil and simulation/foil overlay results for alternative transducer configuration 1.

An examination of the foil sample for the second configuration of transducers (Fig 6.19) indicated the neat banding effect visualised by the simulation. It also showed how the foil/simulation overlay for this example provided an excellent match with numbers, locations and relative strengths of the erosions matching well.

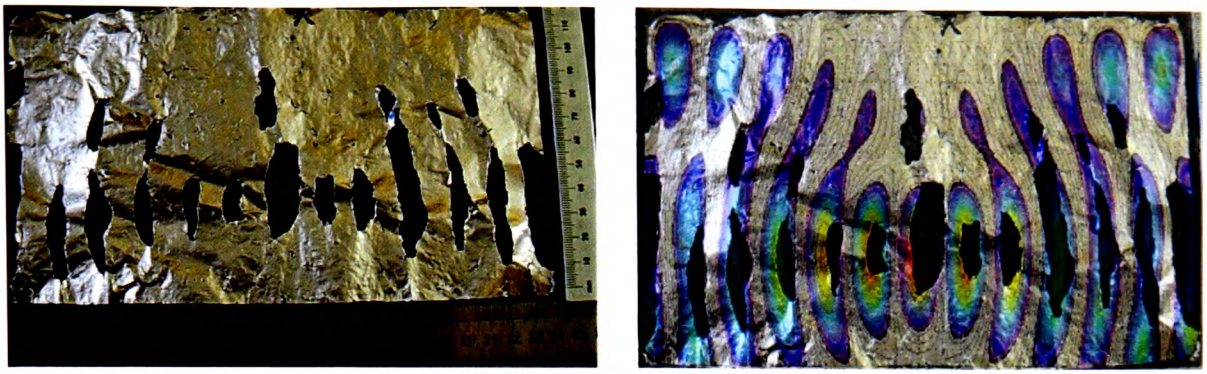

Figure 6.19: foil and simulation/foil overlay results for alternative transducer configuration 2

The small pitting of the foil was once again evident with this configuration of the transducers and the symmetry of erosion was restored along with the symmetry of the transducer placements.

6.5.3 Alternative transducer configurations PPB and NPL probe data

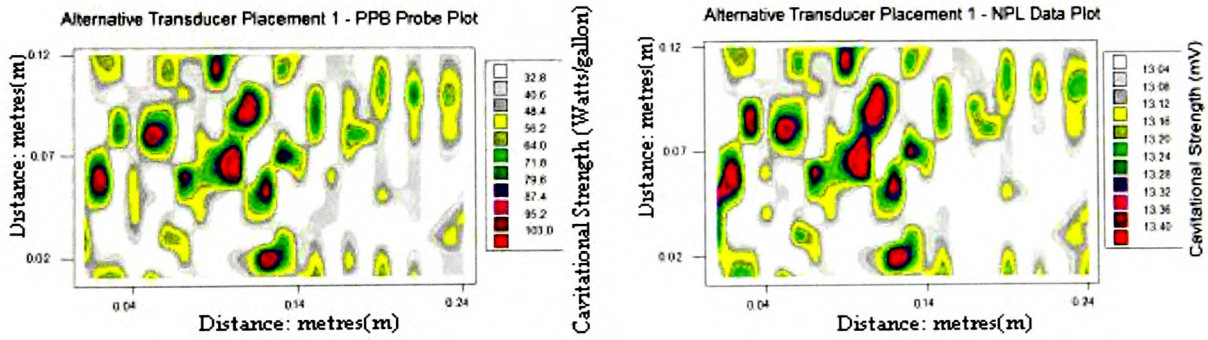

Figure 6.19a and figure 6.19b: PPB and NPL probe data for alternative transducer configuration 1: Base and Bottom bonding

As can be seen from the above contour plots resulting from the probe readings of both the NPL and PPB probes, the cavitational fields provided a reasonable match to the foil and simulation outputs. Both sets of data showed a larger concentration of cavitational energies above the transducers and towards the left hand side of the image, as in the simulation, and foil samples and both sets of data also showed the right hand side of the vessel largely devoid of any significant cavitational activity.

The probe data plots for the second transducer placement also showed a good likeness to the simulation and foil results. Both NPL and PPB meters demonstrate the horizontal banding effect noted from the simulation as shown in figures 6.20a and 6.20b. Both probes also showed a higher cavitational density in the centre of the two transducers with a lower cavitational activity field present above towards the upper areas of the vessel.

Both PPB and NPL show some blurring of fields where two distinctly separate nodes on the simulation and foil appear blended into one. This was again evident in areas with a high cavitational content as shown on the centre left of both probe results.

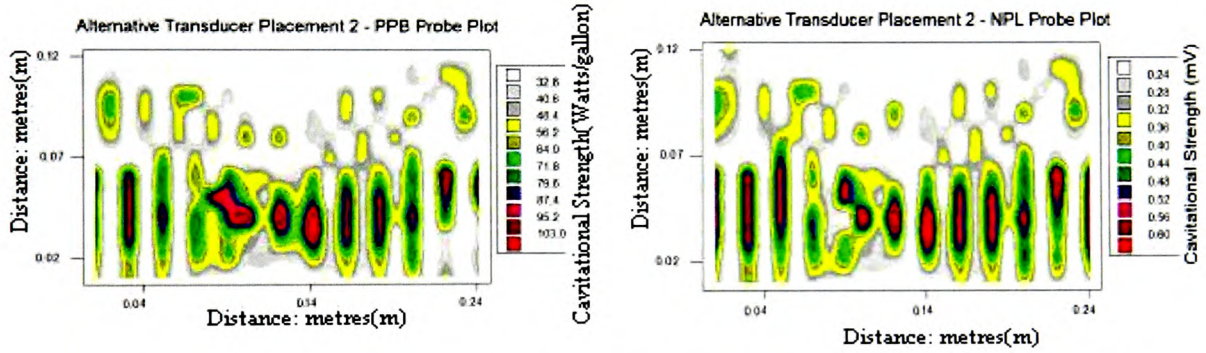

Figure 6.20a and 6.20b: PPB and NPL probe outputs for alternative transducer configuration 2:Transducers on either side.

6.6 Effects of basket mesh on bulk cavitating fields – simulation and practical results

Although the effect of placing a load within the vessel has been examined, it must be noted that loads are not placed within an ultrasonic cleaning bath freely suspended. The literature review concluded that a thin, open mesh basket type is most commonly used by industry, although other types are occasionally utilised such as the punched hole tray described in chapter 5.3.6. Again no literature was available as to the effects, if any the

design of basket holds upon the cavitating field and hence the cleaning capabilities of an ultrasonic cleaning vessel.

In this set of experiments the effects of both types of basket were compared to the unimpeded radiating field shown in figure 6.7b to assess how the field would be affected by each basket type.

6.6.1 Simulation results of open mesh and a punched hole basket

The simulation outputs of the open mesh basket and the punched hole basket types are shown in figures 6.21a and 6.21b respectively.

The results of the open mesh basket show how the pressure radiation field appeared very similar to that of the unimpeded field in fig 6.7b. The only discernable difference was the blurring of the once clear antinodes in the pressure field, especially towards the upper regions of the model (Above the line of the suspended basket mesh).

By stark comparison, the simulation output of the punched hole basket mesh was very different to the unimpeded field and that of the open mesh. Pressure both above and below the basket level was reformed to horizontal bands with the pressure profile above the line of the basket mesh appearing extremely weak although a little more disperse than its open mesh. Pressure above the line of this second basket type was greatest right above the basket itself.

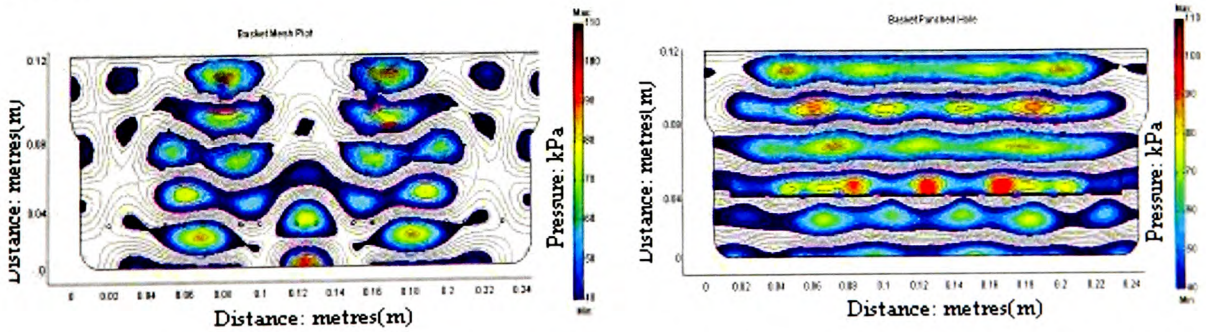

Figure 6.21a and 6.21b: Simulation outputs of the open mesh and punched hole basket type

6.6.2 Foil testing results for basket mesh varieties

The foil sample below (fig 6.22a) shows a foil sample taken from above the basket mesh in the ultrasonic cleaning vessel. The foil erosion shows a number of regions of erosion consistant with those predicted by the simulation output. The small pitting observed upon the foil was very heavy directly above the basket mesh itself. The superposition of the foil and simulation results however highlighted that, despite a correct number of regions of erosion, the locations deviate slightly from those predicted by the simulation output.

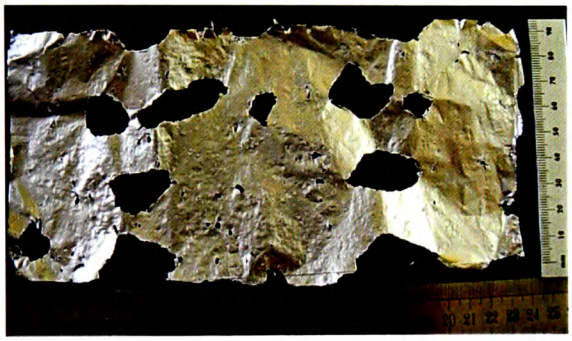

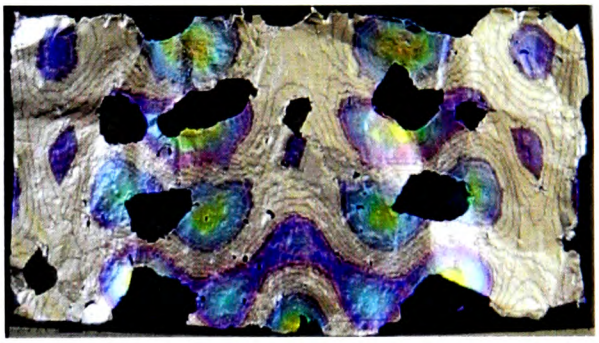

Figure 6.22a and 6.22b: Foil and superposition of foil/simulation results for mesh-type-basket

The foil samples for the punched hole basket type also showed a good correlation with the simulation results. The banding could clearly be seen and an overlay of the foil with simulation images showed that the locations of the areas of maximum erosion coincided well with those predicted by the simulation outputs.

A slight deviation from the simulated output could be noted in fig.6.23b where the foil was overlaid onto the simulation output and the locations of the uppermost regions of cavitation appear shifted from the predicted simulation output.

The levels of erosion noted from this punched hole basket were far weaker than the free field or the open mesh type basket. Possible causes for this weakness and implications will be further discussed in the conclusions chapter (section 7.6.6).

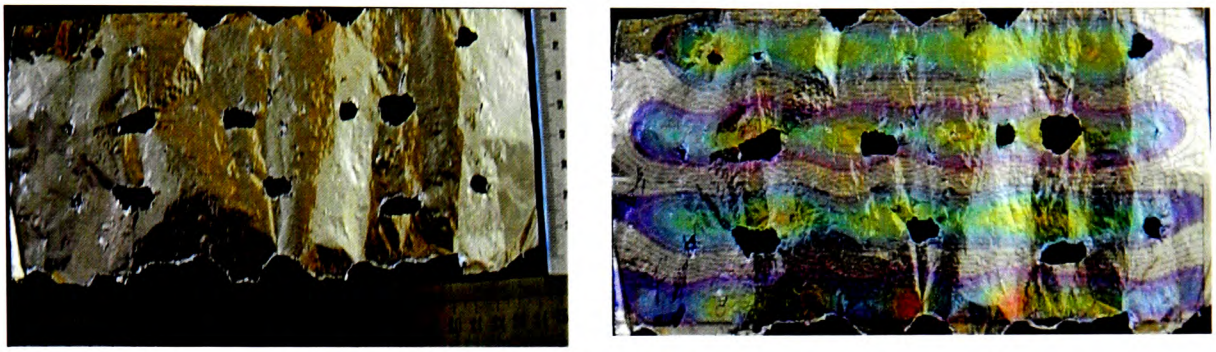

Figures 6.23a and 6.23b foil test result for punched hole type basket

6.6.3 Probe results for the basket variation tests

The figures below show the outputs of the NPL and PPB meters above the basket mesh lines for the open mesh basket. These compared reasonably with the simulation and foil samples presented earlier. A comparison of these figures with those for the unimpeded radiating field in figures 6.10a and 6.10b show a similarity in the data outputs indicating (as with the simulation and foils) that the open mesh does not present much of an obstacle to the radiating field of the transducers.

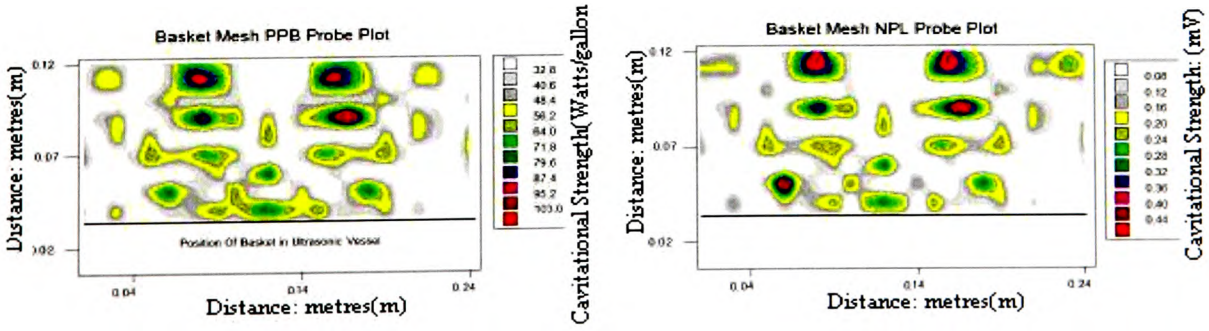

Figure 6.24a and 6.24b: Probe data for the open mesh basket

The probe data outputs for the punched hole basked however showed a marked variation on those of the open mesh and free radiating transducers. Figs 6.25a and 6.25b show the probe outputs that were closely correlated with the simulation outputs and the foil samples. Both data sets show the ordered bands of cavitational activity predicted by the simulations and verified by the foil testing.

The NPL probe also indicated some of the cavitational blurring towards the top of the image that would explain the shift in cavitational positions noted on the foil sampling.

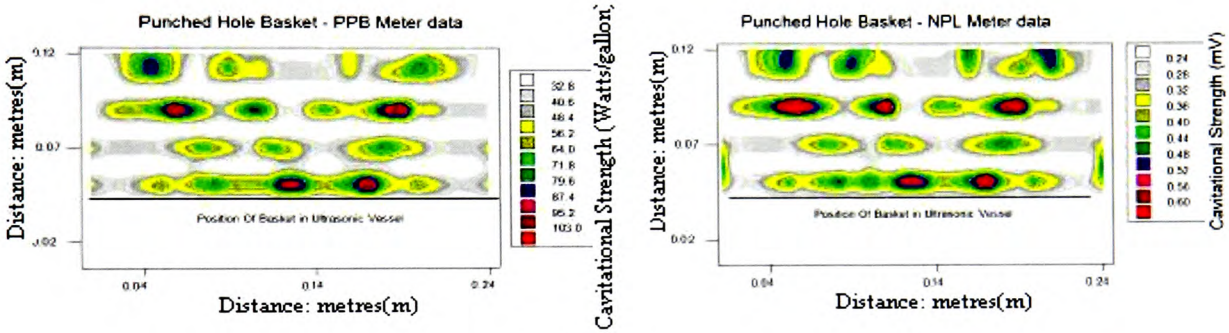

Figure 25a and 25b: Probe data for the punched hole basket type.

Chapter 7 – Conclusions

7.0 Introduction to conclusions.

The results presented in chapter 6 were examined and certain conclusions regarding ultrasonic cavitation, both as a general subject and specifically concerning the experiments performed have been abstracted. Additionally on narrow subsets of experiments with a well defined industrial relevance, (examples of which include the introduction of a load to the cavitating fluid and transducer positioning) have been analysed. This chapter of the thesis critically examines the results obtained and provides a unifying rationale to the various threads noted throughout the previous sections, explaining the relevant logic underlying any conclusions reached. The conclusions also reflect upon the choices made throughout the investigation, both in simulation methodology and test methods chosen, reviewing the appropriateness of each with the benefit of hindsight.

The chapter has been ordered into general observations concerning the modelling methodology, common practical observations and themes common to all experiments. The conclusions sections focus on each set of experiments in turn, examining the specific relevance of the results, particularly with reference to the ultrasonic cleaning industry.

From these observations, further detailed concepts for future work programmes that have arisen, reflecting the desire for this thesis to act as both a catalyst and a platform by which future researchers may base their work.

7.1 General observations on the selection of modelling methodology

A detailed review of the available literature on ultrasonic cleaning and an intimate examination of the needs of an industry producing ultrasonic cleaning vessels concluded that there was a strong need within both academia and industry for a new, practical product modelling system and a related design methodology capable of accurately

predicting the bulk cavitating fields within liquids. Hence one of the stated aims of the project was the development of a system capable of simulating cavitating fields within a given geometry, and further using that simulation capability to probe many of the unanswered topics in the field of ultrasonic cleaning. In doing so the project aimed to provide a strong industrial relevance to the project and to add significantly to the available knowledge.

The selection of the modelling and simulation package aimed to provide a powerful, yet flexible solver that could be adapted to the particular needs of the task whilst still retaining an ease of use that would aid rapid development of simulations. The selection of FEMLAB and the finite element methodology met these challenges and this was confirmed by an independent, external review. The use of the finite element method facilitated the solving of models with complex internal geometries such as meshed baskets while keeping computing overheads to an acceptable level for general PC computing; an essential quality if the methodology was to be generally accepted by industry.

The FEMLAB package came pre-supplied with a number of features that greatly eased the development of the simulation methodology. Partial Differential Equations (PDE's) of the 3-dimensional pressure wave equation, along with many of the boundary conditions required for the development process could be selected as part of the acoustics mode of FEMLAB and the multi-physics and equation editors allowed the insertion of auxiliary equations, such as the "bubbly fluid formula" and the resultant transmition losses.

FEMLAB also included a CAD package and post-processing capabilities that enhanced the speed of model development which allowed the outputs to be efficiently compared with experimental results facilitating rapid evaluation of the developed process.

7.2 General Observations on the selected test methods

7.2.1 The foil ablation testing

In selecting practical testing methodologies, methods were sought that would allow a visualisation of the bulk cavitating field whilst providing numeric data that would enable quantitative comparisons of the relative strength of the cavitating fields under differing circumstances. To this end the project implemented a two phase approach to the practical verification of the simulation results to ensure consistency and accuracy..

The first method, which intended to provide a qualitative view of the cavitating field, was the foil ablation test. Foil erosion was noted as having served as an industry standard test despite its subjective nature (REF), and in comparison to other qualitative means of assessing fields, such as the Savazyan dye method or soil removal test , it proved to be a quick, trusted and valuable method. However, practical issues surrounded the use of suspended foil sheets and they occasionally proved to be a cumbersome method of testing. The foil sheets were prone to movement in the pressure fields unless weighted or clamped and preparation of the foil samples was both time consuming and delicate. Any crease or indent in the surface of the foil prior to beginning the testing attracted significant cavitation and rendered the experiment void.

However, despite some of the operational difficulties encountered with the foil test, consideration of the outcomes of the experiment made the selection of foil a worthwhile endeavour. The outputs of the foil tests provided a striking qualitative indicator and were used to good effect by overlaying images with the simulation outputs, showing the positions and sizes of cavitational hotspots against simulated expectations. The foil test was also utilised as a rapid experimental test during the prototyping phase of the project to assess the accuracy of initial models.

Consideration was given to the various alternatives to the foil test noted during the literature review, however the conclusion was reached that foil ablation would remain the method of choice. The Savazyan dye technique would require the same preparation and positioning of sheets within the pressure field and would have the added problem of

introducing the methyl blue dye to the liquid. Adding the dye would alter the properties of the liquid and could introduce a further source of error to the experimental set up.

The primary function of an ultrasonic vessel is to clean immersed loads and it would seem that particle removal or the cleaning of test strips would provide a better method of assessment of the cleaning field. However significant challenges were uncovered that made the use of load testing impractical. Commercially available soil strips, such as the 'Brownes' strips were not adequately sized and under the test conditions were subject to removal of all the test soil coating within seconds of starting the ultrasonic field. It was considered that such a short time would not be adequate to allow a steady state field to form in the liquid and could thus provide the potential for spurious results.

The possibility also arose of using a test soil that could be applied to any surface and left to dry, thus solving the issue of the size of test strip required. This method however was found to have a disadvantage in that the application of the test soil could not be guaranteed to be consistent across the surface. In order to validate these considerations the topic was raised in a session of the IEEE UFFC conference (2006) and it was confirmed by other researchers from the prestigious National Physical Laboratory (NPL) that this was indeed an issue and thus far no solution to the problem of the 'unit cleaning load' had been devised.

Given the relative subjectivity of the other qualitative methods considered and the potential pitfalls, it is still considered that the use of the foil ablation test and the results obtained justified its use.

7.2.3 Selection of quantitative methods

A review of the potential methods for quantitative measurement of the cavitating field lead to the selection of a cavitation meter that gave a numeric output relative to the strength of the field at that location. The PPB meter initially selected for its useful features proved to be a prudent choice. The in-built time averaging of cavitation values and the automatic recording of the standard deviation from this averaged value helped

both negate small fluctuations within the field and observe the variations in the field over the measured time scale.

The method of mapping the tank by 'walking' the probe through multiple data points was time consuming, but the results, when processed to form banded value contour plots, as shown in figures 6.4, 6.10a etc, gave a remarkable indicator, not only of the locations of cavitational activity, but also its relative strength in comparison to other regions within the vessel.

One major disadvantage in the use of the PPB probe was the inability of the probe to measure beneath objects suspended in the vessel, for example the load placement experiment and the basket mesh tests. This inability to penetrate all areas of the cavitating field meant that verification of some of the more startling results, such as the large predicted cavitating field beneath a suspended load (section 6.4), could not be verified directly by this probe, even if the areas that could be tested gave sufficient confidence in the simulation to validate the results.

Although initially only one probe method was selected to provide data on the project, due to links developed with the research centre of NPL, the author was invited to participate in testing of the new 'Cavimeter', an ultrasonic cavitation probe developed by the NPL team specifically to measure the cavitating fields in ultrasonic cleaning vessels. The 'Cavimeter' was used to collect ancillary data for each set of tests in the same manner as the PPB probe and had the advantage of a smaller probe receiver with a more stable output reading. Although the smaller receiver face could be used to provide a more accurate spatial resolution of results, during this thesis the resolution of data points was kept equal between the PPB and NPL probes for consistency.

Correlation of the data outputs of the two probes show a remarkable consistency in the plots produced. Figures 6.13a, 6.13b and 6.13c show the closeness of the measured results in both plots, indicating the stability of the cavitating field presented to the faces of both receivers while an examination of the output values show a relationship between

the highest and lowest values obtained over specific models. Dividing the output values into a number of predefined bands in the results section has helped highlight this link.

The scale of the individual probes has been presented in their original format out of a desire to further highlight the similarity of both sets of outputs without having to resort to normalisation of the data values. Also at present no standard measure for ultrasonically induced cavitation exists.

However, an active debate was undertaken with members of the 'Cavimeter' development team regarding the development of a comparative standard measurement unit for ultrasonic vessels and this became an aim of the project alongside the 'Cavimeter' trails.

In some results, it is noted that the PPB and NPL probes differ in both strength and location of measured hotspots. Figures 6.15a and 6.15b show not only a difference in predicted strengths, but also a deviation in the measured locations of cavitational activity. A possible explanation of this difference is that the NPL probe data was recorded several months after the PPB meter data was taken and as noted in the literature review, PZT disk transducers are prone to degradation in output values leading to a shift in strength and field distribution over a period of weeks.

It should be noted that many of these deviations occurred along the upper end of the data points (away from the radiating transducers faces and closer to the water/air boundary) and one possible cause of these fluctuations may be explained by the limitations of the model used to represent the water/air interface. These limitations will be further discussed in section 7.3, but it can be noted here that the standard deviation from averaged values recorded on the PPB meter showed a marked increase nearer the water/air boundary from an average of +/-5% to nearer 10% in some boundary regions. (A sample measurement along with measured deviations is shown in Appendix 2).

7.3 Conclusions on the general accuracy of the simulations.

From the results presented in chapter 6, it can be shown that the simulations provided a good representation of the bulk cavitating field within the ultrasonic vessels under consideration. The initial two-dimensional axis-symmetric case showed how the simulation correctly predicted the number of high cavitating regions, their position and the relative strength of each location.

The overlay of the foil and simulation output demonstrated this close correlation visually, with the positions of the heaviest eroded regions of foil overlaying those areas predicted by the model as being of sufficient negative pressure to induce cavitation in the fluid. Further corroboration of the link between the foil erosion and the simulations prediction of cavitation was seen throughout the results with the foil overlay of the simulation output matching well. A particularly good example of this can be seen in the liquid depth test in figure 12c where the positions of foil ablation match the simulation output almost perfectly, which gave confidence in the model.

There were a few discrepancies noted in the general field between the simulation and foil. Figure 6.9 highlights how although the erosions of the foil can be seen to match the number of predicted locations of cavitation, the heavy erosion and the simulation predictions deviate in locality the further from the transducer face the simulation proceeded. In particular in figure 6.9 it can be seen that the positions of actual cavitation in the centre and left of the model appear shifted somewhat left of those predicted.

A possible cause of this deviation may well be minor differences in the bonding of the transducer pair which is almost inevitable in such an experimental arrangement. Care was taken to match the transducers according to age and capacitance, but slight variation in the poling characteristics may also have lead to a slightly varied field.

A further possibility considered was that the simulation methodology displays an intrinsic error as the field diverges from the face of the transducers. Figures 6.12a to 6.12c which chart the lowering of liquid level appeared to show the match between

simulations and foil data improving as liquid level was lowered. Two prime possibilities put forth for this divergence as the field furthers from the transducer field could exist in that either the bubbly liquid clouds cause a heavier scattering of the pressure field than is accounted for in the model, or that the representation of the transducer face does not sufficiently model the pressure dispersal.

For either scenario, there is a possibility of an increasing error as the field progresses from the face of the transducers by either being progressively further dispersed by successive cavitating regions or the uneven radiation of the pressure waves diverging further as they propagate through the vessel.

Despite this relatively small deviation, the modelling methodology presented a very viable method of predicting the cavitating field. The divergence from the foil results was in most cases minor and within a few millimetres of the predicted position.

Similarly, the data outputs from the probes showed a high level of correlation with the predicted cavitational values. The placing of the data into contour plots provided a quick visual cross matching between the results and once again it was noted that the numbers and locations of bulk cavitation spots were well represented and matched the data results.

In simulations with large, clearly spaced cavitating regions, the probe contour plots show marked regions of cavitational energy spaced as almost exactly as predicted by the models. Figure 6.5, the contour plot of the axis-symmetric vessel shows this clearly, with marked divisions between the regions of cavitation.

The advantage of the probes over the use of foil was that they also differentiate between relative strengths within the bulk cavitating fields and provided qualitative output. It was also seen that the areas of higher cavitational density appear to correlate with the higher pressure markers predicted within the simulations. Figure 6.7 of the simulated cross section of the three dimensional vessel predicts a higher cavitational field in the regions

just above the face of the transducers, and again at the top of the vessel, just below the water air interface. The corresponding probe plots shown in Figs 6.10a and 6.10b also showed this higher density of cavitation above the transducers and just below the liquid/air boundary.

A perceived disadvantage of the use of the probes was in regions where high cavitational densities were spaced closely, producing a blurring of the fields on the resulting contour plots. This blurring was very evident in figures 6.9a and 6.9b where the regions towards the centre right of the vessel were blurred on the contour plots. The simulation and foil however (6.16a and 6.16b respectively) show the corresponding regions as individual cavitation spots. A potential cause of this effect may be related to the resolution of the probe measurement locations and future work undertaken will have to address the need for tighter spatial resolution of measurement if this level of resolution needed to be improved.

7.4 Discrepancies at the water/air boundary

Although the general pattern of bulk cavitation demonstrated a pleasing degree of accuracy, both in strength and location to the simulation outputs, one interesting area of deviation between the simulation and practical testing was observed. Heavy foil pitting was constantly noted on the foil test results, but was not predicted by the simulations along the upper edges of the foil sheets in the region of the water/air boundaries.

This region, in areas of the simulation with insignificant pressure amplitude to initiate cavitation, consistently demonstrated a band of pitting, some 1mm wide, heavier than other predicted null regions within the vessels. The explanation for this unpredicted cavitation may coincide with the representation of the boundary between the liquid sub domain and the air above. As a generalisation, the model parameters assumed a perfectly flat boundary condition allowing the type of specular reflection noted in section 2.2 of the literature review.

Observation of the surface of the liquid during transducer operation however showed a distinct ripple forming along the water surface that appeared to be time harmonic and possibly related to the frequency and amplitude of the transducers. This rippling effect would initiate a more diffuse scattering of the incident pressure waves leading to the superposition of reflected waves just beneath the boundary surface. It is possible that these superimposed waves generate significant negative pressures over a narrow band gap to initiate cavitation along the observed region.

An alternative viable theory to the above suggests that once again ripples in the boundary occur as observed, but rather than reflected, superimposed waves being the primary cause by exceeding the cavitation threshold, the rippling effect allows the mixing of air into the surface water increasing the dissolved gas content of the narrow band just below the surface. As noted in the literature review, small gas bubbles free floating in the liquid act as a nucleation site for cavitation by weakening the tensile strength of the fluid in the immediate vicinity. With this decrease in the tensile strength would come a corresponding drop in the negative pressures required to initiate cavitation. Either one, or a combination of both the above factors could contribute to the observed discrepancy between foil and simulation outputs, and a section in the 'future work' summary of this thesis will deal with a methodology to resolve this issue.

The failure of the probes to detect the raised cavitation levels at the surface may be explained by the operating principles of both probes. Neither are recommended for operation outside of liquid and the boundary region exhibiting the rouge cavitation were just outside of the resolution for the probe positioning. Both the resolution of measurement and accuracy of the probes near the liquid/air interface could be regarded as an issue that should be examined both for future work and during future probe developments.

7.5 Rogue homogenous 'small pitting' over foil samples

A further difference between the simulation outputs and the foil and probe results was the issue of 'small pitting' throughout the foil samples. This 'small pitting' is defined as

regions where cavitation was insufficient to completely erode a region of foil, but still peppers the surface with a fine pitting, caused by the implosions of cavitating bubbles outside the antinodes of the predicted standing wave formations. Figure 6.6 highlights a close-up of a region of foil exhibiting this 'small pitting' in detail. The simulation of the vessel geometry implies that the peak negative pressure in these regions should not rise above the values suggested for cavitational inception.

Probe data from both the PPB and NPL Cavimeter confirm the presence of an homogenous distribution of weak cavitational activity throughout the vessel. Both cavitational probes never registered a zero cavitational value in any region of the vessel under test despite regions of extremely weak cavitational activity.

A possible cause for this errant cavitation has already been debated in the preceding section detailing the instability and practical approximations applied to the representation of the water/air interface. The simulations assumed a perfectly flat boundary whereas in practice, the radiated pressure waves caused a rippling of the surface creating a distortion of the primary reflected pressure wave.

Some evidence for this cause is provided by the load placement (section 6.4) and punched hole basket (section 6.6) experiments whereby the foil sampling showed a far lower incidence of 'small pitting' than examples where the primary pressure wave reflected unhindered from the water/air boundaries.

A further possible cause of the manifestation of small pitting was flexure of the vessel walls. Although this flexure was considered negligible when compared to the radiated pressure field, the resultant displacement of liquid caused by vessel wall vibration may have been sufficient to cause a small dispersal of the standing wave field resulting in the observed fine pitting. Although negligible to the bulk cavitating fields responsible for the heavy erosion of the foil, this homogenous fine pitting does represent an area for improvement in the overall model and as such is included in the future work section, whereby possible theoretical solutions to both the above causes are put forward.

7.6 Remarks on specific experimental results

Having made general conclusions drawn from across the spectrum of work, a detailed examination of specific conclusions drawn from individual tests will be made. These were used to assess the flexibility of the model and simulation methodology against a number of test parameters and add significantly to the knowledge base in areas the literature review showed to be lacking in.

7.6.1 Conclusions on the two dimensional axial-symmetric case

The axial-symmetric case was designed to prove the initial mathematics and modelling technique in the development of a full methodology. Its inclusion in the results shows a desire to demonstrate the logical progression from base modelling and proof of concept through to more industrially relevant cases. As such, the single transducer design, coupled with an uncomplicated geometry was considered ideal as a starting point to test the mathematical modelling foundations of the method developed.

Use of a two dimensional axial symmetric mode of computation also demonstrated the low level but memory efficient mode of solving the model, allowing prototypes to be simulated, tested and re-simulated, varying parameters in the fluid and equations to gauge accuracy.

The results provided a reasonable co-incidence with both the foil and probe outputs for the vessel, providing a good level of initial confidence. The number, and position of the major regions of cavitation (the bulk field) were shown by the simulation and subsequently verified by the foil and probe tests. The vessel itself showed that the predominant cavitating field lay in a direct line between the transducer face and the water/air boundary, with little cavitation occurring to the sides of this main beam. The probes also showed that the relative strength of the cavitating field diminished as it radiated away from the source, also as predicted by the simulation, and strengthened toward the liquid/air boundary. This simplified field was a result of both the single transducer and the uncomplicated geometry of the vessel and the resurgence of the

cavitational strength toward the upper region of the vessel a factor of the superimposed reflections from the waters edge.

The cavitating field does however show some regions of fine pitting across the bulk of the foil sample and a line of heavier than predicted erosion beneath the water/air boundary. Both these deviations between foil and data are common to all samples and have been discussed earlier in this chapter.

Although an excellent vessel on which to base initial observations, the axial symmetric mode of simulation can only be applicable to a very limited geometrical range. Vessels exhibiting any variation in geometry, or non-symmetric features such as drainage holes and configurations of multiple transducers cannot be accurately represented by this version of the model and therefore the model is not applicable to the bulk of commercially available vessels.

It should be noted however that for any vessel meeting the specific geometrical needs of the axial symmetric mode of simulation, this method requires a far lower computing overhead and has a quicker solution time that either the two or three dimensional models that follow.

7.6.2 Conclusion of the two dimensional versus three dimensional modelling methodology

Given the geometric limitations of the two dimensional axially symmetric model, it was clear that a simulation method capable of representing enhanced features of ultrasonic cleaners would be required. Often, the centre line of the ultrasonic vessel is of interest when examining the cavitating field and therefore it was possible that a two dimensional approach to the modelling may be applicable. The two dimensional model also represented a logical advance over the axially-symmetric version

The comparison of the two versus three dimensional models was performed to gauge the accuracy of both and help identify a clear path for this thesis. The simulation output of the two dimensional case had the pressure field forming standing waves again between the radiating face of the transducers and the water/air boundaries. The three dimensional slice taken along the same axis as the two dimensional plot for comparison also had the pressure fields predicting a cavitation standing wave pattern above both transducer faces, but in this example a difference of field could be noted from the two dimensional case and significant mixing and spreading of the cavitating regions between the two transducers.

It is surmised that these regions of difference between the two patterns are a result of the reflections from the vessel boundaries not included within the two dimensional case. An examination of the foil and probe results show that although the two dimensional case was seen to exhibit some matches with the practical results, it was the three dimensional model that more accurately described both location and strength of cavitation. The overlay of foil and simulation showed a marked correlation between both, with the deviations towards the upper area of the vessel described earlier in these conclusions.

The probe plots also concur with the simulation outputs quite strongly, marking not only positions of cavitational hotspots, but also giving a good account of the relative strengths of the regions cavitation, predicting high activity in significant regions predicted by the simulation (i.e. directly above the transducer face and in regions just below the water

The results of this test have shown conclusively that in order to represent an ultrasonic vessel of the type commonly available, a three dimensional representation was required. Further advantages of the three dimensional method also included the ability to represent off-centre features of ultrasonic vessels. A peer reviewed paper by the author[109] provided a clear account of this failing of the two dimensional model when faced with an off centre drainage hole common to benchtop units, but with a full three dimensional methodology, such features could be correctly accounted for.

7.6.3 Conclusions on the effect of reducing liquid levels on the cavitating field

Throughout the literature review, it was noted that a distinct lack of data existed on the effects of any environmental variables on ultrasonic cavitating fields. Whereas many of the variables were altered to suit cleaning cycles, such as temperature or liquid viscosity (via the introduction of surfactants), it was noted that the liquid level, a user variable parameter, had no specific information on the effects of varying.

The experiment consisted of reducing the water level in half wavelength steps to assess the effects on both location and strength of the fields. It can be shown from section 6.3 that lowering the wavelength by 0.5λ did not greatly affect the overall field in comparison to the three dimensional case which represented a complete fill level. A corresponding lowering of the number of antinodes in the vessel was noted, which was predicted by theory as forming every half wavelength, and some distortion of the field was also present. However, overall both predicted fields showed similarity.

The foil and probe comparisons to the 0.5λ case showed a good level of correlation but with an increasing deviation from the simulation further away from the transducers, as noted earlier.

The results for lowering the liquid by 1λ and 1.5 λ showed a distinct alteration of the standing wave field when compared to either the full, or 0.5λ cases. Locations of the bulk cavitating field changed significantly as a result of the reflections from the lower liquid level as did the strengths of the predicted pressure fields.

The foil and probe data helped provide verification of these simulations, with the foil especially showing a better degree of accuracy in the lower liquid levels. It was a logical assumption that radiating the same power into a smaller volume of liquid should result in a greater energy density of cavitation within the vessel and these results confirmed this.

This experiment has added to the existing knowledge by showing definitively that liquid level does play an important role in the cavitational effect. A possible development that could stem form this testing would be the simulation of variant liquid levels with a higher resolution than conducted here to ascertain whether an 'ideal' point exists in terms of liquid depth to cavitational strength, or weather beyond a point, the cavitational energy diminishes due to excessive cavitation above the transducer faces.

7.6.4 Conclusions stemming from the introduction of a free suspended load

Considering the intended use of ultrasonic cleaners to remove particles from the surface of an object suspended within the fluid, very little information was uncovered as to any effects of introducing a load upon the cavitating field. Anecdotal evidence within the sponsoring company warned against over filling ultrasonic baskets due to diminished cleaning capabilities, although no actual test data existed. Bretz et al[47] provided the only attempt at simulation of a suspended load uncovered in the literature review, but this consisted of a hollow metal tube placed toward the upper reaches of the test vessel and was unperturbing to the field.

The test undertaken consisted of suspending a large (relative to the vessel geometry) load within the vessel with the particular intention of perturbing the ultrasonic field whilst noting any effect on the cavitation produced.

The simulation output showed a distinct lowering of peak pressure amplitudes in the region above the suspended load whilst predicting an extremely powerful field directly beneath the load. This was surmised to be an effect of the reflection of the pressure waves from the base of the load causing a shadowing effect directly above the load itself.

Due to the positioning of the load and its size, it was not possible to either suspend foil beneath the load, nor to collect probe data from the area. Despite this handicap, the test results obtained above the load surface show a good match to the fields predicted in the simulation. The foil showed strong erosion in a number of predicted regions whilst the probes both confirmed higher cavitational activity present in the zones predicted by the

simulation. Evidence of the shadowing effect predicted by the simulation was found in that the foil sheet showed smaller bulk erosion zones and contained less of the 'fine pitting' over the surface area, as mentioned earlier.

Data from the probes also show a corresponding weakening of the cavitational field above the suspended load, whereas the regions just to the side of the load, where a gap existed between the vessel wall and the load edge show a higher cavitational value where pressure was able to radiate through.

Although no empirical data from beneath the load could be ascertained, due to the accuracy of the model under this test condition, it was concluded with reasonable confidence that the cavitating field beneath the load would be very strong.

The conclusions of this test have important implications for the ultrasonic industry. A weak field and a shadowing effect would equate to a poor cleaning performance and thus baskets should not be over loaded. The presence of the suspected strong field beneath, while at first glance may appear to provide a strong cleaning field, may in fact damage delicate items presented to it. As a result of these findings a careful assessment of load positioning and further testing is advocated in the future work section.

7.6.5 Alternative bonding positions of transducers - conclusions and remarks

The placement of transducers on the base of the vessel, radiating towards the water/air interface appears from the literature review and an examination of the state of the art in industry, to be a standard configuration, although during the research conducted for this thesis no significant explanation was uncovered as to why this would be so. This section of the results aimed to broaden the available knowledge on ultrasonic cleaners by investigating two alternative locations for transducer bonding and cross comparing the results to the standard pattern with a view to critically assessing the benefits and drawbacks of the alternative arrangements.

Initially a test was performed with one transducer bonded centrally to the base of the vessel and another bonded to the vessel side. The results of the simulation showed an interesting dispersal of the standing wave field with reference to the standard pattern shown in figure 6.7b. A superposition of the two transducer pressure fields results in a high pressure field toward the centre of the vessel liable to affect a strong cavitating field. The simulated field however showed a marked asymmetry in the predicted strengths of the left and right hand sides of the vessel, with the right hand side being weaker than left.

An examination of the foil and probe data confirmed this finding with lower erosion and lower cavitational field strengths recorded to the right hand side of the vessel. Again prediction of the erosion becomes less accurate as we move away from the transducer faces, this time towards the right of the vessel. The left hand side however demonstrates a good match.

The second examined configuration of transducer bonding had both transducers bonded to the sides of the vessel with the resultant simulated pattern forming distinctive bands of energy in the horizontal plane of the vessel as a result of superposition. Again the maximum fields were predicted toward the centre of the vessel but once again there was symmetry between both sides of the fields within the vessel.

Probe and foil tests again confirmed the simulation result, with the foil providing perhaps the most closely matched pattern of all the tests conducted. Some blurring and overlapping of what were simulated as clearly defined cavitational areas were noted by the probe readings, but as mentioned above, this may have been due to spatial resolution of the probes.

The results of this subset of tests were deemed highly valuable, not only as they added to the cannon of knowledge concerning ultrasonic cavitation, but also in that, given the results from the load placement experiment with traditional placement of transducers, the alternatives discussed in this section may provide a viable alternative. The first

configuration of transducers would suffer in that the in-homogeneity between the left and right hand sides would result in an uneven cleaning effect. The second transducer configuration however may well yet provide a solution to the reflection of waves from the base of a suspended load by radiating equally across the top and bottom regions of the cleaning load.

7.6.6 Conclusions on the varieties of basket mesh studied for ultrasonic cleaners

From the reviews conducted in the initial phase of this research, it was noted that an essential component of any ultrasonic cleaning system was a system of suspending the load in the liquid. Items could not be placed on the base of ultrasonic vessels due to wear of the vessel and potential damage to the object from the vibrations of the transducers. No literature was uncovered however during the literature review noting the effects of baskets upon the cavitating field. This set of experiments aimed to add to the existing body of knowledge by comparing two varieties of basket mesh, one open, one punched hole and noting the effects on the cavitational field. The results of this set of tests were expected to provide a valuable guideline to the industry as the design and selection of baskets for future use.

The first experiment considered a basket with an open mesh structure which gave simulation results remarkably similar to those without a basket present. A comparison between figures 6.21a (with basket) and 6.7b (without basket) show that the predicted field hardly alters in either locations or strengths of the predicted fields, with the only disconcernable difference being a small blurring of the edges of the pressure zones above the basket mesh in figure 6.21a.

Foil and probe results again could only be gathered from the regions above the basket mesh and the correlation between the two for the open mesh provided a good match. Some regions of expected cavitation from the simulation were misplaced in the regions above the basket mesh, but these were not considered significantly shifted compared to the simulation outputs. The probe data taken in those regions agreed with the locations

provided by the simulation outputs and the strengths of the cavitating fields also reflect the simulations.

The second basket type, with the punched hole base provided a significant variation both in the simulations and the measured outputs. The simulated pressure field altered completely to form bands in the horizontal both above and below the basket mesh, with the strength of field above the mesh significantly reduced. An examination of the foil data showed this to be true, with lower erosion patterns than expected in the regions above the basket and the probe results showing reduced field strength throughout the upper regions of the vessel.

The conclusions drawn from these results showed that the open basket type is preferential to the punched hole variety for the positioning of loads within the ultrasonic vessel. The lowered cavitational strength associated with the punched hole variety may lead to inconsistent cleaning and therefore would not be appropriate under critical cleaning conditions. The punched hole mesh however presents advantages to the mesh variety basket when considering the positioning of small objects within the vessel. It remains to be proven whether varying the aperture or thickness of a mesh type basket would produce better cavitational profiles whilst still maintaining the ability to handle very small objects.

7.7 Future work and directions of study

Throughout this body of work, it has been a stated aim of the project to add significantly to existing academic literature, whilst maintaining a strong industrial relevance. However, whilst the literature review uncovered a direct set of challenges that this thesis has provided answers for, the results obtained raised further questions that this author believes deserves investigation due to their intrinsic relevance both to general ultrasonics and specifically the ultrasonic cleaning industry.

- The intention that the simulation methodology could be applied by industry as a toolset for evaluating ultrasonic cleaning vessel design, one possible avenue of

work should be the optimisation of the modelling methodology to run as efficiently as possible whilst still maintaining an acceptable level of accuracy. To this end, an investigation of alternative modelling techniques or alternative FE packages could be considered against the computational burden and accuracy of the results.

- As an expansion of the above theme, adjustments to the modelling methodology could be considered to improve some of the discrepancies noted both in the results and these conclusions. A possible cause of both the boundary discrepancy and a possible cause of the fine pitting observed across samples was given as the representation of the water/air boundary as a flat interface. A solution to this would be the adaptation of the deforming mesh formulations in recent releases of FEMLAB (Now COMSOL Multiphysics) that use an Arbitrary Lagrangian-Eulerian (ALE) formulation. Coupling this ability to deform the geometry and surrounding mesh to the pressure wave propagation would allow the surface ripples of the vessel to be modeled and hence the reflected pressure profile more adequately represented. It was also noted that the mechanical flexure of the vessel walls may also have lead in part to minor variations between the simulation and practical test data. The ability to couple the pressure and mechanical flexure of vessel walls would be possible within the FEMLAB package and as such could be incorporated into the model.
- The output of the simulation managed successfully to tie regions of high negative pressure to both foil erosion and cavitational power as measured by two independent probes. A further step in the development of this work would consider a method of linking the cavitational power and erosion of foil to cleaning efficacy. Although this may seem a simple step, the development of a unit cleaning load to assess ultrasonic vessels has proved problematic. Some of the issues involved, such as even application of the cleaning load to a surface and what would constitute a typical 'load' have already been discussed earlier in this chapter, but further issues such as the particle size and composition and a quantitative measure of cleanliness would need to be defined.

- It should also be noted that the simulations and tests conducted were only proven over a narrow range of environmental variables. Having found in the literature review a strong cavitational dependence on environmental variables such as temperature, a strong control of experiments program was put in place to prevent destabilisation of the results. Some work was conducted along with the industrial partner into the effects of heat on cavitational strength and also water hardness, but much work remains to be done. A full factorial experiment into the environmental variables would be deeply desirable as would testing the simulation outputs against practical data under a range of environmental conditions.
- Given the high level of confidence developed in the model, a future development may be to use the simulation capabilities to test configurations of ultrasonic tank geometry and transducer placements with a view to developing an optimised tank. Some of the desirable features of this optimised vessel would be an homogenous cavitating field that could prevent shadowing effects from introduced baskets or cleaning loads.
- Given the above view of a homogenous cleaning field and the confidence in the simulation, a method has been simulated by the author as a direct result of this programme of work providing a method of dispersing the standing waves in the cavitational field. Phased arrays have been used in non destructive testing (NDT) as a means of sweeping a focused beam along an object to detect cracks rather than having to physically move the probe along the surface. This technique has been applied by the author to a two disk ultrasonic vessel as used in the bulk of these tests to examine the concept of dispersing the cavitating field by varying the phase of the supply frequency to each individual transducer. The results below show how lagging the phase of the left hand transducer, then lagging the phase of the right hand transducer creates a dramatic sweep of the field. Unfortunately the technology was not available within the sponsoring company to test the concept, but it is felt that the concept is of sufficient merit to pursue further.

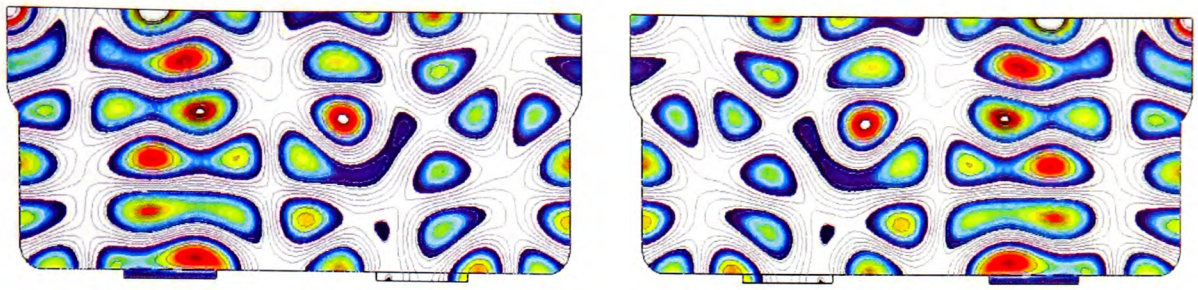

Figure 7.1: Left and right sweeping of the cavitating field as a result of altering phases of the frequency of the transducers by 30°

7.7 Summary

The primary stated aim of the programme of work was to create an original contribution to knowledge, with strong industrial relevance to those industrial sectors utilising ultrasonics. The formulation of the questions that would comprise the backbone of this investigation flowed directly from the comprehensive literature review presented in chapter 2 and fulfilled a two fold purpose. Firstly, the subject area was identified as being under-represented in the academic literature and secondly as being of particular commercial relevance to the manufacturers of ultrasonic cleaners.

The body of this work, having formulated a clear set of aims then describes the methodical development of a mathematical model and simulation toolset. Commencing with fundamental equations, and progressing in logically defined stages to the creation of a full 3D simulation, this toolset has been applied to answer a number of questions of special relevance uncovered in the literature review. Results from these simulations were compared throughout the process to the data from two independent measurement probes and also from foil erosion test data, which showed a pleasing level of correlation.

Comparisons are drawn between 2D axis-symmetric, 2D and 3D cases, assessing the appropriateness of each and highlighting the need for a full 3D simulation for the successful design of the majority of benchtop ultrasonic vessels. The effects of liquid level are also discussed showing how the liquid fill level of an ultrasonic bath should be

strongly considered by manufacturers of ultrasonic baths given the variances of the cavitating field shown during the experiment.

Of particular interest were those experiments where a load and basket mesh were introduced to the vessel creating a clear 'shadowing' effect in the cavitating field that would result in a detrimental cleaning effect. Manufacturers of ultrasonic vessels should pay particular heed to these results, in particular the design of basket meshes where an open mesh was shown to cause considerably less disruption and shadowing of the cavitating field than a 'punched hole' basket variety.

A potential solution to the shadowing effect of load and basket placement is however discussed, whereby the location of the bonded transducers were investigated, demonstrating a dispersal of the cavitating field that could negate the shadowing effects previously mentioned.

Minor deviations from the predicted field were however noted in the results, and a discussion of the potential causes, implications and solutions to these discrepancies are developed in the concluding chapters, some of which form a list of future work that has been identified from the experiments undertaken.

Overall it is shown that this body of work adds significant new knowledge to the existing cannon of ultrasonics, answering a number of relevant questions through a logical thought process and competent investigative techniques. However, more than presenting a set of informative results, it is hoped that the work contained in this thesis will act as a guide to industry in its thinking on some of the many parameters affecting cavitation and ultimately form the basis for future researchers wishing to advance our knowledge of this fascinating topic.

References

[1] Eisenberg R. (1992) *Radiology: an illustrated history*. St. Louis: Mosby

[2] J. J. Knight. (1968) Effects of airborne ultrasound on man. *Ultrasonics*, 6(1), 39–41.

[3] Howard, Carl Q., Hansen, Colin H. & Zander, Anthony C. (2005) Review of Current Recommendations for Airborne Ultrasound Exposure Limits *Proceedings of Acoustics 2005 9-11 November* Busselton, Western Australia pp1-4

[4] Becker, J.F. (1994) Ultrasonic Frequency Selection for Aqueous Fine Cleaning. NASA Report No NASA -CR-200308 Presented at *Aerospace Environmental Technology Conference*, Huntsville, AL, USA 10th August 1994

[5] Puskas, William L. (2005) *Systems and methods for ultrasonically processing delicate parts*. US patent No. 6016,812. Jan 25, 2000

[6] Young, Ronald F. (2005) *Sonoluminescence*: Florida: CRC press

[7] Qi, Quan., Johnson, Robert E., & O'Brien, Jr., William D. (1994) Ultrasonic cleaning of the skin surface, *The Journal of the Acoustical Society of America*, 95(5), 2830

[8] Cafruny, WA., Brunick, A., Nelson, D.M. & Nelson, R.F. (1995) Effectiveness of ultrasonic cleaning of dental instruments. *American Journal of Dentistry* 1995 Jun; Vol 8(3), 152-6.

[9] Detweiler. M.S. (1989) Ultrasonic cleaning in the hospital. *Journal of healthcare Management*. 7(3,) 46-48

[10] Bubb. J.R. & Bradley, C.R. (1995) Endoscope decontamination: where do we go from here. *Journal of Hospital infection*. 30(1,) 543-551

[11] Watmough, D.J. (1994) Role of ultrasonic cleaning in control of cross infection in dentistry. *Ultrasonics*, 32(4), 315-317

[12] Sabir, N. & Ramachandra, V. (2004) Decontamination of anesthetic equipment. *British journal of Anesthesia – Continuing education in anesthesia, critical care and pain*. 4(4), 103-106

[13] Frazer, Lance. (2004) A Cleaner Doctor's Kit: Tiny Bubbles Mean Huge Improvements, *Environmental Health Perspectives*, 112(2), A108-A111

[14] Marangopoulos, I.P., Martin, C.J. & Hutchinson, J.M.S. (1995) Measurements of field distributions in ultrasonic cleaning baths: implications for efficiency. *Physics in Medicine and Biology* 40(11) 1897-1908

[15] Sherman, C.H. (1975) Underwater sound – A review. Pt (1) Underwater sound transducers. *IEEE Transactions on Sonics and Ultrasonics*, 22(5), 281-290

[16] Woollett, R.S. (1957) Transducer comparison methods based on the electromechanical coupling coefficient concept. *IRE National convention Record*, pt.9, pp23-27.

[17] Savage, H.T., Clark, A.E. & Powers, J.M. (1975) Magnetomechanical coupling and ΔE Effect in highly magnetostrictive rare earth FE_2 Compounds. *The 13th international conference on magnetics*, April 1975

[18] Pomirleanu, R. & Giurgiutiu, V. (2004) High-Field Characterization of Piezoelectric and Magnetostrictive Actuators. *Journal of Intelligent Material Systems and Structures*, 15(3), 161-180

[19] Katzir S. (2003) From explanation to description: Molecular and phenomenological theories of piezoelectricity. *Historical studies in the physical and biological sciences.* 34(1), 69-94.

[20] Susslick, K.S., Medleleni, M. & Ries, J.T. (1997) Chemistry induced by hydrodynamic cavitation. *Journal of the American Chemical Society,* 40(11), 9303-9304

[21] Moholkar, V.S., Nierstrasz, V.A. & Wamoeskerken, M.M.C.G. (2003) Intensification of mass transfer in wet textile processes by power ultrasound. *Autex Research Journal,* 3(3),

[22] Berliner, S. (2000) *Keywords* [online] Available from: http://home.att.net/~Berliner-Ultrasonics/ [Accessed August 2005]

[23] Mason, T.J. (1999) Sonochemistry: Current Uses and Future Prospects in the Chemical and Processing Industries, *Acoustic Cavitation and Sonoluminescence,* 357(1751), 355-369

[24] Gendanken, A. (2004) Using sonochemistry for the fabrication of nanomaterials. *istry,* April 11(2), 47-55

[25] Gaitan F.D. & Holt G.R. (1996) Observation of Stability Boundaries in the Parameter Space of Single Bubble Sonoluminescence. *Physics Review Letters* (77), 3791 - 3794

[26] Taleyarhkhan, Rusi P. Dr. (2002) Evidence for Nuclear Emissions during Acoustic Cavitation, *Science* , 295(5561), 1868-1873.

[27] Morgan, Alan. (2005) *Guidance on EC Regulation No 2037/2000 on substances that deplete the ozone layer*, (online) Department of Trade and Industry. Available from http://www.dti.gov.uk/innovation/sustainability/ods/page29091.html (Accessed October 05)

[28] BCC Research (nda) *The Ultrasonics business and markets in the U.S.* Available from http://www.bccresearch.com/mfg/MFG013B.asp (Copy obtained march '06)

[29] Apfel, R.E. (1984) Acoustic cavitation inception. *Ultrasonics*, 22, 167-173.

[30] Chen, W., Chen, X., Lu, M., Miao, G. & Wei, R. (2002) Single bubble sonoluminescence driven by a non simple harmonic ultrasounds. *Journal of Acoustical Society of America*, 3(6), 2632

[31] NASA (2001) Procedures for cleaning of systems and equipment for oxygen service. *NASA Langley research center* (document number LAPG 1740.5), July

[33] Zeqiri, B., Hodnett, M. & Gelat, P. (2000) *Establishing a reference ultrasonic cleaning vessel.* NPL Report CMAM55, (Sept)

[34] Chivate, M.M. & Pandit, A.B. (1995) Quantification of cavitation intensity in fluid bulk. *Ultrasonics Sonochemistry,* 2(1)

[35] Wu, Y., Franklin, C., Bran, M. & Fraser, B. (1999) Acoustic property characterization of a single wafer megasonic cleaner. *The Electrochemical Society conference on Cleaning Technology in semi-conductor device manufacturing VI.* pp360-368, October 1999, Honolulu.

[36] Blitz, J. (1971) *Ultrasonics – Methods and Applications*. London: Butterworth and Co

[37] Papadakis, E. (1999) *Ultrasonic instruments and devices.* Academic press.

[38] Bereziat, D., Doche, M.L., Chaillet, P., Lorimer, J.P., Mason, T.J. & Pollet, B. (2000) *Double structured ultrasonic high frequency reactor using an optimized slant bottom. Ultrasonics Sonochemistry,* (7) 201-205

[39] Ceramtec group. (nda) (online) Available at www.ceramtec.com (Accessed January 2005)

[40] Moreno, E.; Acevedo, P.; Fuentes, M.; Sotomayor, A.; Borroto, L.; Villafuerte, M.E.; Leija, L. (2005) Design and construction of a bolt-clamped Langevin transducer. *2nd International Conference on Electrical and Electronics Engineering*, 7-9 Sept. : 393 - 395

[41] V. V. Goncharuk and V. V. Malyarenko. (2007) The study of sound absorption in water, *Journal of Water Chemistry and Technology*, 29(2), 65-71

[42] Suslick, K.S. (1989) The chemical effects of ultrasound. *Scientific American*, Feb 80-85

[43] Becker, J.F. *Ultrasonic frequency selection for aqueous fine cleaning*. NASA Report No NASA-CR-200308. Presented at the Aerospace Environmental Technology Conference. Huntsville, USA (10th August, 1994)

[44] McQueen, D.H. (1985) Frequency dependence of Ultrasonic Cleaning. *Ultrasonics*, (24), 273-280

[45] Ziskin, M.C., Lewis, P.A. & Ziskin, P. (1993) *Ultrasonic exposimetry*. Florida: CRC Press

[2.16] Notting, G. & Neppiras E.A. (1980) Acoustic cavitation. *Physics Reports* 61, 159-251

[47] Bretz, N., Strobel, J., Kaltenbacher, M. & Lerch, R. (2004) Numerical simulation of ultrasonic waves in cavitating fluids with special consideration of ultrasonic cleaning. *Presented at the IEEE UFFC symposium.*

[48] Qi, Q., O'Brien, D(Jr)., & Harris, J.G. (1995) The propagation of Ultrasonic Waves through a bubbly liquid into tissue: A linear analysis. *IEEE Transactions on Ultrasonics, Ferroelectrics and Frequency Control*, Vol 42(1).

[49] Suslick, K.S. (1989) The Chemical Effects Of Ultrasound. *Scientific American*. (Feb), 80-86

[50] Halliday, D. & Resnick, R. (1970) *Fundamentals of Physics*, New York: Wiley and Sons Inc pp323-325.

[51] Shu, J. (2003) Modeling vaporous cavitation on fluid transients. *International journal of pressure vessels and piping*, 80, 187-195.

[52] Or, D., & Tuller, M. (2002) Cavitation during desaturation of pourus media under tension. *Water Resources Research*, 38(5), 19-22.

[53] Newnham, R.E., Hiremath, B.V. & Rosen, C.Z. (1992) *Introduction to underwater acoustics*. Springer

[54] Etter, P.C. *Underwater and acoustic modeling and simulation (3rd ed)*. UK: Spon Press

[55] Elmore, W., Heald, M. & Bhatia, A. (1985) *Physics of waves*. Dover: Courier Publications

[56] Kirkup, S. (nda) *The Boundary element method in acoustics (1st ed)*. (online) Science books.net. Available at www.boundary-element-method.com/acoustics/manual/chap1/index.htm [Accessed 21/05/05]

[57] Ericson, K.R., Fry, F.J., & Jones, F.J. (1974) Ultrasound in medicine – a review. *IEEE Transactions on Sonics and Ultrasonics*, SU-21(3)

[58] Kwak, H.Y. &Panton, R.L. (1985) Tensile strength of simple liquids predicted by a model of molecular interactions. *Journal of PhysicsD: Applied Physics* 18, 647

[59] Herbet, E., Balibar, S. & Caupin, F. (2006) *Cavitation pressure in water. Phys.Rev.E.*, 41603-41625

[60] Trevena, D.H. (1967) The behavior of liquids under tension. *Contemporary Physics*, 8, 185-195

[61] Message, D., Sette, D. & Wanderlingh, F. (1967) Effects of solid impurities on cavitation neuclei in water. *Journal of Acoustical Society of America*, 41, 573-583

[62] Crum, L.A. (1979) Tensile strength of water. Nature, 278, 148-149

[63] Private correspondence, Professor Min Joo Choi (Visiting professor at the NPL high powerd ultrasound research group)

[64] Leighton, T.G, Richards, S.D. White, P.R (2004) Wall of sound: The bubble nets of humpback whales. *Institute of acoustics bulletin*, 29(1). 26-31 (Jan/Feb).

[65] Bechet, E. Cuilliere, J.C. Trochu, F. (2002) Generation of a finite element mesh from stereo-lithography (STL) files. *Computer Aided Design*. 34(1), 1-17.

[66] Schechter, R. Simmonds, K. Batra, N. Mignogna, R. Delsarto, R. (1999) Use of a transient wave propagation code for 3D simulation of CW related transducer fields. *Ultrasonics*, 37, 89-96.

[67] Harari, I. & Hughes, T.J.R. (1992) A cost comparison of Boundary element and finite element methods for problems of time harmonic acoustics. *Applied mechanics and engineering*, 97, 77-102

[68] Nikitin, I. Nikitin, L. Frolou, P. Goebbels, G. Goebel, M. (2002) Real time simulation of elastic objects in virtual environments using finite element method and computed Green's functions. *Eighth Eurographics workshop on virtual environments*, pp46-51

[69] Ottosen, N. and Peterson, H. (1982) Introduction to the finite element method. Prentice Hall: London.

[70] Huang, C.H. Ma, C.C., Lin, Y.C. (2005) Theoretical, numerical and experimental investigation on resonant vibrations of piezoceramic annular disks. *IEEE Transactions on Ultrasonics, Ferroelectrics and frequency control*, 52(8), 1204-1216

[71] Yong, X. Chun, P. Xuelian, P. Shi, K. Xigang, X and Wenlong, S. (2004) Study of mixing frequency phased array. Proceedings of the 16th world conference on Non-Destructive Testing (WCNDT2004) 393-400.

[72] (2002) *S.A Pressure waves induced by megasonic agitation in a LIGA development tank*. Sandia National Laboratories for the US Department of Energy. Report SAND2002-8333. (online) Available at www.ca.sandia.gov/liga/pdfs/02_8333.pdf] [Accessed May 2005]

[73] Harkin, A., Nadim, A. & Kaper, J. (1999) On acoustic cavitation of slightly sub-critical bubbles. *Physics of fluids*, 2, 274-287.

[74] Crighton, D.G. (1991) Non-linear acoustics of bubbly liquids. *In* Kuwick, A. (ed) *Non-linear waves in real fluids*. Springer publishing

[75] Olson, L.G. (1998) Finite element model for ultrasonic cleaning. *Journal of sound and vibration*, 126(3), 387-495

[76] Olson, L.G. & Yang, Y. (1993) Simplified models for ultrasonic cleaning: wave incidence and angle effect. *Computational mechanics*, 12(4), 245-254

[77] Dahnke, S. Swamy, K.M. & Keil, F.J. (1999) Modeling of three dimensional pressure fields in sonochemical reactors with an inhomogeneous density distribution of cavitational bubbles. Comparison of theoretical and experimental results. *Ultrasonics Sonochemistry*, 6, 31-41.

[78] Dahnke, S. and Keil, F.J. (1998) Modeling of three dimensional linear pressure fields in sonochemical reactors with homogenous and inhomogeneous density distributions of cavitation bubbles. *Industrial and Engineering Chemistry Research* 57(5)

[79] Shimada, M. Kobayashi, T. & Matsumoto, Y. (1999) Dynamics of the cloud cavitation and cavitation erosion. *The 3rd ASME/JSME Joint fluids engineering conference*. San-Francisco, California. pp6775-6777

[80] Lauterborn, W., Mettin, R. and Krefting, D. (2004) High speed observation of acoustic cavitation erosion on multi-bubble systems. *Ultrasonics Sonochemistry*, 11(3-4), 19-23.

[81] Health Technical Memorandum 2030: *Washer disinfectors – validation and verification*. London: The stationary office pp145-148 (1997)

[82] Sarvazyan, A.P. Pashoukin, T.N. & Shilinkov, G.V. (1985) An extremely simple and rapid method of registration of ultrasonic field patterns. *Proc.Ultrasonics.International* London:Butterworths, pp127-133

[83] Watmough, D.J. (1994) Role of ultrasonic cleaning in control of cross-infection in dentistry. Ultrasonics, 32(4), 315-5.

[84] Van Eldik, D.A. Zilm, P.S. Rogers, A.H. & Marin, P.D. (2004) An SEM evaluation of debris removed from endontic files after cleaning and steam sterilization procedures. *Australian Dental Journal*, 49(3), 128-135.

[85] Hodnett, M. Zeqiri, B. Lee, N. (2003) Novel sensors for the occurrence of acoustic cavitation. *Proceedings of the Institute of Acoustics*, 25(1).

[86] Walmsley, A.D. and Williams, A.R. (1991) *Measurement of cavitational activity within an ultrasonic bath.* Journal of Dentistry, 19(1), 62-6.

[87] Yao, G. & Wang, L.V. (1999) Full field mapping of an ultrasonic field by light source synchronized projection. *Journal of the Acoustical Society of America*, 106(4), 36-49.

[88] Martin, C.J. & Law, A.N.R. (1980) The use of thermistor probes to measure energy distribution in ultrasound fields. *Ultrasonics*, 18, 127-33.

[89] Wong, K. George, S & Lixue, W. (2002) High power ultrasound standard. *Journal of the Acoustical Society of America*, 3(4), 1791-1799

[90] Lihn, J.Y., Bereziat , D., Doche, M.L., Challiet, P., Lorimez, J.P. Mason, T.J. & Pollet, B. (2000) Double-structured ultrasonic high frequency reactor using slant bottom. *Ultrasonics Sonochemistry,* (7), 201-205.

[91] Flynn, H.G. (1984) Physics of acoustic cavitation in liquids *In* Mason, W.P. (ed) *Physical acoustics,* New York: Academic

[92] Gachagan, A., Spiers, D. & McNab, A. (2003) The design of high powered ultrasonic test cell using finite element modeling techniques. *Ultrasonics,* 41, 283-288

[93] Abramov, Oleg V. (1998) *High Intensity Ultrasonics: Theory and Industrial Applications.* Taylor & Francis

[94] Ottosen, Niels. & Peterson, Hans. (1992) *Introduction to the Finite Element Method.* London: Prentice Hall

[95] Frolkovic, P. (1998) Maximum principle and load mass balance for numerical solutions of transport equation coupled with variable density flow. *Acta Mathematica Universitatis Comenianae,* LXVII (1), 137-157

[96] Mish, K.D., Mellow, J. (1998) Computer Aided Engineering. *In* Kreith, F. (ed) *Mechanical Engineers Handbook.* Boca Raton: CRC Press p43

[97] Wu, R.S. & Xie, X.B. (1995) A complex screen method for modeling elastic wave reflections. *SEG Technical Program Expanded abstracts: 2169-1273*

[98] Padilla, F. Bossy, E. Laugier, P. (2006) Simulation of ultrasound propogation through three dimensional trabecular bone structures: comparison with experimental data. *Japanese Journal of Applied Physics,* 45(8a), 6496-6500

[99] Standards Association of Australia (1999) *Ultrasonic cleaners for healthcare facilities,* Australian standard AS2773-1999

[100] Becker, Joann F. 91994) Ultrasonic frequency selection for aqueous fine cleaning. *Aerospace Environmental technology conference, Huntsville, AL, USA* (NASA-CR-200308)

[101] Jenderka, K. & Koch, C. (2006) Investigation of special distribution of sound field parameters in ultrasound cleaning baths under the influence of cavitation. *Ultrasonics,* 44(1), E401- E406

[102] Hoddnett, M., Chow, R., Zeguiri, B. (2004) High frequency acoustic emissions generated by a 20 KHz sonochemical horn processor detected using a novel broadband acoustic sensor: a preliminary study *Ultrasonics Sonochemistry*, 11, 441-454

[103] Zeqiri, B., Gelart, P.N., Hodnett, M. & Lee, N.D. (2003) A novel sensor for monitoring acoustic cavitation. Part 1: concept, theory, and prototype development. *IEEE Transactions on Ultrasonics, ferroelectrics and frequency control*, 50(10), 1342-1350.

[104] World Forum for Hospital Sterile Supply (WFHSS) (2006) *recommendations by the quality task group: Cleaning and disinfection in the ultrasonic bath (part 1)* (online) Available at http://www.efhss.com/html/educ/qtg/qtg_0008.php [Accessed June 2006]

[105] Comsol (2004) *FEMLAB modeling guide version 3*. Software package. Oxford, UK.

[106] Wellington, J. & Conroy, B. (1995): *The IGES/PDES Organization (IPO) 1994 Annual Report*. PRO Exchange, National Institute of Standards and Technology, Gaithersburg, MD

[107] Solid works 3D computer aided design package. Available online from www.solidworks.com

[108] Moser, F., Jacobs, J.L. & Qu, J. (1999) Modeling elastic wave propagation in waveguides with the finite element method. *Non-destructive testing and evaluation international*, 32, 225-234.

[109] Lewis, J.P., Gardner, S. & Corp, I. (2005) effects of non-symmetric geometry on bulk cavitation fields – finite element simulation and practical results. *European Simulation and Modeling Conference, Porto, Portugal.* 495-500. Gent, Belgium: EUROSIS –ETI

[110] www.megasonics.com

[111] www.minitab.com

[112] Zeqiri, B., Gelart, P.N., Hodnett, M. & Lee, N.D. (2003) A novel sensor for monitoring acoustic cavitation. Part 2: prototype performance and evaluation. *IEEE Transactions on Ultrasonics, ferroelectrics and frequency control*, 50(10), 1351-1362.

Appendix 1 – weekly PPB probe calibration data

To ensure the reliability of the cavitational power reading from the PPB meter, a weekly calibration check was performed. The probe receiver was immersed at a fixed level within a single disk ultrasonic bath with known parameters (I.e. constant water temperature, no surfactant dosing, set liquid level.

The results shown below represent the data obtained during each weekly test by week number. Note that year one data is incomplete, as the probe was not received until part way through the year.

Zero marks on the probe data denote periods where it was unfeasible to conduct testing (Holiday periods and other absences).

Year one PPB calibration chart.

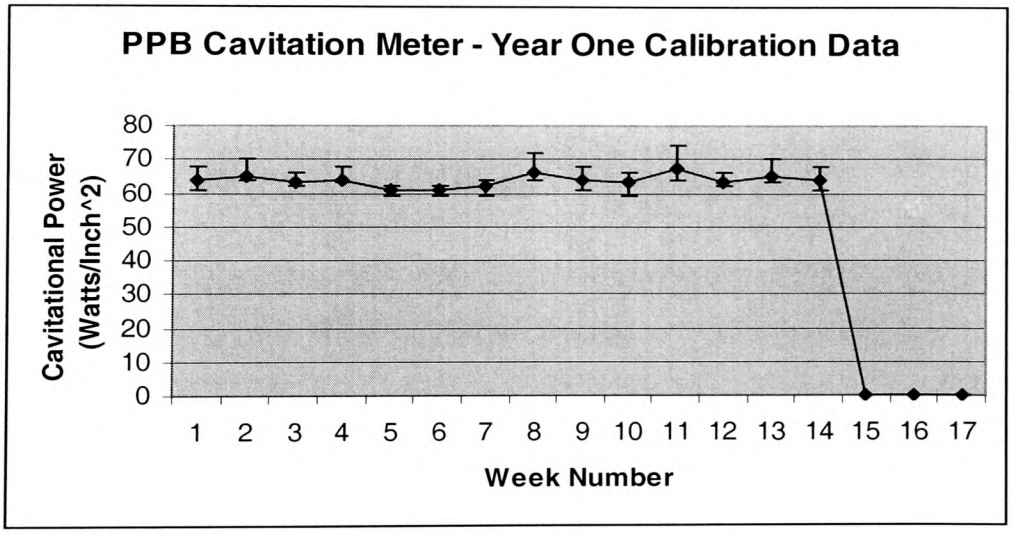

Figure A1: Year One Calibration data for PPB probe.

Note that the solid line depicts the average cavitational reading whereas the Y-axis error bars show localised maxima and minima.

Year two PPB calibration chart.

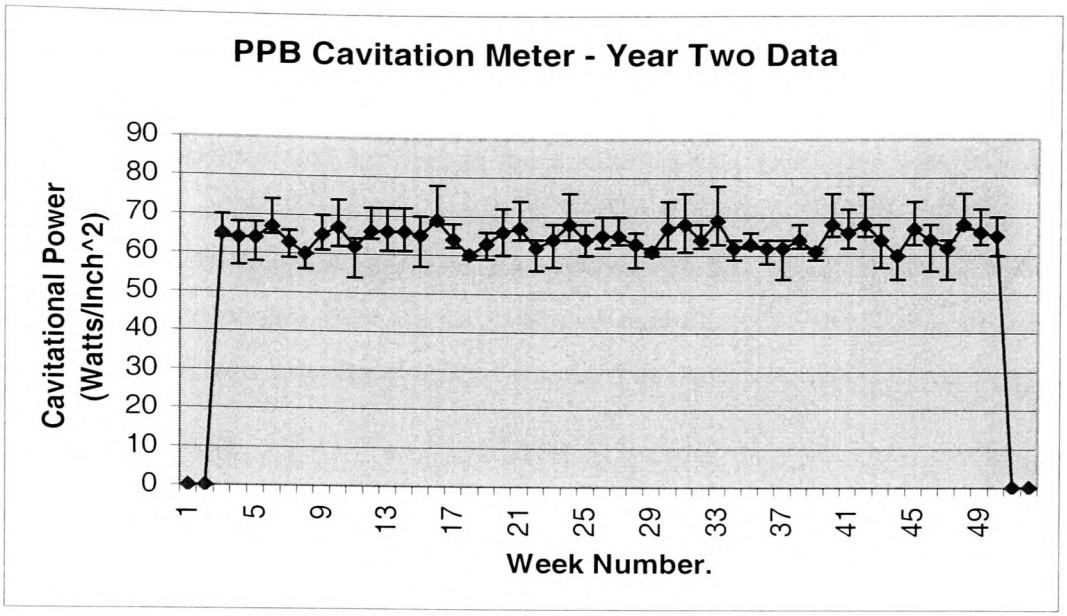

Figure A2: Year two probe calibration chart showing cavitational power by week number.

Year Three PPB calibration Data

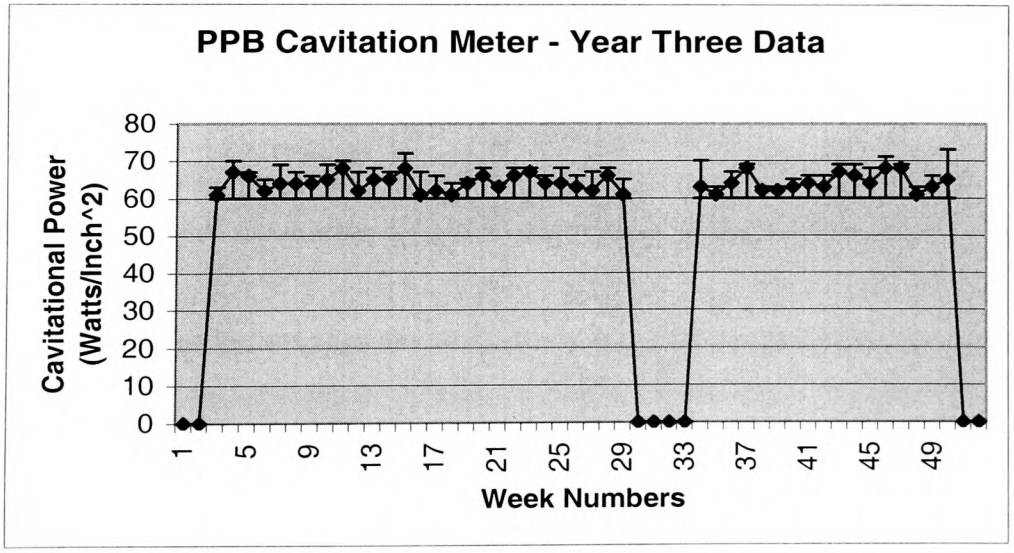

Figure A3: Year Three PPB probe calibration data showing cavitational strength by week number.

Appendix 2 – Deviation from averaged values with distance from the transducer face

It is noted during the results that some practical readings taken with the probes show a variation in both position and strength of the cavitating field from those predicted by the simulation out put as the simulation proceeds further from the radiating transducer face. Figure A4 below shows a reading taken along the centre line of an ultrasonic bath (two transducer, 32 KHz model) showing the averaged cavitating field strengths measured with the PPB probe and also the averaged standard deviation recorded at each location.

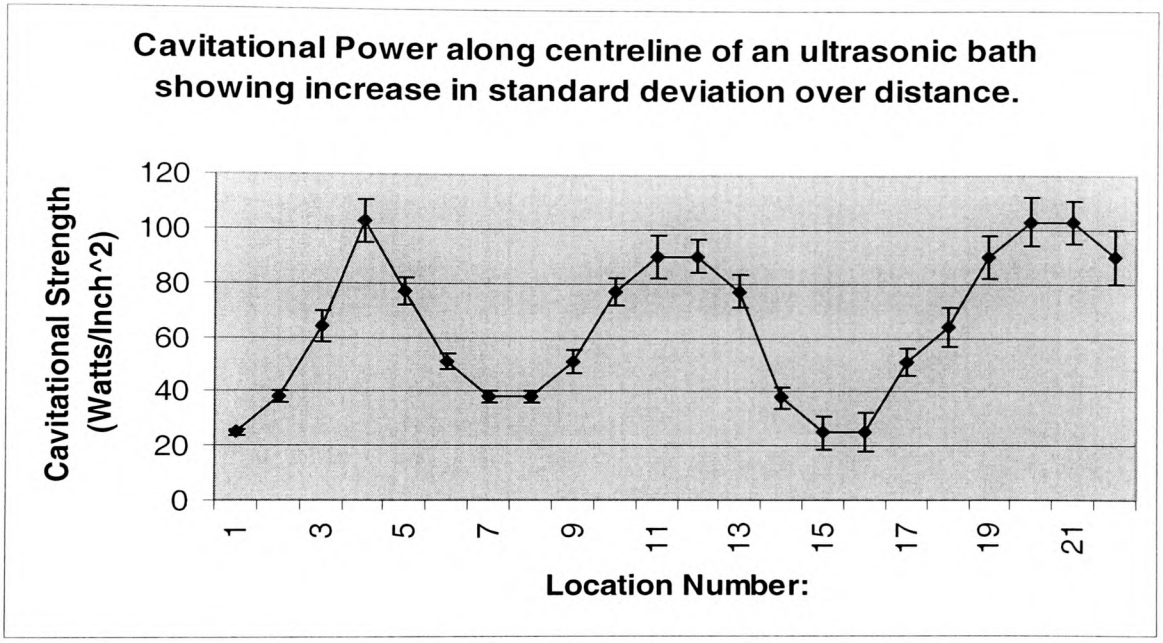

Figure A4: Cavitational field strengths and averaged deviations.

Note the tendency for the average deviation to increase both with higher cavitational powers and the marked increase in average deviation toward the liquid/air interface (Location number 1 represents the measurement location closest to the radiating face of the transducer, Location number 22 represents the measurement taken closest to the water air interface.).

Figure A5 shows the actual averaged deviation values for each location without the cavitational strength. Again location 1 represents the measurements taken closest to the radiating face of the transducer.

Note the increase in the value of the deviation as both cavitational strength increases and with proximity to the water/air boundary (measurement location number 22).

The increased deviation is discussed as a possible cause of discrepancy between the simulation and the practical data in Chapter 7 (conclusions) and is also put forward as a possible cause of the heavier than predicted cavitations located towards the liquid/air surface on the foil test data.

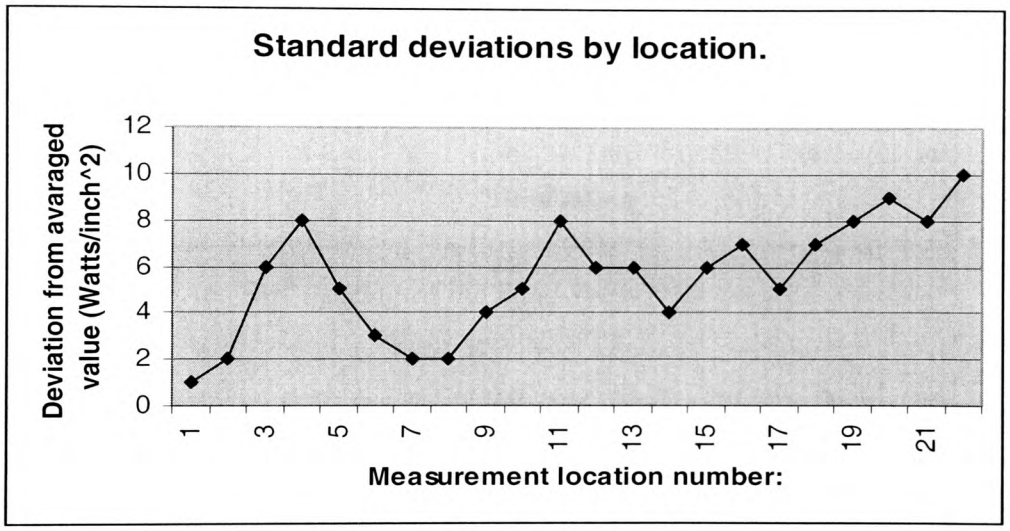

Figure A5: Standard deviations from the averaged cavitational field strength reading with increasing distance from the transducer radiating face.

Appendix 3 – Temperature rise during operation of an ultrasonic bath

The liquid within an ultrasonic vessel was found by experimentation to self-heat during prolonged operation. Figure A6 shows the self-heating recorded with a digital thermal probe suspended in the vessel during operation.

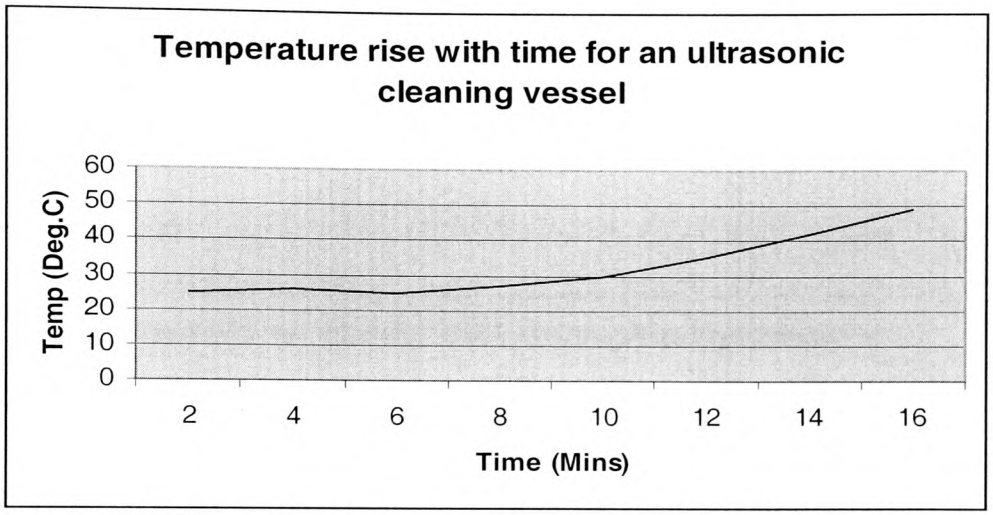

Figure A6: Self-heating of the fluid during ultrasonic agitation.

The self-heating is discussed during the thesis as a function of transducer operation and effects of energy dissipation into the liquid during cavitation. Discussions with CERAMTEC, suppliers of piezo-ceramic rings to the sponsoring company, also noted poor matching of the transducers to the generators would also result in heavy heating of the transducers and hence liquid.

The temperature rise can be shown from the above to have a roughly exponential rise over time. Given the discussed parameters affecting cavitation (Chapter 2, literature review) alter with changing temperature, the 25°C mark was deemed most stable for conducting experimentation and hence to simulate.

Appendix 4 shows the results of temperature heating on the cavitational field strength at a given location with an ultrasonic vessel.

Appendix 4 – Variation in cavitational intensity with temperature rise

Given evidence from the literature review noting change of cavitational activity with increasing temperature, an experiment was conducted to gauge the effect of temperature rise on the cavitational field strength as measured by the PPB cavitation meter.

The meter was suspended at a fixed location in the ultrasonic vessel and the temperature increased from 0°C to 85°C using the inbuilt heaters of the ultrasonic vessel. Cavitation measurements were taken every 5°C change in the liquid temperature as measured by a digital probe.

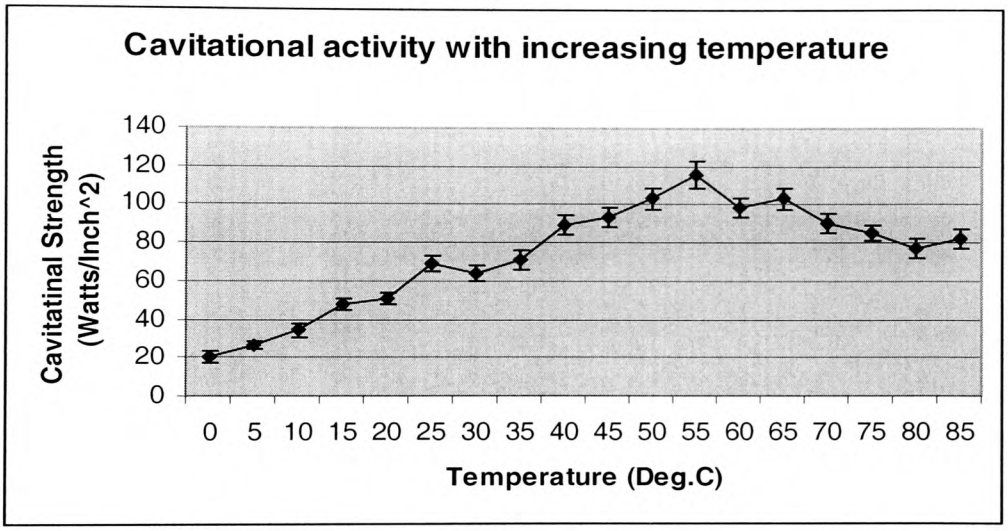

Figure A7: Change of cavitational activity at a fixed locale for changes in temperature.

The results show in figure A7 above note a rise in cavitational activity with temperature until the 55°C marker. Subsequent rises in temperature produced a slight lowering of the cavitational field strength. Causes of this raising and lowering of the cavitational values were discussed during the literature review in chapter 2.

Note also the rise in the deviation from the averaged value (shown by the error bars in the Y-axis) with increased cavitational activity. This finding is in line with the similar rises in deviation outlined in Appendix 2.

The results of this test helped crystallise the decision to include a fixed temperature as an essential feature of the control of experiments protocol as described in chapter 4.

Appendix 5 – Peer reviewed publications and summary of content

The following publications represent peer-reviewed work stemming from the simulation and modeling work conducted as part of this thesis.

A brief summary of each work is included to inform the reader of the content.

1) Lewis JP, Gardner S and Corp I. (2005) *2D Modelling of Ultrasonic Cleaning Vessels – A Finite Element Approach.* Proceedings of the 24th IASTED International Conference on Modelling, Identification and Control. M.H.Hamza (Ed) 475-480

Presented to an audience of simulation researchers, this paper details initial simulation work performed on a two dimensional, single disk ultrasonic vessel (Operating at 40 KHz). Simulation results predict a distinct standing wave set up in the cavitational field and results gained from PPB probe and foil erosion testing concur strongly with the simulation output. Discrepancies in the results are noted and a three dimensional approach is advocated as a possible solution to some variances between practical and simulation results.

2) Lewis JP, Gardner S and Corp I. *Finite Element Simulation of a Long Narrow Workload Immersed in an Ultrasonic Cleaning Bath: Practical Comparisons and Implications for Cleaning Efficacy.* Proceedings of the IEEE UFFC International Ultrasonics Symposium (Rotterdam, the Netherlands. September 19-21, 2005) P415 (Abstract only).

Showing the strong industrial relevance of the research work, this paper discussed the modeling constraints involved in investigating the introduction of a long, narrow load into the cavitating field. Probe and foil testing is used to validate the simulated outputs and shows a good correlation. The paper's results show the shadowing effect caused by the introduction of such a workload and discusses the industrial relevance and importance of the results to ultrasonic cleaning bath design.

3) Lewis JP, Gardner S and Corp I. *Effects of Non-Symmetric Geometry on Bulk Cavitating Fields – Finite Element Simulation and Practical Results.* Proceedings of the 2005 European Simulation and Modelling Conference. Feliz-Teixeira J and Brito A.E (Eds) (Porto, Portugal, 24th – 26th October 2005) P495-499

Acknowledging that many ultrasonic cleaning vessels have non-symmetrical features, this paper explores the simulation of a vessel with a non-symmetric drainage hole in two dimensions and finds that the introduction of this feature raises significant errors between the simulation output and practical data. The error is found to be more significant near the regions of the vessel where the drainage hole is located. The paper highlights the limitations of both 2D axial-symmetry and full 2D modeling and advocates the need for 3D modeling.

4) Lewis JP, Gardner S and Corp I. 3D Simulation of an Ultrasonic Cleaning Vessel – Modelling Methodology and Practical Comparisons. Proceedings of the Institute of Physics Anglo-French Physical Acoustics Conference 2006. (Kent, UK. 17-19 January 2006). P4 (Abstract only).

Presenting to the Institute of Physics, this paper details the mathematical rational behind the three-dimensional models developed. The paper presents as an example several cross-sectional regions from a 3D simulation showing foil and probe comparisons to the simulated output. The practical data is found to be in reasonable agreement with the modelling outputs and possible causes of small discrepancies are discussed in the conclusions.

5) Lewis JP, Gardner S and Corp I. (2006) A 2D Finite Element Analysis of an Ultrasonic Cleaning Vessel: Results and Comparisons. International Journal of Modelling and Simulation. Accepted for publication August 2006. Scheduled for publication in Vol 27 (2) 2007.

This paper is an expanded version of the paper presented to the IASTED conference detailed in (1) above. The theme of the modelling work is expanded upon, providing more detail concerning the simulation methodology and results gained.